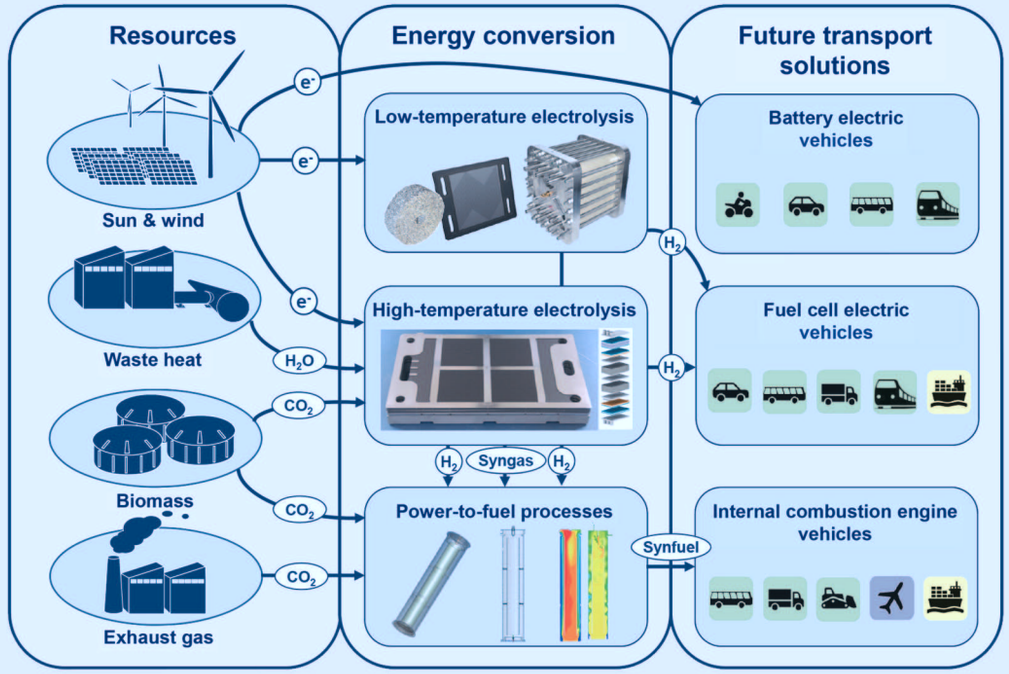

IEK-3 Report 2019

Tailor-Made Energy Conversion for Sustainable Fuels

Detlef Stolten, Bernd Emonts (Editors)

Energie & Umwelt / Energy & Environment
Band / Volume 484
ISBN 978-3-95806-451-5

Mitglied der Helmholtz-Gemeinschaft

JÜLICH
Forschungszentrum

Schriften des Forschungszentrums Jülich
Reihe Energie & Umwelt / Energy & Environment Band / Volume 484

Forschungszentrum Jülich GmbH
Institut für Energie- und Klimaforschung
Elektrochemische Verfahrenstechnik (IEK-3)

IEK-3 Report 2019
Tailor-Made Energy Conversion for Sustainable Fuels

Detlef Stolten, Bernd Emonts (Editors)

Schriften des Forschungszentrums Jülich
Reihe Energie & Umwelt / Energy & Environment Band / Volume 484

ISSN 1866-1793 ISBN 978-3-95806-451-5

Bibliografische Information der Deutschen Nationalbibliothek.
Die Deutsche Nationalbibliothek verzeichnet diese Publikation in der
Deutschen Nationalbibliografie; detaillierte Bibliografische Daten
sind im Internet über http://dnb.d-nb.de abrufbar.

Herausgeber und Vertrieb:	Forschungszentrum Jülich GmbH Zentralbibliothek, Verlag 52425 Jülich Tel.: +49 2461 61-5368 Fax: +49 2461 61-6103 zb-publikation@fz-juelich.de www.fz-juelich.de/zb
Umschlaggestaltung:	Grafische Medien, Forschungszentrum Jülich GmbH
Druck:	Grafische Medien, Forschungszentrum Jülich GmbH
Copyright:	Forschungszentrum Jülich 2020

Schriften des Forschungszentrums Jülich
Reihe Energie & Umwelt / Energy & Environment, Band / Volume 484

ISSN 1866-1793
ISBN 978-3-95806-451-5

Vollständig frei verfügbar über das Publikationsportal des Forschungszentrums Jülich (JuSER)
unter www.fz-juelich.de/zb/openaccess.

Foreword **2**

1 Contributions to International Conferences **5**

1.1 21st International Conference on Solid State Ionics SSI21 6

1.2 Preparation, organization, and result of TRENDS 2017 8

2 Education and Training **13**

2.1 Univeristy education 14

2.2 Contributions to information, further education, and training 19

3 Scientific and Technical Reports **25**

3.1 Solid-oxide converters 26

3.2 Fuel Processing and Systems 38

3.3 Polymer Electrolyte Fuel Cells 49

3.4 Direct Methanol Fuel Cells 65

3.5 Water electrolysis 73

3.6 Rocess and Systems Analysis 82

3.7 Physicochemical principles/electrochemistry 96

4 Selected Results **107**

4.1 Jülich high-temperature fuel cell passes lifetime test of more than ten years 108

4.2 Reduction of noble metal loading 109

4.3 Infrastructural study 112

5 Outlook for New R&D Projects **117**

5.1 Solid oxide cells for reduced operating temperatures from 400 to 600°C 118

5.2 In-Situ TEM study of electrocatalysts 119

5.3 Approaches to developing medium-temperature cells and systems 121

5.4 Supply systems for alternative fuels 122

5.5 Evaluative research on sustainable energy systems 129

6 Data, Facts and Figures **133**

6.1 The Institute of Energy and Climate Research – Electrochemical Process Engineering (IEK-3) 134

6.2 Overview of Department Expertise 137

6.3 Publications, technology transfer, and resources 141

6.4 Prizes and awards 144

6.5 Commitee work 145

6.6 Contributions to trade fairs and exhibitions 152

6.7 How to reach us 155

6.8 List of Abbreviations 158

Foreword

Dear Readers,

Even if the implementation does not always quite keep up with the growing promises, the transformation of the German energy sector is making progress in its implementation, and is even making great progress conceptually speaking in terms of the overall sector. When compared internationally, Germany occupies a leading position with regard to networked infrastructure systems. The principal stimuli and even technologies are no longer coming from the USA, as was the case only recently, but from Asia. There, the focus is also increasingly turning towards infrastructure, and hydrogen is coming to the fore compared to pure electric vehicles.

In response to the major challenge of infrastructure, the topics tackled by IEK-3 have also increasingly shifted towards electrolysis. Electrolysis activities have been boosted considerably in the fields of both polymer electrolyte membrane electrolysis (PEM electrolysis) and alkaline electrolysis. The thematic priority of systems for auxiliary power units has been developed into an activity to research future liquid fuels. This has brought the extensive fuel know-how and many years of experience in reactor design and catalysis to bear on a new pioneering field within the scope of the transformation of the German energy sector. The activities for high-temperature polymer electrolyte fuel cells are focused on PEM electrolysis and fuel cells.

The systems analysis activities have been expanded in a focused manner and now apply to the overall energy system. Hydrogen still plays a role in this, however it is assigned a neutral value in the system considerations just like every other technology. A study on behalf of H2 Mobility compared the infrastructure for battery electric vehicles with that of hydrogen vehicles. With this study, which shows that a hydrogen infrastructure is much more affordable than previously thought, even in the initial phase, the visibility of IEK-3’s systems analysis has increased sharply.

The SOFC stack with the longest operating time to date has been switched off after 100,000 operating hours. This stack was able to show that no new catastrophic degradation mechanisms arise as the stack approaches the end of its lifetime, even over such a long operating time. The stack was subject to degradation that was typical for the length of time over which it was operated, but the degradation of new stacks has, in the meantime, been greatly reduced by means of intermediate layers and material changes.

This has greatly strengthened already strong fields of development in the institute and the focus has been moved completely to technologies that are directly related to the transformation of the energy sector and that also have the potential for a high quantitative impact.

Jülich, August 2019

1

Conferences

Contributions to International Conferences

- 21st International Conference on Solid State Ionics SSI-21
- Preparation, organization, and result of TRENDS 2017

1.1 21st International Conference on Solid State Ionics SSI21

The International Conference on Solid State Ionics is a major event in the field, which is held every two years and attracts a world-wide audience. During June 18th and 23rd the conference takes place in Padua, Italy. The general schedule of the SSI-21 shows Fig. 1. The topics of SSI-21 covered fundamental and applied aspects of ion-conducting materials, both conventional and innovative.

<table>
<tr><th>TIME SCHEDULING</th><th>SATURDAY 17th JUNE</th><th colspan="3">SUNDAY 18th JUNE</th><th>MONDAY 19th JUNE</th><th>TUESDAY 20th JUNE</th><th>WEDNESDAY 21st JUNE</th><th>THURSDAY 22nd JUNE</th><th>FRIDAY 23rd JUNE</th></tr>
<tr><td>8:00 - 9:00</td><td></td><td rowspan="5">Registration</td><td></td><td rowspan="3">TUTORIAL Impedance Spectroscopy</td><td>Plenary session Udo Kragl</td><td>Plenary session Masakazu Aono</td><td>Plenary session Mogens Mogensen</td><td>Plenary session Stanley Whittingham</td><td rowspan="2">Parallel sessions</td></tr>
<tr><td>9:00 - 10:00</td><td></td><td></td><td rowspan="2">Parallel sessions</td><td rowspan="2">Parallel sessions</td><td rowspan="2">Parallel sessions</td><td>ISSI Elections</td></tr>
<tr><td>10:00 - 11:00</td><td></td><td></td><td>Coffee Break</td><td>Coffee Break</td><td>Coffee Break</td><td>Coffee Break</td><td>Coffee Break</td></tr>
<tr><td>11:00 - 12:00</td><td></td><td rowspan="2">Parallel sessions</td><td rowspan="2">TUTORIAL Nuclear Magnetic Resonance</td><td rowspan="2">Parallel sessions</td><td rowspan="2">Parallel sessions</td><td rowspan="2">Parallel sessions</td><td rowspan="2">Parallel sessions</td><td>Parallel sessions</td></tr>
<tr><td>12:00 - 13:00</td><td></td><td>Parallel session Michael Grätzel</td></tr>
<tr><td>13:00 - 14:00</td><td></td><td rowspan="2">Lunch</td><td></td><td rowspan="2">Lunch</td><td rowspan="2">Lunch</td><td rowspan="2">Lunch</td><td rowspan="2">Lunch</td><td>Closing Ceremony</td></tr>
<tr><td>14:00 - 15:00</td><td rowspan="5">Registration</td><td rowspan="2">TUTORIAL Nanoionics</td><td rowspan="2">Parallel sessions</td><td rowspan="2">Parallel sessions</td><td rowspan="4">Excursion / Banquet</td><td rowspan="2">Parallel sessions</td><td></td></tr>
<tr><td>15:00 - 16:00</td><td>Coffee Break</td><td rowspan="3">TUTORIAL Neutro Scattering Techniques</td><td></td></tr>
<tr><td>16:00 - 17:00</td><td rowspan="2">Parallel sessions</td><td>Coffee Break</td><td>Coffee Break</td><td>Coffee Break</td><td>Coffee Break</td><td></td></tr>
<tr><td>17:00 - 18:00</td><td></td><td>Parallel sessions</td><td>Parallel sessions</td><td>Parallel sessions</td><td></td></tr>
<tr><td>18:00 - 19:00</td><td></td><td></td><td></td><td rowspan="2">Poster session</td><td rowspan="2">Presentations of YSA finalists and Mid-Career Researcher Award recipient</td><td rowspan="2">Poster session</td><td></td></tr>
<tr><td>19:00 - 20:00</td><td></td><td colspan="3" rowspan="2">Opening Ceremony & Welcome Party
Palazzo della Ragione</td><td></td></tr>
<tr><td>20:00 - 21:00</td><td></td><td></td><td></td><td></td><td></td></tr>
<tr><td>21:00 - 22:00</td><td></td><td></td><td></td><td></td><td></td><td rowspan="2">Opera Concert</td><td></td><td></td><td></td></tr>
<tr><td>22:00 - 23:00</td><td></td><td></td><td></td><td></td><td></td><td></td><td></td><td></td><td></td></tr>
</table>

Fig. 1: General schedule of the SSI-21

The session “High-temperature proton-conducting polymer membrane” was organized by Werner Lehnert together with other international experts in this field. High-temperature polymer electrolyte fuel cells are beneficial for stationary applications as well as for applications as auxiliary power units in trucks, trains and airplanes. At present, however, the cost and performance of fuel cells operating above 100°C are not yet satisfactory enough to envisage a widespread alternative to conventional technologies. In this frame, the most recent research efforts have been focused on the development of both catalysts and proton-conducting membranes. Concerning the former topic, the major issues are: (i) minimizing the overall Pt content in the catalysts; (ii) improving sluggish kinetics of the ORR at the cathode. Concerning the latter one, the attention is chiefly devoted to: (i) maximizing membrane durability, and (ii) increasing membrane proton conductivity without causing losses in stability.

This symposium aimed at discussing the most recent developments in the field of proton-conducting, polymer-based membranes for high temperature polymer electrolyte fuel cells and related applications. In particular, it treated, the following topics: (i) development of new composite and blended materials with improved proton conductivity, chemical and electrochemical stability and durability; (ii) new in situ and operando characterization techniques of MEAs; (iii) multi-scale modeling (micro-, meso- and macro-scale) of isothermal

and non-isothermal processes in membranes and interfaces; (iv) theoretical/experimental investigation of transport mechanisms in complex systems. The working temperature range considered in this symposium was 100 - 300°C. The attention was be chiefly focused on materials based on polybenzimidazole, however also other systems (pyridine-based, etc.) were discussed.

1.2 Preparation, organization, and result of TRENDS 2017

On 5–6 December 2017, IEK-3 hosted a panel of experts in Aachen entitled TRENDS – Transition to Renewable Energy Devices and Systems. A group of around 20 scientists discussed relevant topics which might contribute to the transition of today's energy system to an energy supply based on sustainable primary energy sources. The aim of the expert panel was to identify high-impact core topics and missing components which will be decisive in achieving an 80 % reduction in CO_2 emissions by 2050. The electrification of the transport sector will continue to rise in future. Thematically, the conference focused on the use of hydrogen for transport and essential drive concepts. With regard to fuels, the potential of alternative fuels, their production pathways, and cost aspects were discussed.

There are various approaches for integrating electric power generation from renewable energy sources as efficiently as possible into the current, and above all the future, energy system – in spite of its volatility. Suitable storage technologies must therefore be developed to balance out the fluctuating nature of power generation. The main topics of the conference were the state of the art and the prospects of hydrogen and battery electric vehicles, power-to-fuel technology, and DC/DC grids, in addition to ideas on sector coupling and the integration of climate zones.

Most of the presentations held at TRENDS 2017 have been compiled into conference proceedings complete with a brief summary[1].

Sector coupling in the German energy system will be primarily realized between the sectors of electric power generation and transport until 2050. IEK-3's energy system is modeled on an installed capacity of 60 GW, based on an annual power generation of 528 TWh. This means that until 2050, renewable power generation must be expanded by 59 GW of offshore wind power, 132 GW of onshore wind power, and 120 GW of photovoltaic power, which corresponds to a total of 311 GW. This will produce 629 TWh of electric power. The strong superstructure is a consequence of the fluctuation of renewables. Energy amounting to 101 TWh will be made available via electrolysis in the form of 2.1 million tons of hydrogen for fuel cell vehicles. The latter will represent 75 % of the passenger car fleet by 2050. A further 200 TWh must be stored temporarily. In this sector, tightening CO_2 reduction targets within the range of 80–95 % is viewed as an equal challenge to a general reduction by 80 %. However, the use of power-to-X technologies will further increase the demand for electrical energy. An investigation into the production of hydrogen in Patagonia with subsequent transportation to Japan analyzed how renewable energy can in future be distributed internationally. This scenario results in costs of 4.44 €/kg of hydrogen. Annual production amounts to 8.8 million tons of hydrogen. The costs can be broken down as follows: roughly one quarter for wind power, one quarter for electrolysis, one quarter for naval transport in liquid form, and roughly one eighth each for liquefaction and storage for pipeline transport.

Power-to-fuel processes represent another way of producing fuel: regeneratively produced hydrogen is combined with carbon dioxide separated in industrial processes to form fuels. Ethers, alcohols, and alkanes are all considered. In particular, ethers such as dimethyl ether and polyoxymethylene dimethyl ether (PODE) offer advantages in terms of the emission of

[1] D. Stolten, R. Peters (Eds.), TRENDS 2017 – Transition to Renewable Energy Devices and Systems, Schriften des Forschungszentrums Jülich, Reihe Energie & Umwelt / Energy & Environment, Band 447, ISBN 978-3-95806-376-1

nitrogen oxides and particles during combustion in engines. Approximately 3 million tons of hydrogen from electrolysis could be used to produce approximately 7.5 million tons of fuel in the form of alkane cuts. The efficiencies of fuel production amount to 30–50 %, depending on the process and the chemical target substance. The analyses were focused on Fischer–Tropsch products, on the one hand, and PODE, on the other. Positive insights into Fischer–Tropsch products include their good “drop-in” ability and their good engine combustion properties. The synthesis of carbon monoxide and hydrogen ultimately leads to the formation of waxes. Targeted reaction control and product processing therefore requires a range of additional instruments such as a reverse water–gas shift reactor, a cracker for cracking the wax chains, and a still. Important insights concerning PODE mixtures include their limited drop-in capability but also their good emission properties during technical combustion. Since direct synthesis is impossible here, a complex synthesis path must be taken. In these material systems in particular, the thermodynamics are characterized by a multitude of nonidealties.

Carbon dioxide is needed for the power-to-fuel path. In current discussions, biomass and industrial waste gases as well as the separation of CO_2 from air are cited as options. In a contribution to the TRENDS 2017 conference, a techno-economic analysis for a potential further process is presented. The energy expenditure for such a system is calculated to be 3.65 GJ/t CO_2. This high level of energy demand results primarily from the installation of two compressors that compress air and CO_2. The efficiency is between 7.52 % and 11.83 %, depending on thermal integration. The costs of preventing CO_2 emissions vary between 824 \$/t CO_2 and 1,333 \$/t CO_2, in accordance with the energy source used. In comparison to other values specified in literature, these analysis results reveal higher values for both energy demand and costs. The reasons for this deviation include frequently flawed balance limits, oversimplified process schematics, and overly positive assumptions. Further case studies show that enormous amounts of land and very high investments are required to reduce the expected quantities of CO_2 in the atmosphere to below the level of 1990 by 2050. A comparison between the removal of CO_2 from the atmosphere and the technology for carbon capture and storage from coal-fired power plants shows that air separation is not viable in the medium term from a techno-economic perspective. In the long term, the separation of CO_2 from atmospheric air can continue to play a decisive role in carbon capture.

In terms of the automotive industry, various manufacturers have presented their own concepts for the further development of battery electric and fuel cell vehicles. Their associated statements are supported by numerous project activities.

The use of hydrogen in public transport has reached a high level of development. The city of Hamburg is an interesting example: like any metropolitan area, Hamburg faces the challenge of a growing population, the associated rise in traffic, and the increase in emissions this causes. Hamburg is therefore pursuing an ambitious program to increase electromobility through batteries and hydrogen-operated fuel cells. The Hamburg Senate has decided to purchase only emission-free buses from 2020. Various projects are currently aiming to increase the number of electric vehicles and simultaneously expand the charging infrastructure to include fast-charging stations. In terms of buses, an “innovation line” was introduced: only buses with innovative electric drives are used on this line so that various innovative drivetrains can be compared under the same conditions. The fleet currently comprises series electric hybrid buses, parallel Diesel-electric hybrid buses, battery buses

with fuel cells as range extenders, and plug-in buses. The results are collected and compared to determine what systems are used in future.

IEK-3 conducted a systems analysis study on hydrogen infrastructure for fuel cell vehicles compared to charging infrastructure for battery electric vehicles. With large proportions of renewable wind and solar power, even a perfect grid does not prevent surplus energy. Hydrogen is necessary for storing energy in order to balance out the volatility of power generation and demand. At 80 % renewable energy, a third of the surplus electric power can supply 50 % of the German vehicle fleet with hydrogen. The fueling infrastructure for fuel cell vehicles is extremely (time-) efficient, particularly compared to charging batteries. The more vehicles that use this technology, the more that the economies of scale are in favor of the hydrogen infrastructure. At 100,000 vehicles, the costs for both infrastructure are approximately the same. At 1 million electric vehicles, the investment costs for hydrogen fueling stations are lower than those for charging stations. Investments in environmentally friendly H_2 production and storage lead to a situation in which the costs for the H_2 infrastructure are temporarily higher than investment costs for battery electric vehicles. At higher vehicle numbers, however, the increase of additional infrastructure investments is steeper for battery systems than for fuel cell systems. Investment costs in infrastructure for the production and storage of 100 % environmentally friendly hydrogen for refueling 20 million fuel cell vehicles are approximately € 11 billion lower than those required for a charging structure for the same number of battery electric vehicles.

The “Tailor-Made Fuels from Biomass” (TMFB) Cluster of Excellence at RWTH Aachen University has the holistic aim of co-optimizing biofuel production and combustion through the molecular structure of the fuel (or its composition in the case of mixtures) as the most important degree of freedom in design in order to find the most suitable fuel. Conceptionally, the challenge is to identify oxygen-containing fuel components that permit high-efficiency, low-emission combustion. The associated production pathways should be efficient and sustainable. The focus is on converting lignocellulosic materials into liquid biofuels through selective catalytic refunctionalization of biomass monomers. The panel of experts gave an overview of model-based strategies and tools for an integrated product and path design.

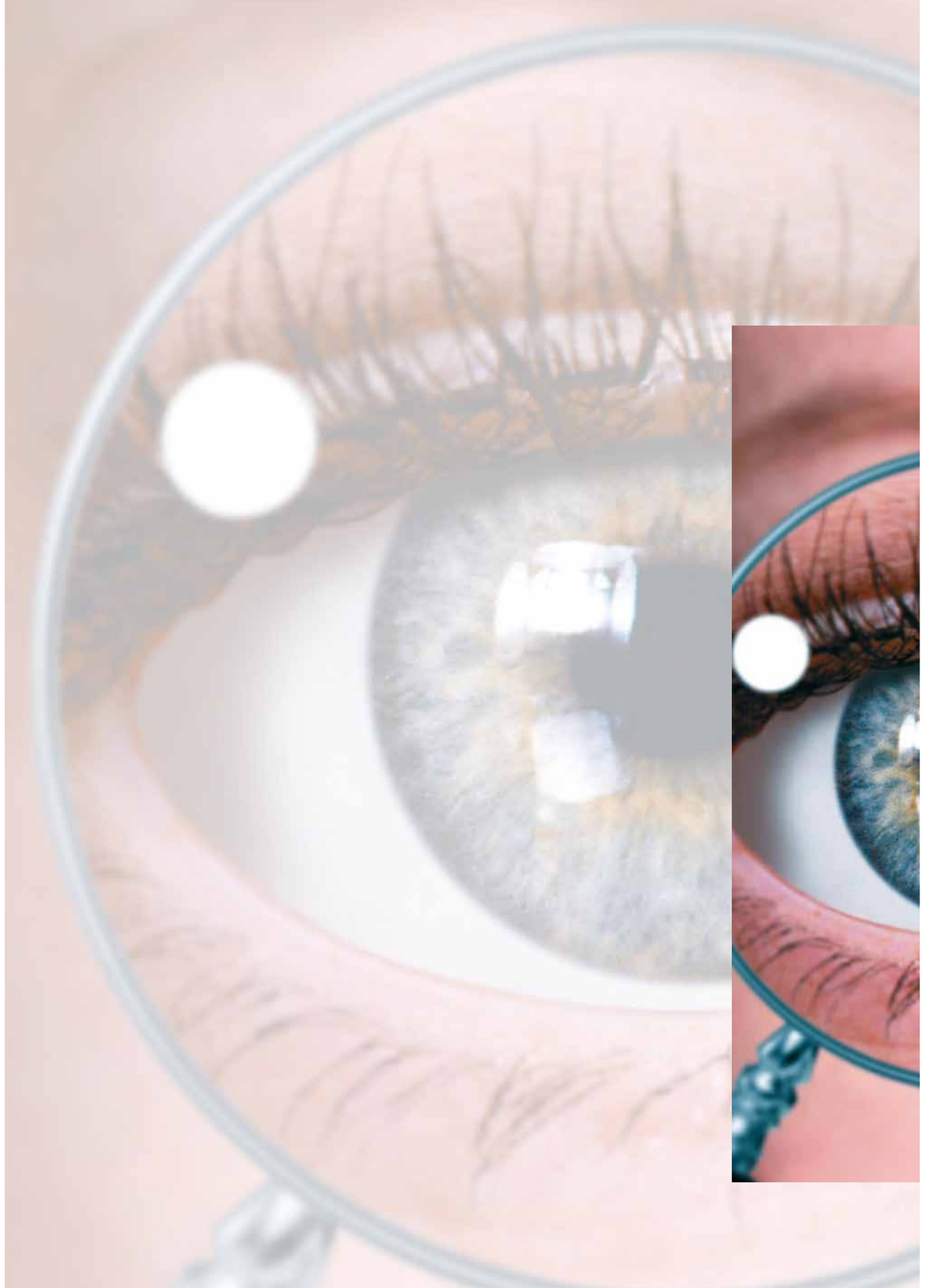

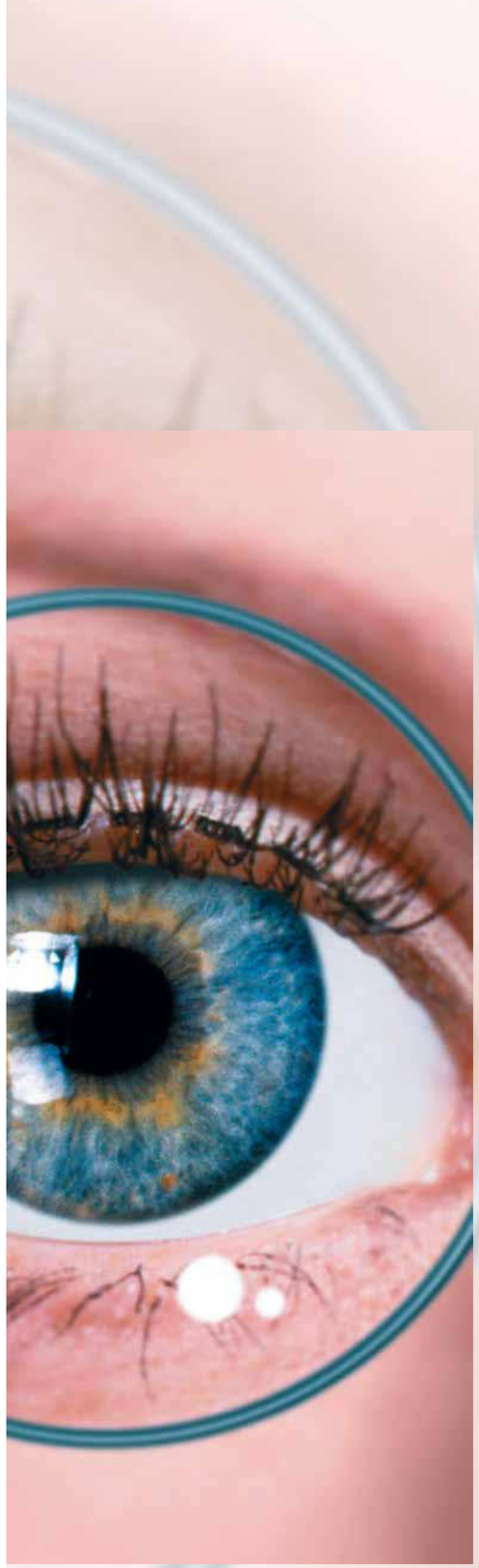

2

Education

Education and Training

- University education
- Contributions to information provision, further education, and training

In addition to disseminating knowledge on pioneering energy conversion technologies, several scientists at IEK-3 are active in the continuing professional development and training of specific target groups. They are involved in educating young scientists, teaching at universities and universities of applied sciences as well as supervising doctoral researchers in their work. Laboratory technicians and mathematical-technical software developers enrolled in dual study programs receive practical guidance and experience at the institute. School children in grade 10 and above also benefit from lessons on energy technology given by IEK-3 employees.

2.1 Univeristy education

Teaching at universities is a fundamental responsibility of selected research scientists at IEK-3 in addition to their research and development work. Within the framework of the Jülich model, IEK-3 has one full professorship (grade W3) at RWTH Aachen University, which is currently held by Prof. Dr.-Ing. Detlef Stolten. Dr. Martin Müller supports Prof. Stolten, teaching tutorials that accompany the lectures and conducting oral examinations at undergraduate level. Prof. Dr. rer. nat. Werner Lehnert is a grade-W2 professor at RWTH Aachen University in the Scientific Faculty. His lectures are accompanied by tutorials given by Dr. Uwe Reimer. Privatdozent Dr. Carsten Korte also teaches at RWTH Aachen University. Dr.-Ing. Martin Robinius has been teaching at RWTH Aachen University since 2016, where he teaches two block courses as part of Prof. Aaron Praktiknjo's lecture course. In addition, Dr. Robinius gives two block lecture courses each year at TU Berlin Campus El Gouna in Egypt.

RHEINISCH-WESTFÄLISCHE TECHNISCHE HOCHSCHULE AACHEN	http:///www.rwth-aachen.de/
Technische Universität Berlin	http://www.tu-berlin.de/
FH AACHEN UNIVERSITY OF APPLIED SCIENCES	http://www.fh-aachen.de/

Fig. 2: Universities where IEK-3 scientists lecture

Two other grade-W2 professorships are held at Aachen University of Applied Sciences Campus Jülich by Prof. Dr.-Ing. Ralf Peters and Prof. Dipl.-Ing. Ludger Blum. Dr.-Ing. Dipl.-Wirt.Ing. Thomas Grube supports Prof. Peters, teaching tutorials accompanying his lectures and conducting written examinations at undergraduate level. Dr.-Ing. Jochen Linßen and Dr.-Ing. Peter Stenzel share the lecturing of another course at Aachen University of Applied

Sciences Campus Jülich. Fig. 2 shows the Internet addresses of the three universities at which IEK-3 scientists teach young scientists.

The spectrum of topics taught ranges from the fundamentals of science and theoretical modeling and simulation methods to detailed technical information and the characterization of technical applications. Each semester, five lecture courses, three tutorial courses, and four block lecture courses are taught. Prof. Stolten's lecture course additionally involves practical work experience lasting a half day. Between 10 and 80 students participate in the individual courses each semester. IEK-3 scientists also play an important role in supervising semester papers, bachelor's and master's dissertations, and doctoral theses. In 2017, 2 bachelor's dissertations, 24 master's dissertations, and 4 doctoral theses were successfully completed. In 2018, 3 bachelor's dissertations, 31 master's dissertations, and 11 doctoral theses were successfully completed.

2.1.1 University courses taught by professors

Table 1 provides an overview of the courses taught at universities by IEK-3 professors.

Name	Topic	Type/hours semester		University
Prof. Dr. D. Stolten	Grundlagen und Technik der Brennstoffzellen	V/2 Ü/2	WS	RWTH Aachen
Prof. Dr. W. Lehnert	Modellierung in der Elektro-chemischen Verfahrenstechnik	V/2 Ü/2	WS	RTWH Aachen
Prof. Dr. R. Peters	Basics and applications of chemical reaction theory – simulation of dynamic processes in energy systems with MATLAB/Simulink	V/2 Ü/2	WS	FH Aachen Standort Jülich
Prof. L. Blum	Brennstoffzellen - Die Zukunft der dezentralen Energieversorgung!?	V/2	WS	FH Aachen Standort Jülich
	Fuel Cells – The Future for Dispersed Power Supply!?	V/2	WS	

Table 1: University courses taught by professors

2.1.1.1 Principles and technology of fuel cells

Prof. Dr.-Ing. Detlef Stolten holds the Chair for Fuel Cells at RWTH Aachen University. The lectures deal with the conversion of renewable and fossil energy carriers for use in fuel cells with portable, stationary, and mobile applications. The process engineering and systems technology aspects include high-temperature and low-temperature fuel cells, as well as fuel processing specifically for fuel cells. These aspects are accompanied by an examination of the basic physicochemical principles. Systems analyses of energy process engineering, which include cost estimates, serve as a comprehensive examination with a view to future market launch. As part of the existing cooperation with Forschungszentrum Jülich, university

students have the opportunity to write semester papers and undergraduate dissertations at Jülich and to work on projects as research assistants.

2.1.1.2 Modeling in electrochemical process engineering

Prof. Werner Lehnert teaches modeling in electrochemical process engineering at RWTH Aachen University. His lecture course focuses on the mathematical description of electrochemical converter systems. In addition to the basic approach for modeling, different modeling techniques are outlined. Using low- and high-temperature fuel cells as examples, 1D, 2D, and 3D models of varying complexity are developed and their validity is then discussed. These examples of application form the basis for mathematical descriptions of the interactions of mass and heat transport with the electrochemical processes. Particular attention is paid to the description of processes in the porous components of fuel cells.

2.1.1.3 Basics and applications of chemical reaction theory – simulation of dynamic processes in ernergy systems with MATLAB/Simulink

Prof. Ralf Peters teaches energy process engineering at Aachen University of Applied Sciences Campus Jülich. The course “Basics and Applications of Chemical Reaction Theory” links the basic principles of chemical process engineering with dynamic simulations of reactors. The lectures and tutorials look at examples of fuel cell systems for hydrogen-powered vehicles and in combination with fuel processing for auxiliary power supply based on diesel. The course is compulsory for students enrolled in the Master of Science in Energy Systems.

2.1.1.4 Fuel cells – the future of dispersed power supply!?

Prof. Ludger Blum teaches fuel cell technology at Aachen University of Applied Sciences Campus Jülich. The optional module “Fuel cells for dispersed power supply” in the bachelor’s course on energy and environmental technology and the master’s course on energy systems covers the function, design, behavior, advantages, and disadvantages of different fuel cell types. It also lays the groundwork for the process engineering design of fuel cell systems. The topics include: fundamentals of fuel cells; fuel supply; efficiency, function, and design of different fuel cell types; requirements on the fuel cell system; process engineering of different fuel cells for different applications; energy balance in a fuel cell system; state of the technology. An average of 20–30 students in the master’s program and an average of 10 in the bachelor’s program take these courses.

2.1.2 Courses taught by university lectures

Table 2 provides an overview of the courses taught at universities by IEK-3 lecturers.

Name	Topic	Type/hours semester		University
PD Dr. C. Korte	Physikalische Chemie I für Chemie (Lehramt) (V), Quantenmechanik	V/2 (Ü/1)	WS	RWTH Aachen
Dr. M. Robinius	Projektmodul Energiesystemische Forschung	V/2 Block	SS	RWTH Aachen
	Technikbasierte Energiesystemanalyse	S CP/5	WS	RWTH Aachen
	Sector Coupling and Market Simulation	V/2 Block	WS	TU Berlin Außencampus El Gouna, EG
Dr. M. Müller	Grundlagen und Technik der Brennstoff-zellen (Beitrag zur Lehrveranstaltung von Prof. Stolten)	Ü/2	WS	RWTH Aachen
Dr. J. Linßen **Dr. P. Stenzel**	Energiespeichertechnologien	V/2 Ü/1 P/2 Block	SS	FH Aachen Standort Jülich
Dr. T. Grube	Basics and Applications of Chemical Reaction Theory – Simulation of Dynamic Processes in Energy Systems with Matlab/Simulink (Beitrag zur Lehrveranstaltung von Prof. Peters)	Ü/2	WS	FH Aachen Standort Jülich
CP: Credit Points				

Table 2: Courses taught by university lecturers

2.1.2.1 Physical chemistry I, quantum mechanics

Privatdozent Dr. Carsten Korte lectures chemistry to trainee chemistry teachers at the Department of Chemistry in the Faculty of Mathematics, Computer Science and Natural Sciences at RWTH Aachen University. His lecture course on physical chemistry I is part of the lecture module physical chemistry B for students in their third semester. The lecture (2 SWS) and the accompanying tutorial (1 SWS, taught by Junior-Prof. F. Hausen from IEK-9) teach the students about the structure of matter and spectroscopy. Students are given an introduction to quantum mechanics before learning about the spectroscopic methods used in chemistry as well as the atomic structure and various forms of chemical bonds. In 2017, 28 students and in 2018, 24 students registered for the lecture and seminar in winter semester.

2.1.2.2 Energy systems research and technology-based energy systems analysis

Dr. Martin Robinius works with Prof. Dr. Aaron Praktiknjo (Assistant professor of energy resource and innovation economics), teaching a joint lecture course and tutorial on technology-based energy systems analysis. Their collaboration is part of the Jülich Aachen Research Alliance (JARA), which is a cooperation between Forschungszentrum Jülich and RWTH Aachen University. Extensive technical expertise was pooled in the ENERGY section of JARA concerning the fields of process engineering, mechanical engineering, electrical engineering, geoscience, biotechnology, and chemistry, and the corresponding research institutes agreed to take part in an interdisciplinary collaboration. Triggered by the increasing demands on systems analysis in comprehensively evaluating technological innovations expected to compete economically with conventional technologies already on the market, the dovetailing of engineering and scientific competence with economic and sociological expertise is crucial. The courses aim to teach the students the importance of this in an appropriate manner.

2.1.2.3 Sector Coupling and Market Simulation

Dr. Martin Robinius teaches a block lecture course entitled “Sector Coupling and Market Simulation” at TU Berlin’s Campus El Gouna in Egypt. Students taking the lecture are introduced to programming in Python and given an overview of the energy industry, including sector coupling and energy markets in general. They learn how to design techno-economic models using the “FINE”[2]environment developed at IEK-3 and how to apply more detailed models, for example to model renewable energy feed-in[3]. The course involves a group project, where students work together on their own research question and design relevant energy system models. They analyze their results in a written paper.

2.1.2.4 Energy storage technologies

Students learn about energy storage technologies, their application, and their design. The knowledge required for the efficient planning of energy storage is taught and applied to practical problems. The lecture, tutorial, and practical element deal with the requirements to be met by energy storage systems, areas of application, principles of storing electrical energy and heat, technical design of storage systems, new and unconventional storage options, technical and economic design, and the role of energy storage in supplying energy.

[2] https://github.com/FZJ-IEK3-VSA/FINE
[3] https://github.com/FZJ-IEK3-VSA/glaes

2.2 Contributions to information, further education, and training

Based on existing multidisciplinary expertise and building on experience from previous years, IEK-3 organizes a variety of events, contributes to external events at various levels, and works with other institutions preparing, coordinating, and advising. The expansion and consolidation of these activities is the aim of existing and planned partnerships providing interested target groups with information and further education.

2.2.1 Organization of tours, seminars, work experience, information events, and visits to the institute

The topics of the events are tailored to the requirements and needs of each target group. The spectrum ranges from information events and training courses for secondary-school students, university students, teachers, tradesmen, technicians, engineers, and scientists to work experience for secondary-school students, as well as vocational training and internships for university students. These courses last between a half day to several weeks, depending on requirements. The tasks assigned to secondary-school students and university students during a placement include shadowing technical and scientific personnel at the institute as well as supervised, independent work on practical projects.

- Information events and visits to the institute for those interested in Jülich's contribution to R&D for fuel cell and hydrogen technology. Tours of the institute are given by two IEK-3 doctoral researchers and an average of 60 tours take place each year at IEK-3 with around 20 people per tour.
- Every year, IEK-3 offers secondary-school students from local schools work experience and placements in the area of fuel cell and hydrogen technology (2017: 3 school students on placement; 2018: 4 school students on placement). Laboratory work experience is also available to secondary-school students, covering a wide range of topics over a period of one or two weeks.
- A day of experiments related to fuel cells was also organized by JuLab together with scientists at IEK-3. In 2017, it took place on three dates and groups of 26–31 school students familiarized themselves with how the electrochemical converter works. In 2018, the day of experiments was run again on three dates for groups of 8–18 school students.
- One-day supervised project work on an R&D fuel-cell topic was part of JuLab's work experience program on the topic of mobility, attracting 10 school students in July 2017 and 10 in July 2018.
- As one of the activities within JuLab's science work experience program on energy, school students (8 in 2017 and 10 in 2018) were given a comprehensive introduction to the world of fuel cells.
- As part of JuLab's teacher training program in 2018, 2 teachers were given a tour of the institute and 30 trainee teachers attended a lecture, providing an introduction to the principles, structure, function, and application of fuel cells.
- In cooperation with ProNIMat and JuLab, a university student learnt how a fuel cell works as part of a two-day work placement in IEK-3's laboratories.

2.2.2 Involvement in extrernal events

Several scientists from IEK-3 were involved in diverse external events including training courses, workshops, and continuing professional development courses as invited speakers, experts, and coordinators, giving introductory and specialist presentations on renewable energy, hydrogen, and fuel cells.

- Master's seminar on systems innovation and sustainability using the energy transition as an example

  Dr. Bernd Emonts gave a lecture to students taking the master's degree at the Chair of Economic Geography, RWTH Aachen University, on a project house for technology-based energy systems analysis. In this 90-minute lecture, Dr. Emonts talked about the stakeholders, work, and results of the scientific project as well as coordinated approaches for a sustainable German energy scenario.

- Master Class Course Conference "Renewable Energies"

  The Master Class Course Conference is a five-day conference series focusing on renewable energy. Each year, the conference focuses on a different topic. The speakers are the big names in politics, industry, and research. Different universities also present their research projects. The program additionally features forums, excursions, and discussions. IEK-3 was represented in 2017 by Dr. Peter Markewitz, who was also one of the coordinators, and Dr. Peter Stenzel. In 2018, Dr. Peter Markewitz und Peter Lopion gave presentations.

- Dialogue on research, society, and the future

  Organized by Sustainable Campus at Forschungszentrum Jülich, Region Aachen Zweckverband, and EnergyAgency.NRW, the dialogue began in 2017 and looked at whether de-fossilizing the energy supply is a dream or reality in our region. It continued in 2018 focusing on hydrogen as an important element in coupling sectors. The dialogue aims to bring players from research, industry, and politics together to discuss topics relevant to the future. Several scientists from IEK-3 took part in both events, giving presentations and showcasing examples of research and application.

- Day of Science

  In 2017, Forschungszentrum Jülich ran a Day of Science for the first time, providing colleagues with in-depth insights into research conducted at the institutes on campus. In March 2017 and June 2018, several hundred researchers came to the foyer in the Central Library for the Day of Science and discussed their work with colleagues. In-depth insights were gained into research at other institutes on campus and new contacts were made.

- Research forum on science in the classroom

  On 22 June 2018, Dr. Bernd Emonts gave a presentation on fuel cells to 20 secondary school students at Sankt Adelheid Gymnasium in Bonn. He spoke about research for the Energiewende, focusing on hydrogen and fuel cells for sustainable mobility, introducing the school students to the most important technologies in a sustainable energy scenario for Germany, and answering their questions at the end.

Fig. 3: Contributions of IEK-3: autothermal reformers (2017, left) and flow visualization in a PEM electrolysis cell (2018, right)

- Expert talk in secondary school Gymnasium Haus Overbach

  School students taking ordinary-level and higher-level chemistry at Gymnasium Haus Overbach are given the opportunity to attend expert talks that take the form of a normal lesson. On 4 July 2018, scientists from IEK-3 spoke about the current state of the art in electrochemistry, hydrogen technologies, fuel cells, and electromobility.

- Conference of the episcopal academy of the diocese of Aachen

  Focusing on energy storage as the key to the Energiewende, the episcopal academy of the diocese of Aachen held a conference on 10–11 November 2018 for members and friends of the German Association for the Promotion of Solar Power (SFV) on how energy can be secured in future from the sun and wind through suitable storage systems. One of the presentations was given by Dr. Peter Stenzel from IEK-3.

2.2.3 Collaboration with other organizations

Work on creating and implementing further education and training and continuing professional development in the field of fuel cell and hydrogen technology is expanding at the same pace as applications with fuel cells and hydrogen infrastructures are being launched on the market. This development is proceeding at a rapid pace in response to growing interest in expertise in the areas of fuel cells and hydrogen on the part of the manufacturing industry and the relevant educational establishments. In order to cater for this demand, special initiatives have been launched. The combination of specialist knowledge and existing opportunities provides an excellent basis for collaboration.

- Involvement in the Fuel Cells Qualification Initiative (IQ-BZ), which aims to implement information and training measures for fuel cell and hydrogen technologies.
- Promotion and sale of a “Fuel Cells” CD-ROM through the Federal Technology Centre for Electrical Engineering and Information Technology (Oldenburg) and Vogel Industrie Medien GmbH (Würzburg) to provide information, increase the acceptance of fuel cells, and promote further training and education.
- Involvement in the school student competition “Fuel Cell Box”, organized annually by the EnergyAgency.NRW: assessment of the theoretical and practical results of 20 teams of

students in the final round of the competition. Fig. 4 shows the winning teams of 2017 and 2018 holding their certificates together with the organizers.

Fig. 4: Group photos of the winning teams of the 2017 (left) and 2018 (right) competitions

- Assessment of the theoretical and practical results of work in the disciplines of technology, the working world, and geo- and space science in the regional heat of the young scientists' competition "Jugend forscht, Schüler experimentieren", which takes place once a year at Forschungszentrum Jülich.

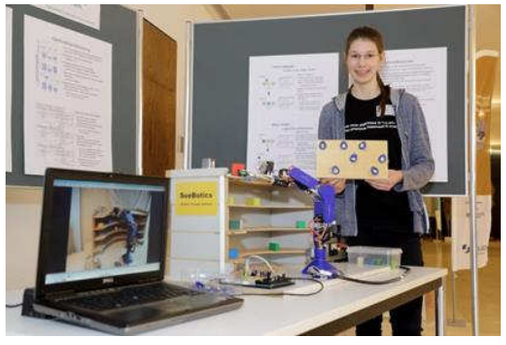

Fig. 5: Winners of the 2017 regional heat of "Jugend forscht"

In 2017, Susanne Rütten from Linnich, from the secondary school Gymnasium Haus Overbach (see Fig. 5) won the regional heat of "Jugend forscht" in the category of the working world. She impressed the jury with her work on effectively utilizing storage capacity by employing a microcontroller-controlled robot. By storing information on free space and used space as well as autonomously putting goods away or fetching them, the robot can fill and manage a chaotic warehouse or storage facility.

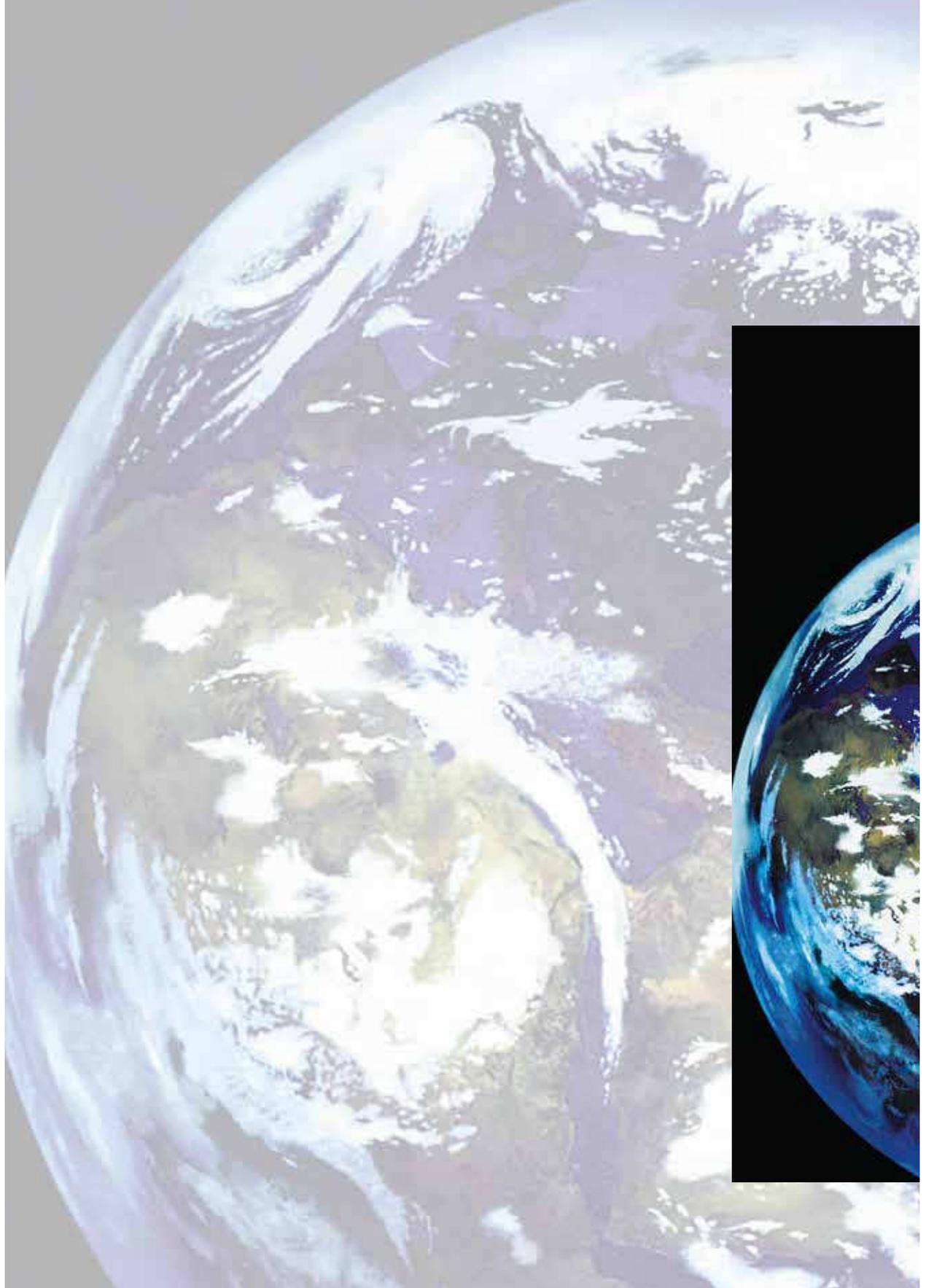

3

Reports

Scientific and Technical Reports

- Solid oxide converters
- Fuel processing and systems
- Polymer electrolyte fuel cells
- Direct methanol fuel cells
- Water electrolysis
- Process and systems analysis
- Physicochemical principles/ electrochemistry

3.1 Solid-oxide converters

3.1.1 Objectives and fields of activity

Cells, components, stacks, and systems are developed within the program topic of high-temperature solid oxide fuel cells (SOFCs) as well as high-temperature solid oxide electrolysis (SOE). The strategic aim of this topic is to provide electrical energy in a highly efficient manner for mobile and stationary applications – both distributed and centralized – on a scale ranging from a few kilowatts to several hundred kilowatts. Work focuses on increasing power density, improving lifetimes, identifying – and preventing – degradation mechanisms in the stack, advanced design, and highly integrated system engineering. The results of this development work encompass materials for cells, thermomechanically improved stacks, and highly integrated system components, as well as demonstration plants. Important supporting activities include the modeling of mechanical and thermal component loads as well as the development and characterization of components for fuel cell systems and their evaluation using process engineering analyses.

3.1.2 Important results

3.1.2.1 Development of lightweight cassette stacks

Alongside F-design-based stack development activities for stationary applications, a lightweight cassette stack design is being developed with the specific aim of reducing manufacturing costs and improving dynamics. Based on experiences with the F-design, thermomechanical robustness was improved. This is a particularly important development, since heating times of 30 min and less are required, for example, for APU applications in vehicles. A known weakness of the cassette design is the insufficient lifetime of the silver solder currently used for soldering cells. By adapting the design, cells with glass ceramics, which exhibit much better long-term stability than the silver solder, were inserted into the frame. An initial 3-layer short stack was subjected to a total of 53 thermal cycles at various heating rates, with no deterioration of gas tightness observed[4]. A 5-layer stack (using a WPS protective coating to prevent chromium vaporization) has since been developed. Its cell voltage characteristics are shown in Fig. 6. A stability test was conducted over approx. 1000 h (see Fig. 7).

[4] Ludger Blum et al., SOC Development at Forschungszentrum Jülich, ECS Transactions, 78 (1) (2017) 1791-1804

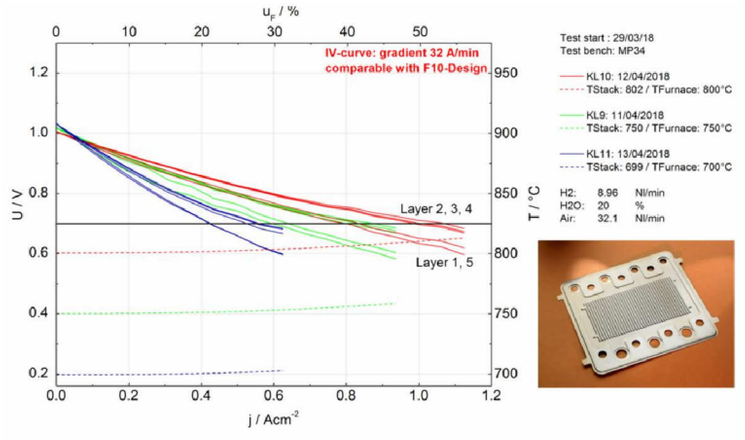

Fig. 6: **Performance of 5-layer cassette stack CS^{V}05-05 with humidified hydrogen in a direct current arrangement at various furnace temperatures**

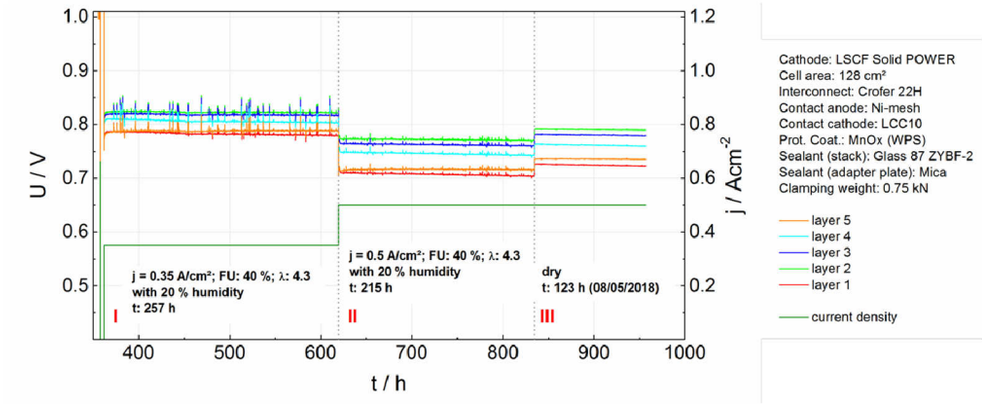

Fig. 7: **Voltage of the 5-layer cassette stack CS^{V}05-05 with dry hydrogen in a direct current arrangement at a furnace temperature of 700 °C, a current density of 0.375 A/cm² and 0.5 A/cm², and fuel utilization of 40 %.**

Thermal cycles were subsequently run with heat being increased from 200 °C to 650 °C within 100 min (and to 700 °C within 160 min). After the first 5 cycles, the stack was cooled to room temperature, removed from the test stand, and subjected to a tightness test: the stack exhibited internal and external tightness. It was then subjected to further thermal cycling. By the end of 2018, a total of 178 cycles had been realized. During this time, the open-circuit voltage (a measure for internal tightness) had not changed (see Fig.8, left). A characteristic curve was measured after each time the stack was heated. The cell voltage values at 0.35 A/cm² are plotted on the right-hand side in Fig.8. After an initially steep drop in voltage, the impact of cycling on cell voltage became increasingly less. In total, the voltage drop amounts to less than 0.02 % per cycle. The fact that layer 1 (red dots) has a much lower voltage is essentially due to the lower temperature caused by the loss of heat via the base of the furnace. The cycling continues to be performed.

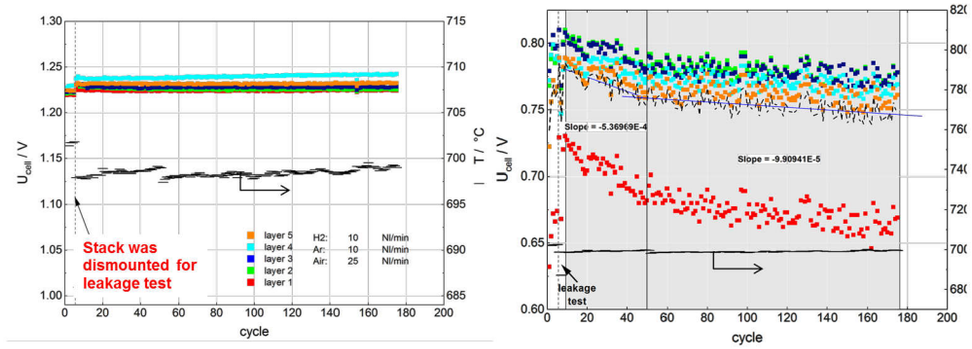

Fig.8: Thermal cycling of 5-layer cassette stack CS^{V}05-05: Left – OCV over 178 thermal cycles; right – cell voltages at 0.35 A/cm² (u_F 40 %) over 178 thermal cycles, eachmeasurement made at 700 °C and with the use of dry hydrogen

3.1.2.2 Short-stack test at 500 °C

Cell development in the past focused on demonstrating the basic functionality of materials and the interaction of materials during the production and operation of the cell. Building on this, work then concentrated on topics such as degradation and the scaling of component fabrication.

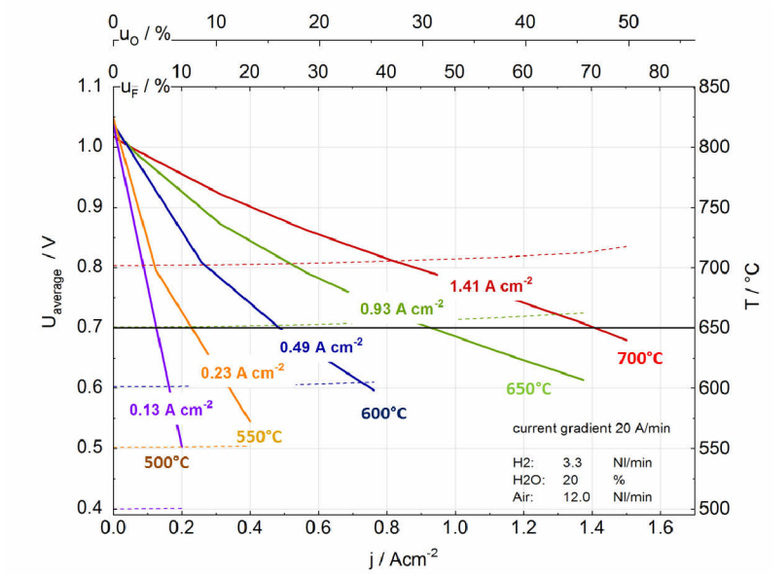

Fig. 9: Characteristic curves of a 3-layer short stack (F1003-02) between 500 °C and 700 °C

Below conventional application temperatures for ASCs (650–800 °C), cell development for a low-temperature SOFC (~ 400–500 °C) is focused on the production of thin electrolyte layers and verifying that the deposition of these layers can take place in a reliable and reproducible manner, and that they can be scaled to the size of cell stacks. To this end, their electrochemical performance should be higher than that of standard cells. This work led to 8YSZ layers with a thickness of 1 µm (development work at IEK-1). Their functionality was demonstrated using a short stack with 10 x 10 cm² cells up to a temperature of 500 °C (see Fig. 9). The stack exhibits the best performance ever measured at Jülich. However, a large gap was found between cell performance and the performance of the stacks. A significant problem is the drastic increase of contact resistance at low temperatures. An evaluation of the underlying mechanisms is a major priority for future work.

3.1.2.3 kW-class stacks with a window-pane design

Forschungszentrum Jülich has modified the design of the kW class towards what is referred to as a window-pane design, in which four 10 x 10 cm² cells are incorporated into one layer. This enables the integration of standard-sized cells from various suppliers. When using the same type of cell, the performance of the window-pane stack design is comparable to that of a short stack with just one cell per layer (see Fig. 10).

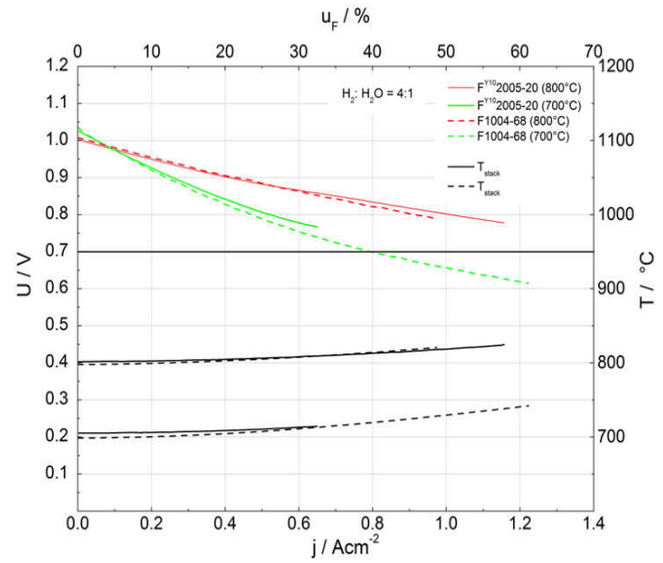

Fig. 10: Comparison of the characteristic curves (average stack voltage) of a F1004-68 short stack (dashed line) with one cell per layer with those of a stack with four 10 × 10 cm² cells per layer (F^{Y10}2005-20)

To achieve the next development goal – the realization of stacks with a performance of at least 15 kW_{DC} – the design of the gas diffusers was adapted in such a way that 120 layers were stacked on top of each other. The design was further adjusted to reduce manufacturing costs and to facilitate the assembly of the stacks. The 5-layer stack F^{Y10}2005-21

demonstrated a good performance, with the exception of layer 1, which exhibited a contact problem particularly at lower temperatures (see Fig. 11).

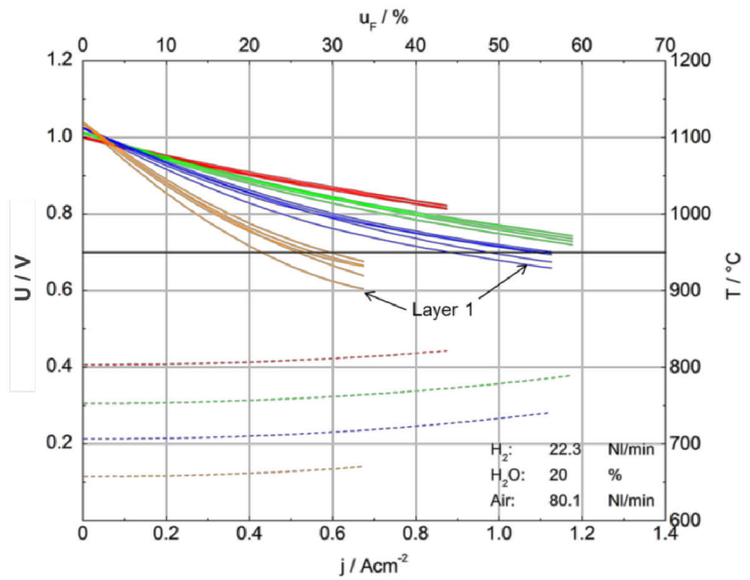

Fig. 11: Performance curves of the 5-layer stack F^{Y10}2005-21, measured at a furnace temperature between 650 °C and 800 °C with humidified hydrogen

3.1.2.3.1 Thermomechanical properties: thermal cycling

In previous investigations, a 5-layer stack with a window-pane design exhibited very good temperature change behavior[5]. A slightly modified design, which enables the stacking of 120 layers and is easier to manufacture, was also subjected to a temperature change test. The tested set-up consists of two 5-layer substacks stacked on top of each other and sealed against each other with a compressive mica seal. This set-up is in line with the design concept for larger stack units. The F^{2S}2010-18 stack is cycled at a rate of 3 K/min at a temperature between 200 °C and 700 °C. Fig. 12 shows the OCV with dry hydrogen as a function of the number of cycles. The tests begin with very high OCV values between 1.23 V and 1.30 V. Between the 20th and 60th cycle, layers 2, 6, 7, and 8 exhibit decreasing OCV. After 80 cycles, however, the voltages are still above 1.15 V, which is sufficient for reliable operation (a voltage of at least 1.10 V is the target value). In Fig. 13, the voltage curves at 0.5 A/cm² are shown (corresponding to an overall performance of 1.25 kW), measured at 700 °C after each thermal cycle. There is no decline in OCV observed here. A similar development is seen for all layers, with voltage decreasing by approx. 0.02 % per cycle.

[5] Ludger Blum et al., SOC Development at Forschungszentrum Jülich, ECS Transactions, 78 (1) (2017) 1791-1804

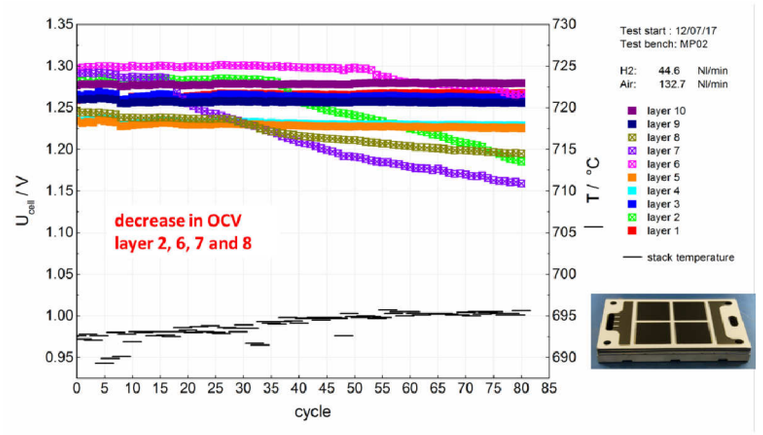

Fig. 12: F[2S]2010-18 stack consisting of two 5-layer substacks: Temperature change between 200 °C and 700 °C, heating rate of 3 K/min – OCV with dry hydrogen as a function of the number of cycles

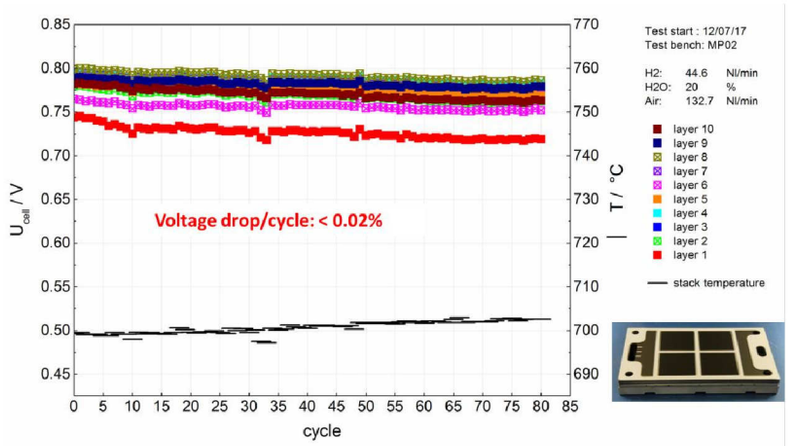

Fig. 13: F[2S]2010-18 stack consisting of two 5-layer substacks: Temperature change between 200 °C and 700 °C, heating rate of 3 K/min – cell voltage with humidified hydrogen at 0.5 A/cm² as a function of the number of cycles

3.1.2.3.2 5 kW Stack

To achieve the next development goal – the realization of a reversible 5 kW SOC system (rSOC) – four 10-layer substacks were manufactured and pre-tested as parts of the 5 kW stack. All substacks exhibited very similar behavior, as can be seen in Fig. 14. Fig. **15** shows the voltage and power of the 40-layer 5 kW stack (F[4S]2040-01) during operation with hydrogen and with methane (steam-to-carbon ratio of 2 with 10 % prereforming) in a direct current configuration.

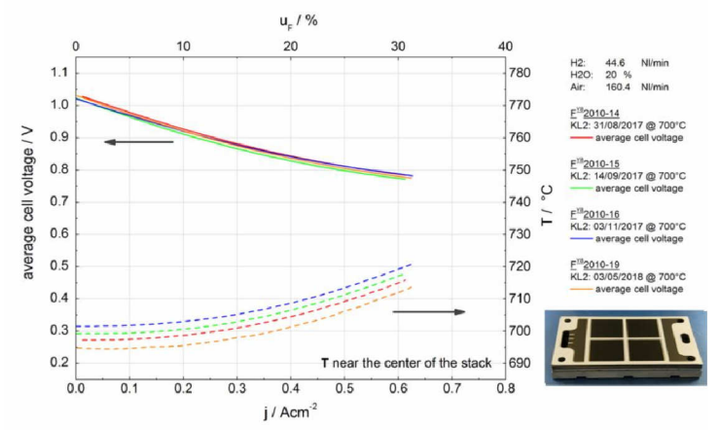

Fig. 14: Performance of four 10-layer F[Y8]2010-14/15/16/19 substacks with humidified hydrogen in a direct current arrangement at a furnace temperature of 700 °C.

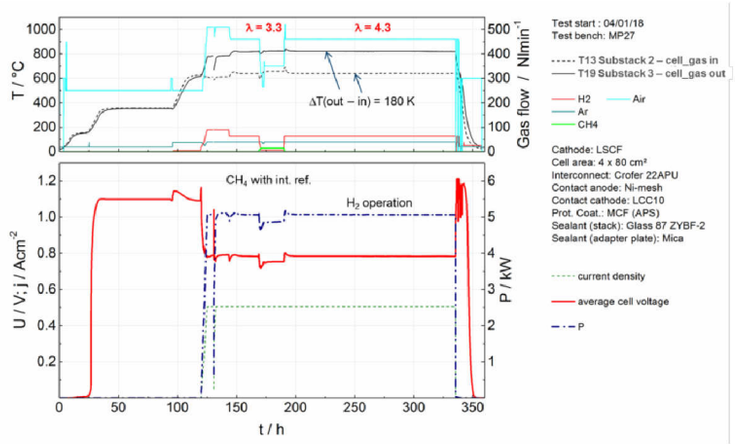

Fig. 15: Average cell voltage and power of F4S2040-01, comprising four 10-layer substacks (FY82010 type) with humidified hydrogen or methane in a direct current arrangement in thermal insulation at an average stack temperature of 700 °C, current density of 0.5 A/cm², and fuel utilization of 70 %.

The stack was operated with thermal insulation provided by a 10-cm-thick microporous material and was heated with preheated air and fuel to an average stack temperature of 700 °C. The stack was operated at a fuel utilization of 70 % and a current density of 0.5 A/cm², achieving 5.1 kW with hydrogen and 4.9 kW with methane and internal reforming. The temperature difference in the solid between the inlet and the outlet amounted to 180 K with excess air of 4.3.

3.1.2.3.3 SOE – High-temperature electorlysis

A solid oxide cell (SOC) short stack comprising two ASCs (anode in fuel cell mode) was operated at temperatures of 700 °C, 750 °C, and 800 °C, a current density of -0.5 A/cm², and a steam utilization rate of 50 % with 50 % humidified H_2 in electrolysis mode. The stack was

also briefly operated in fuel cell mode at 800 °C for one phase of approx. 1500 h without any noticeable deterioration. The entire operation is shown in Fig. 16.

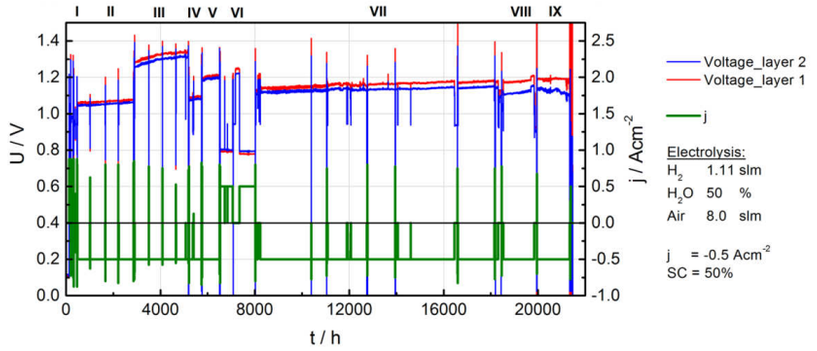

Fig. 16: Long-term operation of the F1002-165 stack at various operating temperatures in electrolysis mode (phases I–V, and VII–IX) and fuel cell mode (phase VI) (H_2O: H_2 = 1:1). Electrolysis mode: -0.5 A/cm², 50 % steam utilization; fuel cell mode: +0.5 A/cm², 50 % fuel utilization

During the first 8000 h of operation, there was almost no deterioration in the gas tightness of the stack and/or cells. The average ASR degradation rates were uniform at roughly 10 %/kh for three temperatures. From 8000 h onwards, the voltage and ASR degradation rates for the next 10,000 h of electrolysis at 800 °C were approx. 0.4 %/kh and 2.7 %/kh, respectively. After 10,000 h of continuous operation, the OCVs of the cells with dry H_2 fell from over 1.2 V to 1.1 V, which later transpired to be a result of a leak in the test stand (leak rate ≤ 3 %). For the 18,460 h of operation before the start of the strong leakage in layer 2, the average degradation rates of the stack – including the losses during all load cycles and the brief operation in fuel cell mode for 1500 h – amounted to 0.6 %/kh for the voltage and 8.2 %/kh for the ASR at a temperature of 800 °C. Impedance measurements and DRT analysis revealed that the main mechanism of degradation was the continuously increasing ohmic resistance, which was mainly due to a decline in the effective conductivity of the fuel cell electrode resulting from Ni depletion in the functional layer of the electrode (see Fig. **17**). This was confirmed by a post mortem analysis (see Fig. 18). Compared with the rise in ohmic resistance, the deterioration in the polarization of the electrodes was practically negligible. During stationary operation, however, a continuous slight increase in polarization in the air electrode was observed. Delamination of the air electrode was also observed after operation in both layers. It is difficult to prove whether the slightly increased polarization of the air electrode is linked to the delamination, since the delamination of the air electrode can also be caused by resin infiltration during post-test preparation. A preliminary post mortem analysis did not reveal any process that significantly influenced stack performance, with the exception of Ni depletion in the functional layer of the fuel cell electrode. Detailed analyses of the cells are currently being performed. The leak rate in layer 2 increased dramatically during the last 2600 h of operation, most likely due to the fire on the fuel inlet side in the stack. The exact correlations have yet to be confirmed, however.

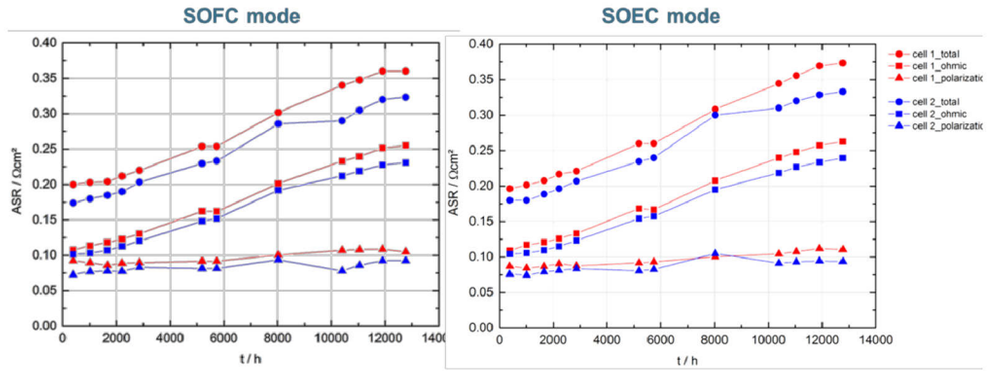

Fig. 17: **F1002-165: ASRs based on Nyquist plots – Ohmic resistance increases continuously (9 ~ 10 %/1000 h), while the polarization remains almost constant.**

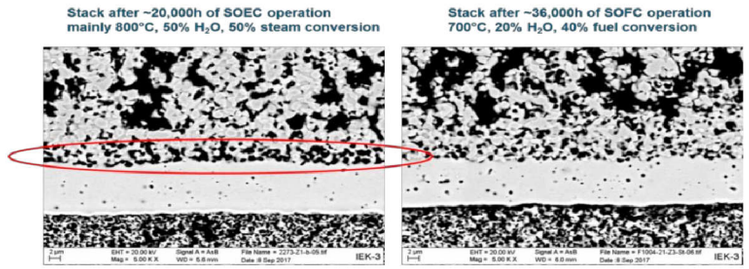

Fig. 18: **Ni depletion at the electrolyte/fuel cell electrode interface during SOEC operation was the main reason for the deterioration of ohmic resistance**

3.1.2.4 System Engineering

System development of 5 kW rSOC

In the last two years, a reversible 5 kW solid oxide cell (rSOC) system was developed. One of the main advantages of the rSOC system is that the same SOC stack can be used as the electrolyzer (SOEC) and as a fuel cell (SOFC). This is ideal for managing the temporal discrepancy between energy demand and supply in systems producing electricity from renewable energy, such as photovoltaics and wind power. In situations of surplus energy, the system can be operated as an electrolyzer, with steam being electrolyzed into storable hydrogen. When electricity is required at a later point in time, the system can be operated in fuel cell mode (SOFC), with electricity being produced from the stored hydrogen. A simulation model of the rSOC system was developed based on experimental data from previous SOFC stack tests and other previous component tests. A plant was developed that is capable of supplying the stack with hydrogen, steam, and air, depending on the mode of operation (Fig. 19).

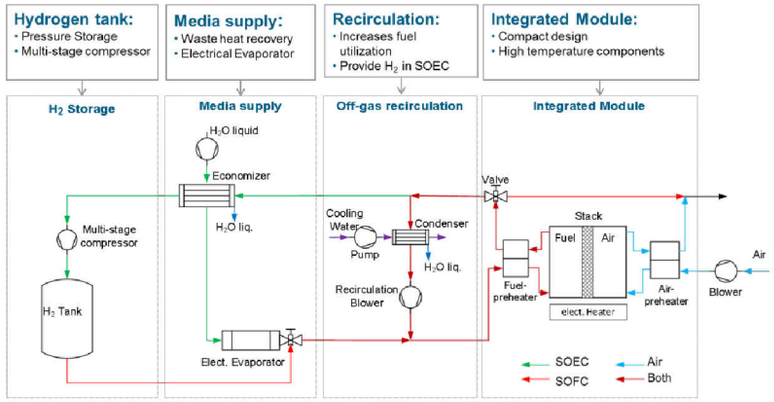

Fig. 19: Flow diagram of rSOC system

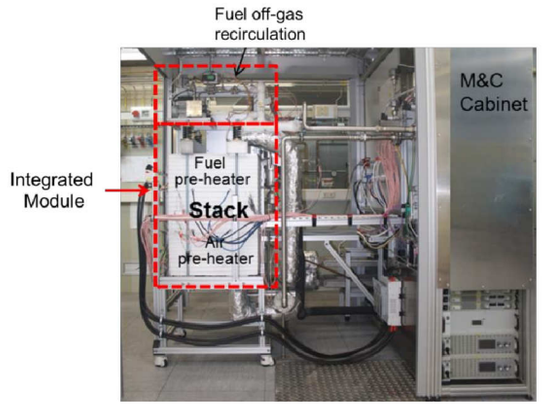

Fig. 20: Image of rSOC system

It is important that the steam required for electrolysis mode is produced in the plant so that no external steam is necessary. To increase the efficiency of both modes of operation, various rSOC concepts were developed and compared. In terms of heat management, a detailed analysis of waste heat recovery was conducted for the entire plant. In both modes of operation, off-gas recirculation was investigated at low temperatures (below 100 °C). The analysis revealed that the condensation in the recirculation loop has many advantages. In SOFC mode, anode off-gas recirculation enables the system to achieve increased fuel utilization in comparison to a plant without recirculation. At a very high recirculation degree of above 90 %, a low level of fuel utilization in the stack is possible. This has two positive effects: Firstly, the air flow required for cooling is reduced due to the significant cooling caused by the anode current. Secondly, the Nernst potential increases due to the increased hydrogen content. This enables a net electrical efficiency of over 60 %. In SOEC mode, the recirculation of hydrogen prevents the degradation of the Ni electrode and limits the use of stored hydrogen to just the start-up phase. If no additional heat or steam is accrued from external processes, net efficiency – in relation to the heating value – in electrolysis mode is around 75 %.

The system (Fig. 20) (without feedwater heater and hydrogen tank) was put into operation in November 2018. In fuel cell operation mode using hydrogen, a net DC efficiency of 62 % was achieved (if taking into account an inverter with 95 % efficiency, this corresponds to a net electrical AC efficiency of 59 % for the system). This was achieved through a high anode off-gas recirculation rate, which led to system fuel utilization of over 97 %.In electrolysis mode, with an electrical input into the system of 14.9 kW, 4.75 Nm³ hydrogen per hour was produced. This corresponds to a system efficiency of 70 %. The system continues to be operated in toggle mode to optimize operating behavior and systems control, and to analyze ways of further increasing efficiency.

3.1.3 Staff members and fields of activity

Name	Tel. (02461-61-) Email	Fields of activity
Prof. L. Blum	6709 l.blum@fz-juelich.de	Head of solid oxide converters
R. Deja	5291 r.deja@fz-juelich.de	System simulation, development and testing of SOC system components
Dr. Q. Fang	1573 q.fang@fz-juelich.de	Head of SOC electrochemical measuring technology, testing of SOC stacks, test evaluation and analysis
K. Fitzek	1573 k.fitzek@fz-juelich.de	SOC, electrochemical measuring technology, testing of SOC stacks and test evaluation
M. Frank	4394 ma.frank@fz-juelich.de	System simulation, development and testing of rSOC system concepts
I. Hoven	4053 i.hoven@fz-juelich.de	Electrical engineering, measurement data acquisition, and systems control
Dr. V.N. Nguyen	8393 v.n.nguyen@fz-juelich.de	Chemical process engineering, development and testing of system components
Fr. U. de Haart	5170 u.de.haart@fz-juelich.de	Testing of SOC stacks, test evaluation, and analytics
Ro. Peters	4664 ro.peters@fz-juelich.de	Head of SOC systems engineering, component development, system design, system engineering and system testing, CFD, component modeling
Y. Yan	5487 y.yan@fz-juelich.de	SOC, electrochemical measuring technology, testing of SOC stacks and test evaluation

3.1.4 Important publications, doctoral theses, and patents

Nguyen, V.N., Deja, R., Peters, Ro., Blum, L., Stolten D.
Study of the catalytic combustion of lean hydrogen-air mixtures in a monolith reactor
International Journal of Hydrogen Energy 43 (36), (2018) 17520-17530

Frank M., Deja R., Peters Ro., Blum L., Stolten D.
Bypassing renewable variability with a reversible solid oxide cell plant
Applied Energy 217 (2018) 101–112

Preuster, P., Fang, Q., Peters, R., Deja, R., Nguyen, V.N., Blum, L., Stolten, D., Wasserscheid, P.
Solid oxide fuel cell operating on liquid organic hydrogen carrier-based hydrogen – making full use of heat integration potentials
International Journal of Hydrogen Energy 43(3) (2018) 1758-1768

Kennouche, D., Fang, Q., Blum, L., Stolten, D.
Analysis of the cathode electrical contact in SOFC stacks
Journal of the Electrochemical Society 165(9) (2018) 677-683

Fang, Q., Frey, C.E., Menzler, N.H., Blum, L.
Electrochemical performance and preliminary post-mortem analysis of a solid oxide cell stack with 20,000 h of operation
Journal of the Electrochemical Society 165(2) (2018) 38-45

Fang Q., Blum L., Menzler N.H., Stolten D.
Solid Oxide Electrolyzer Stack with 20,000 h of Operation
ECS Transactions 78 (1) (2017) 2885-2893

Peters Ro., Engelbracht M., Tiedemann W., Hoven I., Deja R., Nguyen V. N., Blum L., Stolten D.
Development and Test of a Solid Oxide Fuel Cell Subsystem with a Low Temperature Anode Off-gas Recirculation
ECS Transactions, 78 (1) (2017) 2489-2495

Yan Y., Fang Q., Blum L., Lehnert W.
Performance and degradation of an SOEC stack with different cell components
Electrochimica Acta 258 (2017) 1254-1261

Blum, L.
An Analysis of Contact Problems in Solid Oxide Fuel Cell Stacks Arising from Differences in Thermal Expansion Coefficients
Electrochimica Acta 223 (2017) 100-108

Engelbracht M., Peters, Ro., Blum, L., Stolten D.
An On-Demand Safety Gas Generator for Solid Oxide Fuel Cell and Electrolyzer Systems
Fuel Cells, 17 (6) (2017) 882-889

3.2 Fuel Processing and Systems

3.2.1 Objectives and fields of activity

The availability of hydrogen is fundamental to the use of fuel cells in mobile and stationary applications. One option for passenger cars, buses, and fleets of vehicles in the delivery sector is to combine electric motors with hydrogen-powered fuel cells. However, the infrastructure for hydrogen as a future energy carrier must first be established. In future, hydrogen will be produced from renewable and solar power using electrolysis. With a pressure tank of 700 bar, a range of approx. 350–400 km can be achieved. Such ranges are insufficient for trucks, ships, and aircraft. Due to the poor storage properties of liquid and gaseous hydrogen compared to today's fuels (i.e. gasoline, kerosene, and diesel), liquid fuels are preferable for the aforementioned areas of application. The tank system as a whole with its mass- and volume-specific power densities must be considered in analyses. The aforementioned energy carriers are mainly produced today from the fossil primary energy carrier crude oil. In the long term, some of the liquid energy carriers currently required could be produced from biomass or synthesized from carbon dioxide and hydrogen.

Carbon dioxide from industrial off-gases and renewable hydrogen represent the basis for the production of electrofuels, a process often termed "*Power-to-Fuel*". Potential fuels include n-alkanes from Fischer–Tropsch synthesis, alcohols, various ethers and n-alkanes, cycloalkanes, and aromatics from an oligomerization process. In addition to using hydrogen for fuel cell vehicles, this represents a further integration of renewable energy in the transport sector – and a reduction of our dependence on oil. Renewable hydrogen can thus also find its way into goods and passenger transport using ships, aircraft, and trucks. Synthetic fuels also allow engine efficiencies to be improved and limited emissions to be reduced.

Fuel cells are not available in the power classes needed for drives in maritime applications or aviation (i.e. larger than 1 MW_e). In driving mode, the diesel engines used in the truck sector are extremely efficient and have a high mass- and volume-specific power density. When idling, a power of 3–5 kW_e is generated to operate air conditioning or electrical heating as well as to power electrical devices on board. Under these load conditions, diesel engines have an efficiency of only 10–15%. In aviation, on-board power on the runway and sometimes at the gate is generated by auxiliary power units with efficiencies of approx. 20%.

At IEK-3, research in the field of fuel processing is focused on reforming middle distillates, the desulfurization of kerosene, and system development for on-board power supply in combination with HT-PEFCs. Reformers are also being developed for high-temperature SOFCs. All areas of work are supported by relevant modeling. Important tools include CFD simulations on the institute's own cluster and system simulations using the Simulink program to optimize the dynamic performance under load changes and for starting strategies. In future, the use of PEFCs will form the focus of power supply systems.

3.2.2 Important results

3.2.2.1 Development of the next reactor generation for autothermal reforming

In the IEK-3 Report 2017, the ATR 12 was presented in detail, including a description of how it functions and its technological innovations. To summarize again, the technical design of

the superheater in the ATR 12 was modified in such a way that the previously used pipe coil for the transfer of waste heat from the reformate to the mass flow of saturated steam was replaced by concentric shells. This modification results in a reduction of the pressure drop in this part of the reformer and a homogenization of the media flows. The concentric shells also offer sufficient space for an electric heating wire to be integrated. The integration of such a heating element permits the reformer to be started up in a quick and autonomous manner. This brief description can now be expanded to include a number of interesting experimental results. Fig. 21 shows the volume flows of air, the mass flow of water, and the temperatures in the vaporization chamber and the mixing chamber during the start-up process of the ATR 12 as a function of time. To begin with, the control variable of the heating wire was set to 550 °C for the volume flow of air upon entry in the vaporization chamber (3 m^3 h^{-1}). Previous measurement series had shown that lower control variables do not lead to sufficiently high temperatures at all relevant positions within the ATR 12. The heating process – from room temperature to 550 °C – took 27 min and led to temperatures of 421 °C in the vaporization chamber and 442 °C in the mixing chamber of the ATR 12.

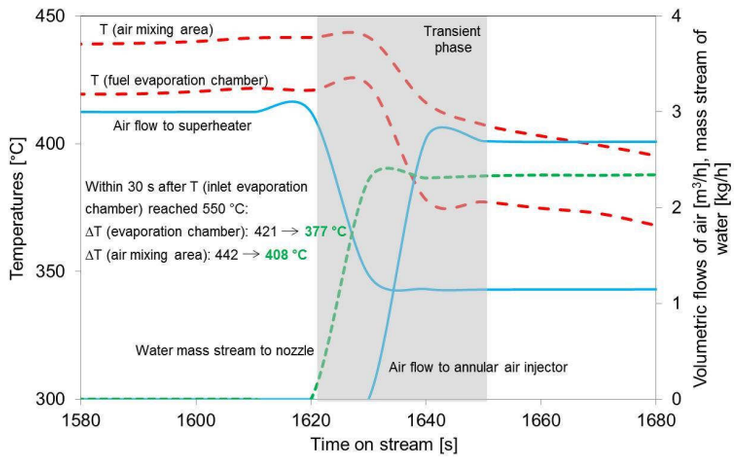

Fig. 21: Volume flows of air, mass flow of water, and temperatures in the vaporization chamber and the mixing chamber during the start-up process of the ATR 12 as a function of time.

Immediately after the control variable was reached, a water mass flow of 2.34 kgh^{-1} was added. A few seconds later, the air flow was distributed to the air pathway (70 %) and the superheater (30 %). This transient phase, in which constant volume and mass flows set in and the temperatures stabilized, lasted around 30 s. During this phase, the temperatures in the vaporization chamber and the mixing chamber fell to 377 °C and 408 °C, respectively. However, the temperatures were high enough that when diesel fuel was added immediately afterwards, the complete vaporization of this fuel was ensured – an absolute prerequisite for stable reformer operation without catalyst ageing. The experimental procedure described above is therefore suitable for a rapid start-up of the ATR 12.

3.2.2.2 Development of the next reactor generation for the water–gas shift reaction

The water–gas shift reactor (WGS) in the fuel processing unit of a fuel cell system has the important function of reducing the concentration of CO in the product gas of the autothermal reforming process to values between 1.0 vol% and 1.5 vol% in order to protect the catalyst in the anode of the fuel cell against irreversible poisoning. In this chapter, IEK-3's latest development in this field is introduced, the WGS 6 in the 5 kW_e class. The WGS 6 is distinguished by a fundamental new concept for the arrangement of high-temperature shift (HTS) and low-temperature shift (LTS) stages. Both stages are now coaxially integrated into a joint housing to obtain higher power density and specific power values. In previous reactor generations, these stages had been arranged in parallel. Fig. 22 shows a schematic view of the new concept for the arrangement of the shift stages.

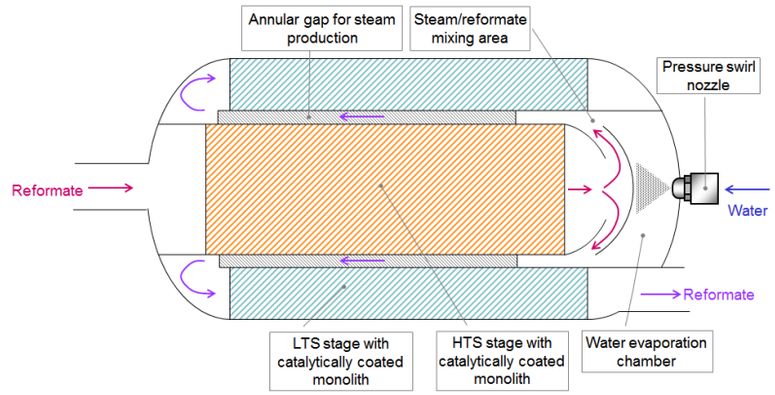

Fig. 22: Schematic concept for the arrangement of high-temperature and low-temperature shift stages in the WGS 6

The reformate from the autothermal reformer (approx. 400 °C) flows into the HTS monolith whose catalytically active layer with a washcoat and noble metal particles helps to reduce the concentration of CO. The hot molecules in the reformate (450 °C) then impact on the underside of a hemispherical impingement area, the upper side of which is injected with a fine mist of water droplets (20 °C) using a nozzle. By means of the impingement area, the enthalpy flow of the hot reformate is then transferred to the cold water droplets. A small proportion of the droplets thus vaporize immediately, while the biggest proportion forms a film on the surface of the impingement area. This film then moves into the annular gap between the HTS and LTS stages. The water film then fully vaporizes and mixes homogeneously with the reformate. At the end of the annular gap, the reformate flow (300 °C) is again redirected by 180 ° and flows into the LTS stage, where the concentration of CO in the reformate is further reduced to values between 0.8 vol% and 1.5 vol%, as shown in Fig. 23. The figure clearly shows that the concentration of CO in the product gas of the WGS 6 remained between these two values for the entire duration (5000 h) of the experiment. To realize the long duration of this experiment, catalysts were regularly regenerated in a hot air flow. The figure only shows a few of these regeneration points. The above-described novel design of the WGS 6 results in a power density of 12.2 kWL^{-1} and a specific power of 11.2 $kWkg^{-1}$. These values are twice as high as those that were achieved for previous reactor generations. Based on the experimental results and the specific reactor data, it can be concluded that the

WGS 6 is suitable for continuous operation in a commercial fuel cell system dedicated to efficient and sustainable energy conversion.

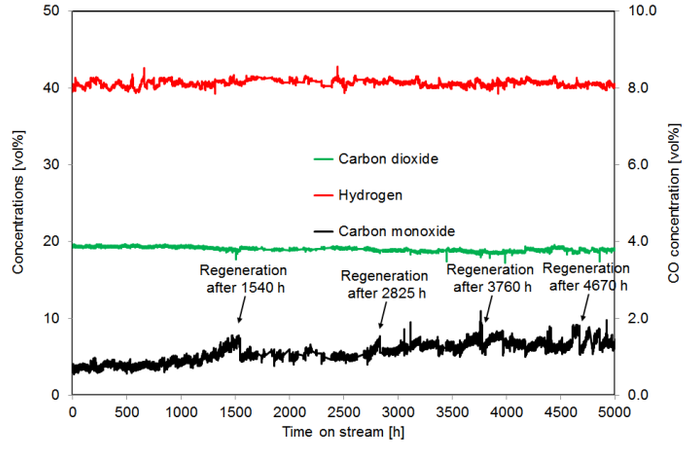

Fig. 23: Concentrations of H_2, CO_2, and CO achieved by the WGS 6 during a long-term experiment for a water–gas shift reaction over 5000 h.

3.2.2.3 Experiments on Pd/γ-Al_2O_3 catalysts for CH_4 oxidation by temporal analysis of products (TAP)

Natural-gas-powered passenger cars and trucks are gaining increasing significance, since – compared with petrol- or diesel-powered cars – they emit relatively low amounts of critical exhaust gases into the environment. However, methane slip, which is caused by the incomplete combustion of methane in engines, requires catalytic exhaust gas aftertreatment for a natural-gas-powered car. Methane has a very high potential (greenhouse warming potential of 28) to act as a climate-damaging greenhouse gas and must not, therefore, be emitted into the environment. It is known from the literature that palladium is the most active catalyst for the oxidation of methane in the temperature range between 200 °C and 500 °C. Previous investigations have shown that catalytic activity is dependent on the relationship between elementary palladium and oxidic palladium species on the catalyst surface. In the series of experiments described here, the catalysts are investigated without special pretreatment (as received) as well as after oxidative and reductive conditioning. The approach of the experiments, which are carried out in collaboration with Forschungszentrum Jülich's Central Institute of Engineering, Electronics and Analytics – Analytics (ZEA-3), is to combine ambient pressure X-ray photoelectron spectroscopy (AP-XPS) with transient kinetic experiments using the temporal analysis of products (TAP) technique. Following this approach, relationships will be explored between the chemical and the electronic state of the catalyst and its catalytic activity for methane oxidation. The TAP experiments with the non-pretreated Pd/γ-Al_2O_3 catalyst revealed an increasing conversion of methane with increasing temperature. At 200 °C, conversion was relatively low at around 14 %. At 250 °C, it increased to around 43 %, and at 300 °C, it increased further still to 87 %. At temperatures of 350 °C and 400 °C, the methane conversion was almost complete. The activation energy for methane oxidation was calculated to be approx. 92.5 $kJmol^{-1}$. It must be noted that these experiments were conducted without the addition of O_2, meaning that the oxidation reactions

were only made possible through chemisorbed O_2 species on the catalyst surface. Fig. 24 shows the outlet intensities of the CH_4 pulse at 350 °C when CH_4 was almost fully converted. All signals are very similar to each other and therefore easily reproducible, with their average being used for the conversion calculation. The pulse outlet intensities for the two reaction products, CO and CO_2, from the same series of experiments suggest that CO was formed more selectively at lower temperatures between 200 °C and 300 °C, while CO_2 occurred more strongly at temperatures of 350 °C and 400 °C. Furthermore, the outlet intensities for CH_4, CO, and CO_2 provide indications that CH_4 decomposed on the catalyst and carbonaceous deposits possibly formed on the catalyst surface. Additional experiments on the adsorption/desorption of CO and CO_2 on the Pd/γ-Al_2O_3 catalyst – without methane being simultaneously pulsed – demonstrated that CO and CO_2 only desorb in small amounts from the catalyst surface in the temperature range between 200 °C and 400 °C. Both molecules are very strongly bound to the active centres. The as-yet incomplete AP-XPS experiments will provide information about which Pd species (metallic or oxidic) exist on the catalyst surface under these reaction conditions and what their numerical ratio is, as well as whether and how these results correlate with catalytic activity.

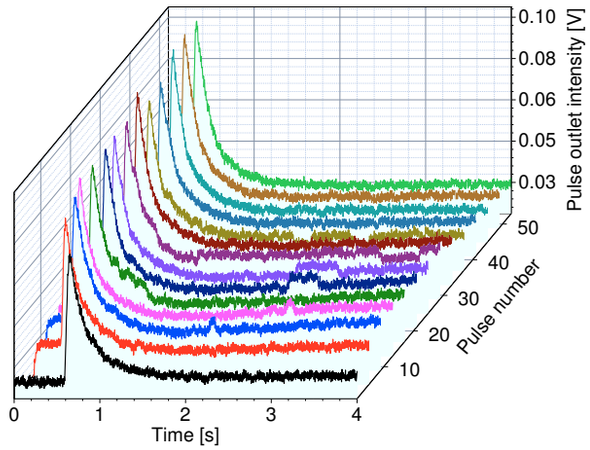

Fig. 24: Outlet intensities of the CH_4 pulses during the oxidation of CH_4 on the Pd/γ-Al_2O_3 catalyst at 350 °C as a function of time and pulse number

3.2.2.4 Diesel reforming systems for on-board power supply

Jülich's fifth-generation fuel processing system (package 5) consists of the following core components: ATR AH3 for autothermal reforming, WGS 4 for the water–gas shift reaction, and CAB 3 for catalytic combustion. These components are complemented by a microstructure heat exchanger produced by the Institute for Micro Process Engineering at the Karlsruhe Institute of Technology (KIT – IMVT) as well as a commercial diesel burner made by Physitron GmbH. In addition, a customized shell and tube heat exchanger was developed at IEK-3 to ensure thermal feedback of the diesel burner's hot off-gases during system start-up. The entire system including insulation amounts to a volume of 74.1 l. Fig. 25 shows the fifth-generation fuel processing system.

Fig. 25: IEK-3's fifth-generation fuel processing system

Im Folgenden werden experimentelle Ergebnisse mit diesem System erläutert. Im ersten Teil wird die Startstrategie präsentiert. Im zweiten Teil folgt der stationäre Betrieb.

Start-up strategy for the fuel processing system

The aim of the start-up strategy is to heat the fuel processing system in the shortest time possible and with minimal energy expenditure, to put the reformer into operation, to switch off the external supply of energy, and to deliver the desired product gas quality for the fuel cell. Fuel processing package 5 has a thermal start-up system based on the use of a diesel burner. The heat of the burner's hot off-gases is initially transferred to the air in the downstream shell and tube heat exchanger. The heated air then preheats the reformer as well as the following downstream system components: WGS, micro heat exchanger, and CAB. After the dew point has been exceeded in all of the system's catalysts, the shell and tube heat exchanger is used as a vaporizer. For this purpose, the shell and tube heat exchanger has an integrated system for injecting liquid water. In the second phase of the start-up strategy, air continues to flow through the shell and tube heat exchanger together with water.

Critical parameters were identified during the first heating tests with the system. At a predefined operating time of 35 min for the diesel burner and a burner output of 8 kW, it was possible to switch to the specified start-up parameters 30 min after the start in order to subsequently begin the reforming process. Energy consumption was calculated at 3.3 kWh. During this test, the catalytic burner was found to be the component preventing a faster start-up procedure. The critical points in the system include the interface as well as the cooling concept between the shift stages, the micro heat exchanger as well as its interface to the shift reactor, and the pipe between the micro heat exchanger and the catalytic burner. Since it was found that the catalytic burner prevents a faster-start-up procedure, a decision was taken to respond to the latter of the critical points in order to reduce the start-up time. The first two critical points were caused by the design of the respective components and cannot be improved using systems technology methods.

Using a commercially available glow plug, integrated into the pipe of the catalytic burner, the above-mentioned heat sink was eliminated and the monolith of the catalytic burner was also

actively heated during the heating process. A second heating test using the glow plug revealed that the starting conditions were achieved after just 20 min. In the first series of tests without the glow plug, the start-up time was still 30 min. As a result of this measure, the limiting component in the system was now the reformer and no longer the catalytic burner. Using the accelerated heating process, the energy consumption of the diesel burner amounted to only 2.5 kWh. The electricity consumption of the glow plug was determined to be 106 Wh.

In a third test to validate the overall strategy, the diesel burner was operated with an output of 8 kW for a preprogrammed time of 25 min. As the diesel burner was put into operation, 12 $m^3_N h^{-1}$ of air was simultaneously fed into the system via the shell and tube heat exchanger. At 12 min after the start, the glow plug was put into operation with an output of 12.1 V and a current of 59.3 A. At the same time, an additional amount of air (10 $m^3_N h^{-1}$) flowed through the glow plug. As early as 18 min after the start, the temperature of the monolith in the catalytic burner amounted to 105 °C, far higher than the dew point. At this point in time, the supply of water to the shell and tube heat exchanger began. After 1 min, the glow plug was switched off and a conversion to the starting values occurred. For diesel this was 999 $g h^{-1}$, while water and air amounts were determined based on H_2O/C and O_2/C molar ratios of 1.9 and 0.47, respectively. A 30 % proportion of the entire amount of air was fed into the reformer through the steam pathway (via the shell and tube heat exchanger).

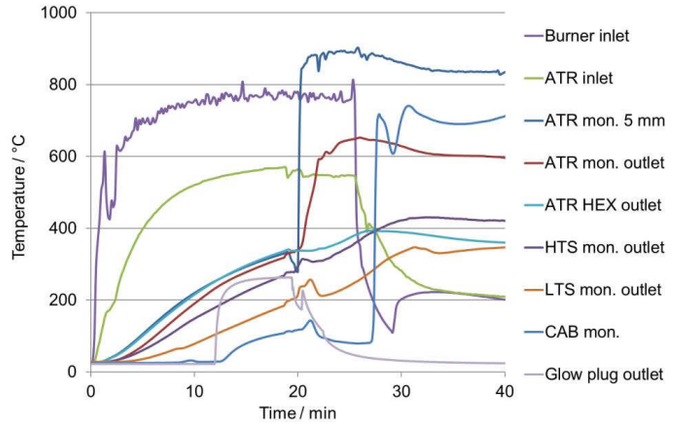

Fig. 26: Temperatures over time in the fuel processing system package 5

Fig. 26 shows a rapid temperature rise in the ATR monolith (5 mm behind the inlet) at this point in time. This increase in temperature is caused by the strongly exothermic oxidation reaction in the reformer. This indicates the beginning of the reforming process in the system. After an additional 3 min, the amount of diesel was increased to 1350 $g h^{-1}$. The maximum performance of the system, which is determined by the shift stages, was thus reached. At 25 min after the start, the supply of diesel to the diesel burner was stopped. After an additional 2 min, the provision of superheated steam for the reforming process was completely covered by the reformer and catalytic burner. Self-sufficient system operation was thus achieved after 27 min. After an additional 4 min, the concentration in the wet product gas was reduced to a value smaller than 1.2 (vol)%. At this concentration, the provided

reformate can be supplied to a high-temperature PEFC, in which electricity and heat are produced from hydrogen-rich reformate.

In summary, using the hybrid start-up strategy with the aid of a diesel burner and a glow plug, the maximum performance of the system was reached within 22 min after the start. In addition, self-sufficient system operation was achieved after 27 min. The start-up procedure was completed after 31 min, in which time a product gas of sufficient quality was produced for a HT-PEFC. This start-up time is in agreement with the 30 min objective set by the US Department of Energy (DOE)[6] for the year 2020 for diesel-powered fuel cell APUs for trucks in the 1–10 kW_{el} power class. During this start-up testing, the energy requirement of the diesel burner, which was calculated from the diesel consumption value, amounted to 2.5 kWh and the electrical energy consumption of the glow plug was 90 Wh.

Stationary operation of the system

In addition to optimizing and validating the system's start-up strategy, its stationary operation was also investigated and optimized. Strategies for the start-up, operation, shut-down, and regeneration of the system are based on the findings from a publication [7]and are not explained in more detail here.

During testing with the NeXBTL diesel fuel, it was shown that the system can be ideally operated at inlet temperatures of 356–400 °C for the high-temperature shift (HTS) stage and 320–330 °C for the low-temperature shift (LTS) stage in order to keep the CO concentration behind the LTS stage below 1.25 (vol)% in the dry product gas. The average CO concentrations were measured between 0.92 (vol)% and 1.2 (vol)%. The operating time was varied between 3 h and 24 h. The system was always operated at its maximum performance. An extreme case was thus simulated for the application of an on-board power supply. The O_2/C and H_2O/C molar ratios in the reformer remained constant at 0.47 and 1.9, respectively. A 70 % proportion of the entire amount of air was fed into the reformer without preheating via the reformer mixing chamber. The remaining amount was preheated and fed into the reformer via the steam pathway together with the superheated steam from the catalytic burner. A 65–75 % proportion of water for the reforming process was vaporized and slightly superheated in the integrated heat exchanger of the catalytic burner. An overview of the results for the CO concentrations achieved behind the respective shift stages as well as the testing duration are shown in Fig. 27.

The tests with desulfurized jet fuel Jet A-1 (HC kerosene) showed that an increased temperature level in the system is required – which is brought about by higher proportions of steam provided in the catalytic burner, higher O_2/C ratios in the reformer, and preheating of the total amount of reforming air – in order to reduce, or even eliminate, the formation of undesirable by-products in the reformer. However, it was found that this increased temperature level in the system also increased the temperatures in the shift stages, which led to higher CO concentrations. Since the target concentration of 1.25 (vol)% was achieved in all tests with HC kerosene (1.03–1.16 (vol)%), it is still advisable to operate the system

---

6 US DOE: US Department of Energy.

7 Samsun et al., J Power Soruces 355 (2017), 44-52

with adjusted parameters (e.g. O_2/C molar ratio of 0.49 instead of 0.47). A detailed list of the test parameters for all experiments can be found in[8].

In the tests with premium diesel (Aral Ultimate Diesel), it was not only advisable but also necessary to operate the reformer with adjusted parameters in order to achieve the target value for CO concentrations with this fuel. The highest (1.50 (vol)%) and lowest (0.83 (vol)%) CO concentrations behind the shift stages were observed during system operation with this diesel fuel. In the optimized case (tests 16 and 17), the reformer was operated with an O_2/C molar ratio of 0.49, a H_2O/C molar ratio of 2.2, complete preheating of the air, and a 75 % proportion of water vaporization in the catalytic burner.

Fig. 27 summarizes the most important results of all tests. For all the fuels used, it was possible to achieve the target CO concentration of 1.25 (vol)% in the dry product gas of the shift reactor, while also demonstrating self-sufficient system operation without an external heat supply.

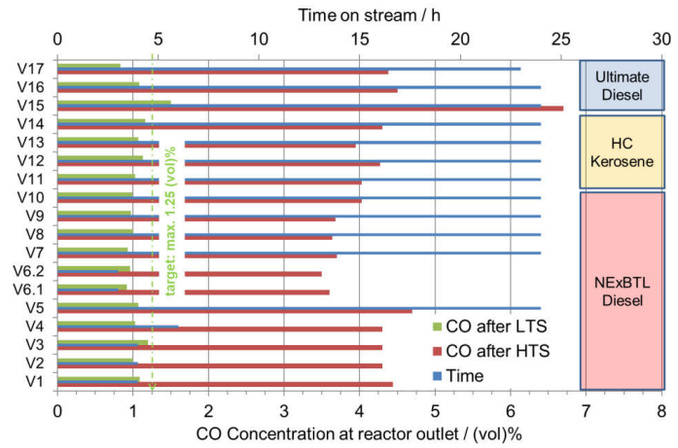

Fig. 27: Summary of the most important test results from stationary operation of fuel processing system package 5.

3.2.3 Staff members and fields of activity

Name	Tel. (02461-61-) Email	Field of activity
Prof. Dr. R. Peters	4260 ra.peters@fz-juelich.de	Head of Fuel Processing Systems
Dr. J. Pasel	5140 j.pasel@fz-juelich.de	Head of Chemistry for Fuel Processing
Dr. R. C. Samsun	4616 r.c.samsun@fz-juelich.de	Head of Systems Engineering for On-Board Power Supply

[8] Samsun et al., Applied Energy 226 (2018), 145-159

A. Tschauder	4547 a.tschauder@fz-juelich.de	Reactor development, reforming, system design
J. Meißner	4306 j.meissner@fz-juelich.de	Catalytic combustion, CO fine cleaning
S. Schemme	2779 s.schemme@fz-juelich.de	Future fuels, process and systems analysis of electrofuels
M. Decker	5322 ma.decker@fz-juelich.de	Future fuels, liquid energy carriers for ships, aircraft, and trucks
S. Weiske	5322 s.weiske@fz-juelich.de	Future fuels, DME synthesis methods, reactor modeling
J. L. Breuer	96984 ja.breuer@fz-juelich.de	Future fuels, traffic and emissions modeling
F. Schorn	4394 f.schorn@fz-juelich.de	Future fuels, process analysis of methanol-based electrofuels
J. Häusler	5393 j.häusler@fz-juelich.de	Future fuels, alcohol synthesis
H. Huang	85193 h.huang@fz-juelich.de	Future fuels, process analysis of membrane processes

3.2.4 Importand publications, doctoral theses, and patents

Publications in peer-reviewed jornals

Pasel, J.; Samsun, R.C.; Tschauder, A.; Peters, R. Stolten, D.
Water-gas shift reactor for fuel cell systems: Stable operation for 5000 hours
International Journal of Hydrogen Energy 43 (2018) 19222-19230

Schemme, S.; Breuer, J.L.; Samsun, R.C.; Peters, R.; Detlef Stolten, D,
Promising catalytic synthesis pathways towards higher alcohols as suitable transport fuels based on H_2 and CO_2
Journal of CO_2 Utilization 27 (2018) 223–237

Samsun, R.C.; Prawitz, M.; Tschauder, A.; Pasel, J.; Pfeifer, P.; Peters, R.; Stolten, D.
An integrated diesel fuel processing system with thermal start-up for fuel cells
Applied Energy 226 (2018) 145–159

Peters. R.; Pasel, J.; Samsun, R.C.; Scharf, F.; Tschauder, A.; Stolten D.
Heat exchanger design for autothermal reforming of diesel,
International Journal of Hydrogen Energy 43 (2018) 11830-11846

Krekel, D.; Samsun, R.C.; Peters, R.; Stolten, D.
The separation of CO_2 from ambient air – A techno-economic assessment
Applied Energy 218 (2018) 361-381

Meißner, J.; Weiske, S.; Faidel, D.; Tschauder, A.; Samsun, R. C.; Pasel, J.; Peters, R.; Stolten, D.

Highly integrated catalytic burner with laser-additive manufactured manifolds
Reaction Chemistry Engineering, 2017, 2, 437

Pasel, J.; Samsun, R.C.; Tschauder, A.; Peters, Stolten, D.
Advances in autothermal reformer design,
Applied Energy 198 (2017) 88-98

Samsun, R.C.; Krekel, D.; Pasel, J.; Prawitz, M.; Peters, R.; Stolten, D.
A diesel fuel processor for fuel-cell-based auxiliary power unit applications
Journal of Power Sources 355 (2017) 44-52

Peters, R.; Pasel, J.; Samsun, R.C.; Scharf. F.; Tschauder, A.; Müller, M.; Müller, A.; Beer, M.; Stolten, D.
Spray formation of middle distillates for autothermal reforming
International Journal of Hydrogen Energy 42 (2017) 16946-16960

Peters, R.
Identification and thermodynamic analysis of reaction pathways of methylal and OME-n formation
Energy 138 (2017) 1221-1246

Schemme, S.; Samsun, R.C.; Peters, R.; Stolten, D.
Power-to-fuel as a key to sustainable transport systems – An analysis of diesel fuels produced from CO_2 and renewable electricity
Fuel 205 (2017) 198–221

Doctoral theses

Krekel, D.
Betriebsstrategien für Brenngaserzeugungssysteme zur Anwendung in HT-PEFC-Hilfsstromaggregaten
Schriften des Forschungszentrums Jülich, Reihe Energie & Umwelt, Band 356, 2017.
ISBN 978-3-95806-203-0

3.3 Polymer Electrolyte Fuel Cells

3.3.1 Objectives and fields of activity

Within the scope of a reorientation, low-temperature polymer electrolyte fuel cells (PEFCs) have become a priority. At the same time, research on high-temperature polymer electrolyte fuel cells (HT-PEFCs) has been scaled back. The expertise gained over the course of more than 10 years of HT-PEFC research has been successfully transferred to PEFC research. This applies to both experimental and theoretical work. The different operating temperatures and materials of PEFCs compared to HT-PEFCs automatically gave rise to new tasks and challenges for the team. One example is two-phase flow. In HT-PEFCs, which have a typical operating temperature of 160 °C, there is no liquid water in the channels or porous transport layers. In contrast, typical operating conditions of PEFCs at ambient pressure mean that liquid water is present in all cell components. This water, which is unwanted on the one hand, is necessary on the other hand, in order to guarantee the conductivity of the polymer membrane. Furthermore, water management in the cells has effects on the lifetime. The water balance in cell components, cells, and stacks has thus become a key topic in process engineering work within PEFC research. One focus within this topic is the modeling and simulation of everything from cell components to the stack. In addition to various simulation methods adapted to the task at hand, the coupling of methods and scales is a major challenge which the department has set itself. The competencies of the physicists, chemists, process engineers, and computer scientists involved complement each other perfectly, making it possible to examine phenomena from different perspectives, leading to innovative modeling approaches. The complexity of the tasks in combination with the required high spatial resolution of the simulations demands a sophisticated IT infrastructure. As part of the Jülich Aachen Research Alliance (JARA), high-performance computers (HPCs) at both RWTH Aachen University and Forschungszentrum Jülich are used to generate numerical solutions. Another important aspect of these theoretical activities is that the simulations and the underlying models are verifiable in the sense of scientific transparency. This is the main, if not decisive, reason why commercial software has lost its significance for our work. The focus shifted several years ago to open source software. The field of computational fluid dynamics (CFD) in particular makes consistent use of OpenFOAM as a basis for simulation work. Exchange with other research groups was significantly expanded in this area and resulted in a leading role within the International Energy Agency's (IEA) Technology Collaboration Programme on Advanced Fuel Cells. One basic prerequisite for reliable conclusions to be drawn from these simulations is experimental validation. This gives the models the validity needed to make the best use of them. Simulation results must agree with current–voltage characteristics, but this alone is insufficient for verifying model validity. Further integrated evidence can be drawn from measuring the pressure drop between cell inlet and cell outlet as a function of current density, stoichiometry, and temperature. Due to the two-phase flow phenomena in PEFCs, flooding effects can be detected. However, local effects must also be considered for model validation. Typically, these are local current density and temperature distributions, as well as the visualization of local water droplet dynamics in a cell. The team works together on this with colleagues from the Paul Scherrer Institute (PSI), Switzerland, as well as colleagues at Hemholtz-Zentrum Berlin (HZB). Furthermore, a nano-CT at IEK-3 is important for ex situ and operando measurements.

3.3.2 Important results

3.3.2.1 Investigations on the influence of GDL mechanics on PEFC operation

During the assembly of polymer electrolyte fuel cells, the individual functional layers are contacted with each other using mechanical clamping devices. Two opposite effects make it difficult to set the optimal contact pressure on the active surface area. To achieve the lowest possible contact resistance, high pressure is needed on the active surface area. High contact pressure, however, leads to an increased diffusion resistance of the gases in the gas diffusion layer (GDL), which in turn leads to a reduced cell voltage since the gas concentration on the active cell surface area decreases.

A test cell from Baltic FuelCells GmbH was used to determine this optimum experimentally. This cell permitted the average contact pressure on the active surface area during fuel cell operation to be varied between 0.1 N/mm² and 2.7 N/mm². The test cell was combined with a membrane electrode assembly (MEA) from W. L. Gore & Associates GmbH for low-temperature PEFCs and various, frequently used GDL materials. Graphite-composite flow field plates with a meandering structure served as flow distributors.

To determine the optimal contact pressure, polarization curves were measured at different contact pressures. To record the effects of mechanically damaged cell components and particularly the effects of the mechanically damaged GDL on cell performance, the contact pressure was increased from the lowest to the highest value and subsequently decreased again. The cell performance for both steps was compared at the individual pressure levels. Some of these measurements are shown in Fig. 28. In Fig. 28, the maximum power density of the cell is plotted against the contact pressure for the GDL materials 29BC from SGL, TGP-H 060 from Toray, and H2315 C2 from Freudenberg.

It is clear from Fig. 28 that these GDL materials behave very differently. The SGL material has a sharp optimum at around 0.6 N/mm², the Toray material has a wide optimal working window of 0.6–1.6 N/mm², and the Freudenberg material is the most robust, exhibiting an almost constant performance maximum until the maximum contact pressure was achieved at 2.6 N/mm².

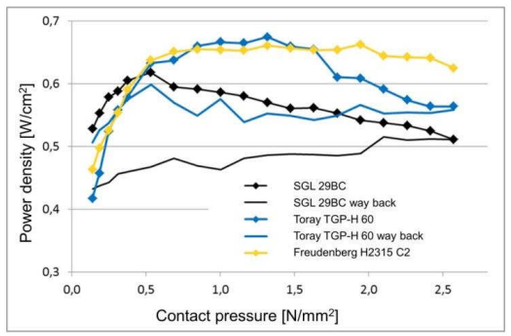

Fig. 28: Maximum power density of a single cell as a function of the average contact pressure for various types of GDL

Once the maximum contact pressure was reached, the pressure was decreased again. The maximum power density of the SGL and Toray materials did not increase again when the

contact pressure was decreased. This indicates permanent mechanical damage of the GDL. For a more detailed analysis of the damage sustained, SEM and nano-CT images of the GDL materials were recorded.

Fig. 29 shows that the mechanical damage is heavily dependent on the type of GDL used. For this analysis, a pressure of 6 N/mm² was applied to the samples since this approximates to the pressure under the rib of the flow field during fuel cell operation due to the channel/rib ratio of 1:1. The SGL and Freudenberg materials appeared unaffected by contact pressures of up to 6 N/mm², while the Toray material exhibited clear damage to the fiber structure.

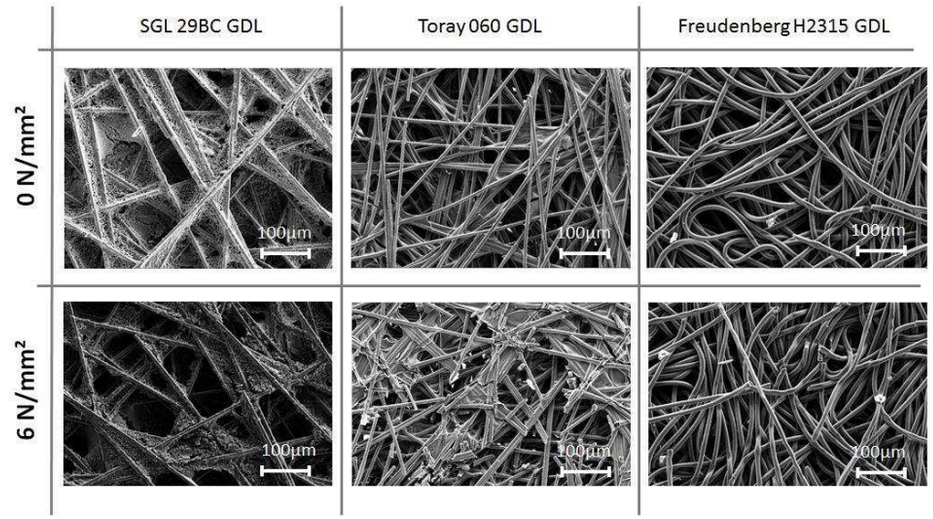

Fig. 29: Mechanical damage to the fibers due to contact pressure

The SEM images only provide information on surface damage of the fiber structure, however. The nano-CT images recorded in the unloaded state after mechanical loading (Fig. 30) show that although the SGL material did not have any fiber fractures, it did have a heavily modified 3D structure. The fibers did not break, but the GDL binder was redistributed and compressed, which led to changes in thickness and thus to impaired porosity and cell performance. Only the Freudenberg material appeared unaffected by pressures of up to 6 N/mm² and its structure was not significantly permanently damaged, which was also clear from the performance characteristics.

To summarize, the mechanics of fuel cells considerably influence the fiber structure of the GDL, which in turn influences porosity as well as mass transport resistance, and ultimately the performance of the fuel cell. How strong this influence is depends on the material used. Depending on the material and the initial situation, selecting the optimal contact pressure can increase electrical performance by up to 15 %. The material H2315 C2 from Freudenberg proved to be the most robust material with no performance limitations. It exhibited fewer fiber fractures and only very small plastic deformations, allowing optimal performance even under high contact pressures.

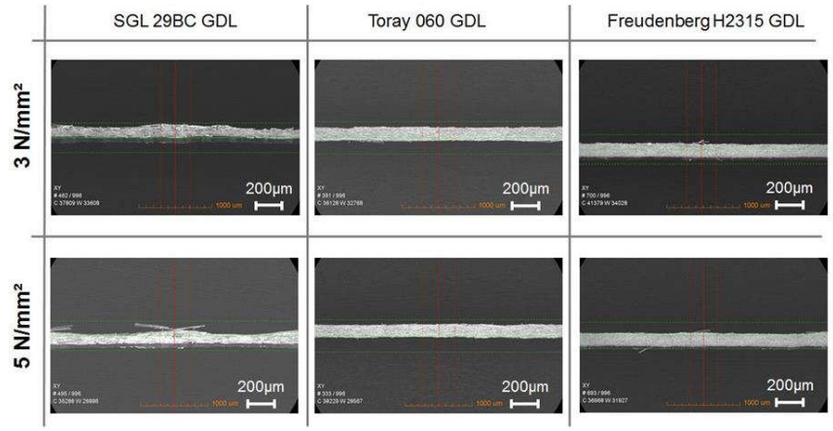

Fig. 30: Nano-CT images of mechanically loaded and subsequently unloaded GDLs

3.3.2.2 Water dynamics in low-temperature PEFCs

For the use of PEFC systems in vehicles, fuel cells must react quickly to achieve the desired performance requirements and to achieve optimum operating conditions during start, stop, acceleration, and braking. These factors require continuous changes in operating conditions and therefore an in-depth understanding of the various time-dependent reactions during PEFC operation. Water is produced at the cathode catalyst layer and transported through the gas diffusion layer during fuel cell operation to the flow channels. Any change in cell operation can lead to the condensation of liquid water in the flow channels, resulting in an altered two-phase pressure drop. In the present case, the cell was subjected to six different load change scenarios. Voltage and pressure drop reactions as well as the ohmic resistance were observed.

a) Assembled test cell b) Flow field and MEA

Fig. 31: Tes cell for experiments

The test cell (shown in Fig. 31) consisted of a MEA with an active surface area of 17.64 cm². The GDL was a carbon fleece from Freudenberg (H2315Cx165) which was coated with a microporous layer (MPL). The flow field consisted of three parallel meandering channel structures. These channels were 1 mm wide and 1 mm deep; the ribs were also 1 mm wide. The operating temperature of the cell was set to 60 °C, the relative humidity of the reaction gases (anode and cathode side) to 90 %, and the stoichiometry of both gas flows to 2.

In this experiment, six tests were conducted with different load change scenarios. The load change scenario in test no. 1 was designated 5-5-5-5. This means that the load was first increased in a linear manner in 5 min from 0.2 A/cm² to 0.6 A/cm². When the target value was reached, it was kept constant for 5 min, and then reduced in a linear manner within the next 5 min from 0.6A /cm² to 0.2 A/cm². When this target value was reached, it was again kept constant for 5 min. The other load change scenarios were as follows: 2.5-5-2.5-5 (test no. 2), 1-5-1-5 (test no. 3), 0-5-0-5 (test no. 4), 5-0-5-0 (test no. 5), and 1-0-1-0 (test no. 6).

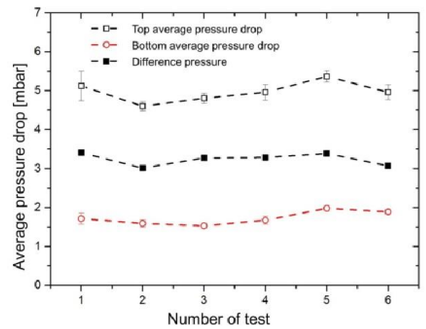

Fig. 32: Average pressure drop

In order to characterize the dynamic behavior of the two-phase pressure drop of the cell for different load change scenarios, the upper average pressure drop (ODD) at 0.6 A/cm² and the lower average pressure drop (UDD) at 0.2 A/cm² were examined in each test. As shown in Fig. 32, the ODD is slightly higher in tests no. 2–4, which feature a steeper ramp rate ($|^{\Delta i}/_{\Delta t}|$). The relevant changes in UDD were, however, not obvious, and neither were the differential changes between ODD and UDD.

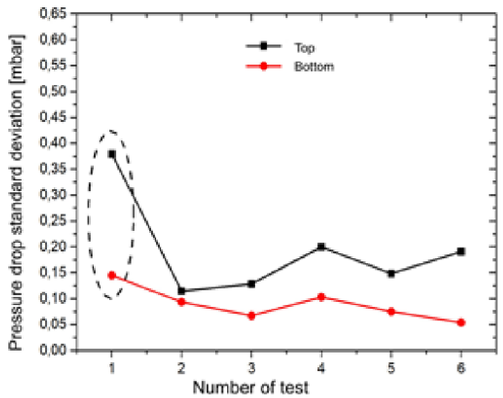

Fig. 33: Standard deviation from upper and lower average pressure drop

Fig. 33 shows the standard deviation of ODD and UDD with different ramp rates. In tests no. 2–4 and tests no. 5–6, the standard deviation from ODD was greater with steeper ramp rates. The reason could be that at lower gradients, the two-phase pressure drop is slower, so that the pressure drop in the constant-current phase reaches its equilibrium. For the steeper ramp rates, however, the change in the water flow produced is greater, and therefore

equilibrium of the two-phase flow is harder to achieve. This leads to a higher pressure drop fluctuation. The results of test no. 1 (highlighted in Fig. 33) were unexpected. Further investigations are necessary here.

Fig. 34 shows the standard deviation of the pressure drop of the individual cycle phases for tests no. 1–4. In test no. 1, it was found that the difference in standard deviations between the upper pressure drop and the lower was largest in the first cycle. The difference decreased in the subsequent cycles. Similar results were also found in tests no. 2–4. During cyclic operation, the two-phase flow appeared to reach a quasi-stationary equilibrium in the cell.

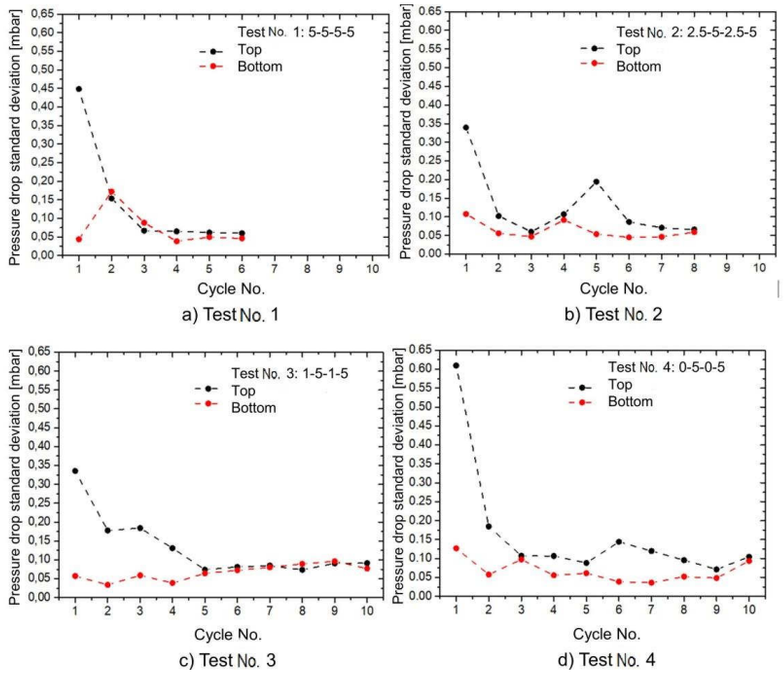

Fig. 34: Standard deviation of upper and lower pressure drop in tests no. 1-4

Fig. 35 shows the ohmic resistance in each cycle for tests no. 1–4 measured using impedance spectroscopy (white and gray lanes). The ohmic resistance was measured in each cycle at 0.6 A/cm² and then at 0.2 A/cm². Before each first cycle began, the ohmic resistance was measured during the initial phase at 0.2 A/cm². It can clearly be seen that the ohmic resistance is considerably higher at the lower current density. This was to be expected because more water is produced at higher current densities and the membrane has a higher water content. This results in higher protonic conductivity. It was also observed that the difference in ohmic resistance between the tests is not significant. The reason could be that there is sufficient water in the cell and the membrane is sufficiently wet.

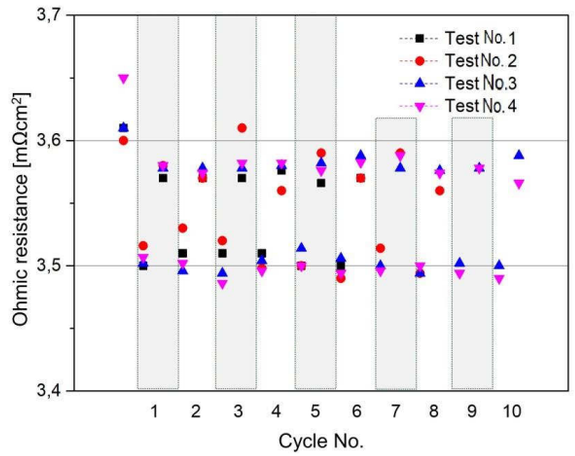

Fig. 35: Ohmic resistance in the different tests and cycles (high value at 0.2 A/cm², low value at 0.6 A/cm²)

3.3.2.3 Characterization of open cell voltage of olymer electrolyte fuel cells

For commercial applications of fuel cells, cell lifetimes of 5,000 h for mobile applications and up to 40,000 h for stationary applications are often required. However, lifetime is decisively influenced by operating cycles. Although unfavorable operating conditions, such as high local current densities, can be prevented by both constructive and operative means using suitable load control, the periodic start-up and shut-down process is a fundamental problem because the fuel cells have to be operated at a relatively high potential of approx. 1 V for a short time. In this potential range, partial oxidation of the platinum surface occurs, which is associated with slow dissolution and thus the loss of the catalyst. Catalyst oxidation is a complex process with several stages from the pure metal surface to adsorbed oxygen molecules and ultimately pronounced oxide layers. Fig. 36 shows a schematic of this reversible process. In simplified terms, the first step involves the formation of an adsorption or oxide layer, which covers only the upper-most platinum atoms as a monolayer. As the process progresses, the transition to PtO_2 occurs, which is associated with a reorientation of the outer layer of the catalyst.

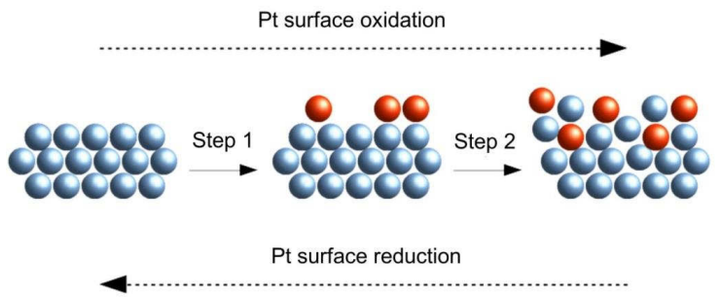

Fig. 36: Simplified depiction of the progressive oxidation of the catalyst surface

This oxidation process was characterized at IEK-3 using a special measuring cell with a classic three-electrode arrangement, which can be employed in the temperature range of 30–80 °C. A polycrystalline Pt disk with a diameter of 2.54 cm served as a model electrode, and a 1 M solution of H_2SO_4 served as the electrolyte. At the beginning of the measurements, the cell was brought to the specified temperature for 60 min and flushed with oxygen in order to achieve the relevant saturation concentration of oxygen in the electrolyte. A cyclic voltammogram (with 8 repetitions) was then recorded, and is shown in Fig. 37.

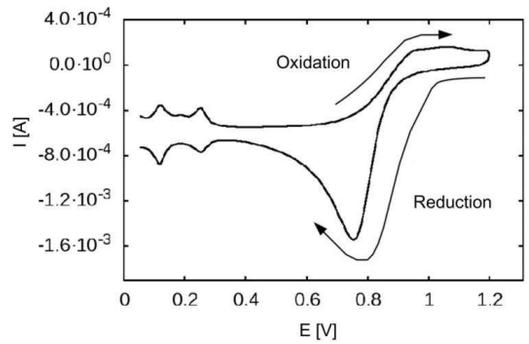

Fig. 37: Cyclic voltammogram of Pt in 1 M H_2SO_4 at 30 °C saturated with O_2 (see Fig. 36 for an allocation of the peaks)

The cyclic voltammogram in Fig. 37 shows the dependence of surface oxidation on electric potential. In the case of the fuel cell, switching off the load leads to a corresponding oxidation of the catalyst surface, whereby the potential can be freely adjusted. The result is an open cell voltage, which changes as a function of time. The time dependence is shown in Fig. 38. It can be described as a function of the kinetics of the electrochemical processes occurring at the electrode surface. Two processes simultaneously determine the potential: surface oxidation and the oxygen reduction reaction. Clarifying these correlations as a function of temperature and electrolyte concentration is the subject of an ongoing doctoral project at IEK-3.

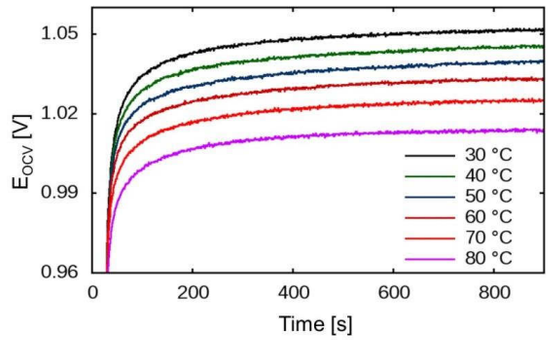

Fig. 38: Free electrode potential (OCV) as a function of time; Pt electrode in 1 M H_2SO_4 at 30 °C saturated with O_2

3.3.2.4 Water transport in gas diffusion layers

The efficiency of PEFCs depends on a multitude of factors. One important aspect is the transport of liquid water in the porous structure of the gas diffusion layer on the cathode side of the fuel cell. The water produced in the catalyst layer must be transported through the porous fiber structure to the air channels, where it is removed by the comparatively fast air stream.

Gases are distributed across the active surface area of a fuel cell by suitable flow distributors (referred to as flow fields). The microstructure of the GDL influences the flow in the channels of the flow distributor. Transport simulations typically comprise only a small section (roughly 1 mm²) of a real GDL, which in a fuel cell measures 20–300 cm². To achieve reliable results despite this, transport simulations are therefore conducted on statistically varied model geometries which are stochastically equivalent to the real microstructure.

The transport of liquid water through the GDL is a factor that considerably influences the efficiency of a fuel cell. The analysis of water transport reveals an irregular shape of the water droplets emerging at the surface of the GDL. Fig. 39 shows a water droplet with an asymmetrical shape at the surface after being transported through the GDL. The deformation of such a water droplet by the flow in the air channel is also shown.

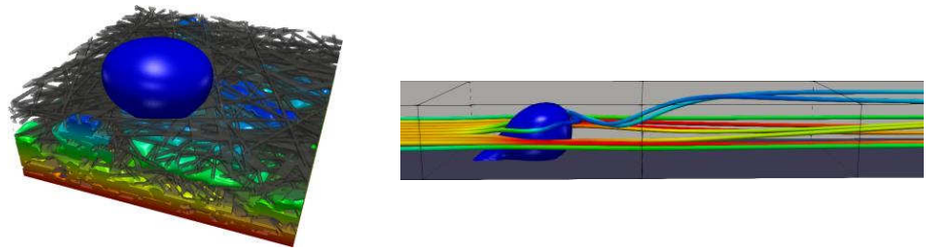

a) Water droplet emerging from the GDL

b) Flow in the air channel around a water droplet emerging from the GDL

Fig. 39: Water transport in the GDL and air channel of a PEFC

Fig. 39 shows the results of simulations on various scales. The GDL consists of microstructures whose basic elements are fibers with a typical diameter of 5–7 µm. Accordingly, the simulation areas have typical dimensions in the mm² range of a GDL. In contrast, the dimensions of simulations in channels are oriented towards the interconnect plates of fuel cells in the cm range. GDLs are often accounted for as a homogenized porous material, the material data of which are incorporated in the transport models as model parameters. One such parameter is the angle formed by a water droplet with the surface of a material. From this contact angle and with the aid of the Young–Laplace equation, the surface tension and interfacial energies can be determined. However, this approach is based on the assumption that the droplet is symmetrical, which has been disproved by the results of transport simulations.

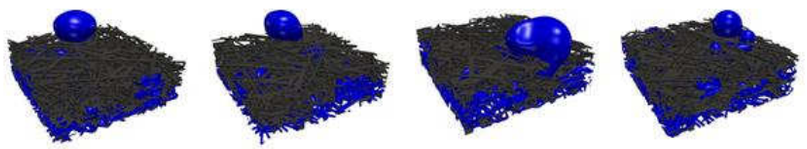

Fig. 40: Emerging water droplets in stochastically equivalent geometries

The results in Fig. 40 show an example of a strong variation in contact angles for four geometries, representing the asymmetrical shape of water droplets emerging from the GDL. Furthermore, the variation in contact angles across the different stochastically equivalent model geometries is in the same order of magnitude, which corresponds to a statistical distribution over the surface area of the GDL. Water droplets at the surface of seven model geometries stochastically equivalent to the real microstructure were analyzed. The contact angles were investigated in four cutting planes: 0°, 30°, 60°, and 90°. For these cutting planes, the variation in contact angles was statistically analyzed.

The transport simulations were performed using hardware at the Jülich Supercomputing Centre (JSC; JURECA project CJIEK30).

3.3.2.5 Simulation von Tropfentransport in PEFC-Kanälen

Ein A typical PEFC flow field contains micro- or minichannels. The continuous removal of liquid water from the channels on the cathode side is a challenge because water droplets that form in the channels can lead to blockages. Oxygen transport to the active sites in the three-phase boundary can thus be blocked. This leads not only to considerable performance loss, but also to an uneven current density distribution, increased degradation rates, and unstable operation. Based on the open source library OpenFOAM, volume of fluid (VOF) models were developed and simulations performed to describe the transport of water droplets at the interface between GDL and channel. The aim was to achieve a better understanding of the two-phase flow in PEFC gas channels and their interaction with the GDL surface.

A gas channel geometry with a liquid inlet, a gas inlet, and a two-phase outlet was used for the simulations. The simulation results were compared to synchrotron measurements from ex situ water injection experiments conducted by colleagues at the Paul Scherrer Institute (PSI) in Switzerland.

Good agreement between was demonstrated between the simulations and the measurements (Fig. 41) in terms of droplet dynamics. The distance between liquid entry and first contact with the wall correlates particularly well. The droplet behavior largely depends on the size of the liquid inlet, the velocity of the gas stream, the channel geometry (height and width), and the contact angle.

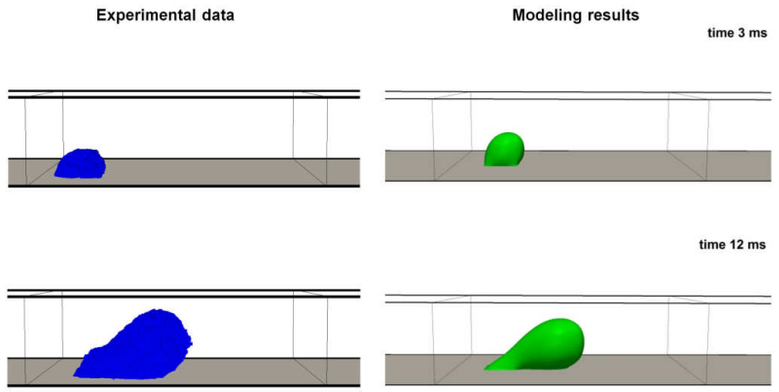

Fig. 41: Comparison of experimental data and VOF simulations with static boundary conditions at 15 m/s; parameters at a temperature of 20 °C

Both experiments and models show separation-free flow in the channel for standard conditions. The droplet can, however, also contact with the GDL surface and the channel wall at the same time when gas velocity and channel height decrease or the size of the liquid inlet increases. Furthermore, water transport can occur in the channel edges at the channel wall opposite the GDL when the gas velocity or the wall contact angle decreases or the size of the liquid inlet increases.

A smaller liquid inlet (constant liquid mass flows for constant stoichiometry) leads to considerably smaller droplets. Increased gas velocity also leads to smaller droplets and the number of droplets per unit of time therefore increases.

The model that assumed static contact angles was expanded to investigate the effects of dynamic contact angles on the transport behavior of water (Fig. 42).

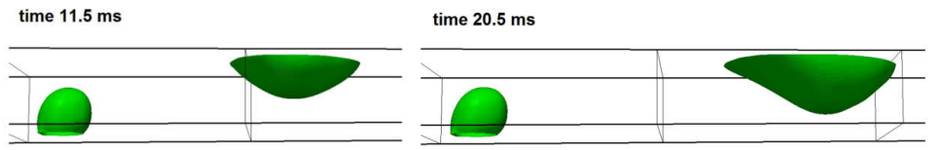

Fig. 42: The first droplet moves very slowly and waits for a second droplet (left). Two merged droplets move along the main flow direction with increased velocity (right). Wall contact angle: 10°/75°; contact angle of the gas diffusion layer: 138°/162°; gas velocity: 10 m/s; parameters at a temperature of 60 °C

The influence of dynamic contact angles on the behavior in a flat channel are described here as an example. The first droplet adheres to the wall opposite the GDL, and slowly moves toward the channel outlet. After it merges with a second droplet, the velocity increases and this larger droplet exits the channel at a high velocity. The droplet continues to adhere to the wall during this transport.

Similar phenomena were not observed using a static contact angle.

Simulations were conducted using computing resources allocated by JARA-HPC at RWTH Aachen University within the scope of the jara0070 project.

3.3.2.6 Modeling and simulation on the cell and stack level

It is difficult and expensive to measure local phenomena in a PEFC. Numerical methods are an alternative and additional means of observing and quantifying these phenomena. High-performance computers (HPCs) make it possible to conduct extensive and detailed simulations within a relatively short period of time. Alongside experimental measurement and analysis methods, numerical models play an important role in designing and optimizing fuel cells. In the past ten years, various PEFC models have been developed. However, these models have not attracted much attention from the PEFC community, mainly because the implementations are based on proprietary software limited by commercial licensing agreements which cannot be readily released or parallelized for large HPC systems. To compensate for these disadvantages, an LT-PEFC cell model and an LT-PEFC stack model were developed and implemented using the open source library OpenFOAM®.

All of the important transport phenomena, including two-phase fluid flow, mass and heat transfer, and ion and electron transfer in the membrane, electrolyte, and bipolar plates were included at the cell level in the model. An Euler–Euler model was used for the flow in the gas channels. A Leverett J-function was used for the transport of liquid water in the porous layers, which accounts for the vaporization/condensation of water. The electrochemical reaction on the anode side as well as the cathode side was described by a Butler–Volmer or a Tafel relation. For the electron and ion transport, a two-potential model was implemented.

In the stack model, all transport phenomena of the cell model were accounted for, with the exception of the detailed electron/ion transport model. In addition, a resistivity analogy (local volume averaging technique) was used to reduce the convergence time. The computational mesh was coarser than the mesh used for simulations on the cell level.

The cell model was validated using experimental polarization curves. The active surface area of the simulated cell measured 1 cm x 1 cm and the operating temperature was T = 353 K. The stoichiometric factor on the anode side was λ = 1.2 and on the cathode side λ = 2.0. The anode was exposed to fully humidified hydrogen, and the cathode to fully humidified air. Fig. 43 shows good agreement between the simulation result and the experiment.

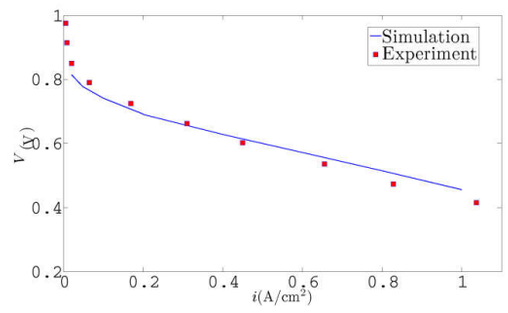

Fig. 43: Comparison of the numerical results and experimental data

Calculations were then performed for an IEK-3-specific PEFC design. The geometry corresponded to that of an ongoing round robin test within the framework of the International Energy Agency's (IEA) Energy Technology Collaboration Programs on Advanced Fuel Cells. The active surface area of the cell was 17.64 cm² (4.2 cm x 4.2 cm).

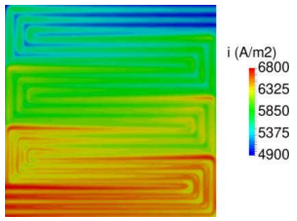

Fig. 44: Simulated current density distribution of a cell with IEA LT-PEFC benchmark geometry

In Fig. 44 ist die simulierte lokale Stromdichteverteilung für eine mittlere Stromdichte von 6000 A/m² dargestellt. Die Betriebstemperatur beträgt T = 343 K. Die relative Luftfeuchtigkeit für Anoden- und Kathodenseite beträgt jeweils 90%, die Stöchiometrien sind λ = 2,0 / 2,0. Die Gase strömen von links unten in die Strömungskanäle ein und treten oben rechts aus. Die Stromdichte nimmt von Einlass zu Auslass ab. Lokale Extrema sind in den Ecken der serpentinenartigen Kanäle zu sehen.

Polymerelektrolytmembran-Elektrolysezellen und -Stacks teilen sich viele physikalische Prozesse mit PEFC-Zellen und -Stacks. Dazu gehören ein zweiphasiger Flüssigkeits- / Gasstrom, ähnliche elektrochemische Reaktionen sowie Wärme- und Stofftransport. Daher können die vorliegenden Zell- und Stackmodelle leicht auf die Wasser-Elektrolyse angepasst werden.

3.3.3 Staff members and fields of activity

Name	Tel. (02461-61-) Email	Fields of activity
Prof. Dr. W. Lehnert	3915 w.lehnert@fz-juelich.de	Head of High-Temperature Polymer Electrolyte Fuel Cells
Prof. Dr. M. Andersson (Gast)	9074 m.andersson@fz-juelich.de	CFD with OpenFOAM, Volume of Fluid
Prof. Dr. S. Beale	8856 s.beale@fz-juelich.de	CFD with OpenFOAM, cell and stack level
Fr. Y. Cai	6484 y.cai@fz-juelich.de	Electrochemical half-cell investigations, OCV
D. Froning	6676 d.froning@fz-juelich.de	Lattice Boltzmann simulations in porous components
E. Hoppe	85192 e.hoppe@fz-juelich.de	HT-PEFC characterization unit
P. Irmscher	9803 p.irmscher@fz-juelich.de	Stack mechanics
Dr. H. Janßen	5082	HT-PEFC stack development

	h.janssen@fz-juelich.de	
A. Kulikovsky, PhD, DSci (Gast)	5396 a.kulikovsky@fz-juelich.de	Analytical fuel cell models
R. Li	96924 r.li@fz-juelich.de	Corrosion of metallic bipolar plates
Y. Lin	9036 y.lin@fz-juelich.de	HT-PEFC membranes
Sh. Liu	8626 Shu.liu@fz-juelich.de	HT-PEFC electrodes
Dr. U. Reimer	3537 u.reimer@fz-juelich.de	HT-PEFC Modeling and Simulation
Y. Shi	1902 y.shi@fz-juelich.de	PEFC water management
Fr. B. Schumacher	5406 b.schumacher@fz-juelich.de	Development of designs for test stands for HT-PEFCs, testing of HT-PEFCs
M. Sietmann	3850 m.sietmann@fz-juelich.de	Quality control bipolar plates
J. Yu	2989 j.yu@fz-juelich.de	Lattice Boltzmann simulations in porous components
S. Zhang	96465 s.zhang@fz-juelich.de	CFD with OpenFOAM, cell and stack level
Fr. W. Zou	9399 w.zou@fz-juelich.de	Modeling of dynamic fuel-cell behavior

3.3.4 Important publications, doctoral theses, and patents

Publications

Yasser Rahim, Holger Janßen, Werner Lehnert
Characterizing Membrane Electrode Assemblies for High Temperature Polymer Electrolyte Membrane Fuel Cells Using Design of Experiments
Int. J. Hydrogen Energy, 42 (2017) 1189-1202

H. Janßen, L. Lüke, J. Ehlert, W. Lehnert, D. Stolten
Setup and experimental validation of a 5 kW HT-PEFC stack
Int. J. Hydrogen Energy 42 (2017) 11596

Liangfei Xu, Junming Hu, Chuan Fang, Siliang Cheng, Jianqiu Li, Minggao Ouyang, Werner Lehnert
Robust control of internal states in a polymer electrolyte membrane fuel cell air-feed system by considering actuator properties
J. Hydrogen Energy 42 (2017) 13171-13191

A Kulikovsky

Impedance of a PEM fuel cell cathode with nonuniform ionomer loading: Analytical and numerical study

Journal of Electroanalytical Chemistry 789 (2017) 174-180

M. Andersson, S. Beale, U. Reimer, W. Lehnert, D. Stolten

Interface resolving two-phase flow simulations inside gas channels relevant for polymer electrolyte fuel cells

Int. J. Hydrogen Energy, 43 (2018) 2961-2976

J. Yu, D. Froning, U. Reimer, W. Lehnert

Apparent contact angles of liquid water droplet breaking through a gas diffusion layer of polymer electrolyte membrane fuel cell

Int. J. Hydrogen Energy 43 (2018) 6318-6330

Junliang Yu, Dieter Froning, Uwe Reimer, Werner Lehnert

Liquid water breakthrough location distances on a gas diffusion layer of polymer electrolyte membrane fuel cells

J. Power Sources 389 (2018) 56-60

D. Froning, J. Yu, U. Reimer, W. Lehnert

Stochastic analysis of the gas flow at the GDL/electrode interface of a high-temperature polymer electrolyte fuel cell

Transp Porous Med 132 (2018) 403-420

S. Beale, U. Reimer, D. Froning, M. Andersson, J.G. Pharoah, W. Lehnert

Stability Issues for Fuel Cell Models in the Activation and Concentration Regimes

ASME Journal of Electrochemical Energy Conversion and Storage, 15 (2018), 041008-1 - 041008-7

Y. Lin, T. Arlt, N. Kardjilov, I. Manke, W. Lehnert

Operando Neutron Radiography Analysis of High Temperature Polymer Electrolyte Fuel Cell based on a Phosphoric Acid-Doped Polybenzimidazole Membrane Using the Hydrogen-Deuterium Contrast Method

Energies 2018, 11(9), 2214;

Shuai Liu, Marcin Rasinski, Yu Lin, Klaus Wippermann, Andreas. Everwand, Werner Lehnert

Effects of constant load operations on platinum bands formation and cathode degradation in high-temperature polymer electrolyte fuel cells

Electrochimica Acta 289 (2018) 354-362

Ruiyu Li, Yun Cai, Klaus Wippermann, Werner Lehnert.

Corrosion and Electrical Properties of SS316L Materials in the Simulated HT-PEFC Environment

J. Electrochem. Soc. 165 (10) (2018) C681-C688

Diankai Qiu, Holger Janßen, Linfa Peng, Philipp Irmscher, Xinmin Lai, Werner Lehnert

Electrical resistance and microstructure of typical gas diffusion layers for the proton exchange membrane fuel cell under compression

Applied energy, 231 (2018) 127-137

Holger Janßen, Achim Edelmann, Thea Mildebrath, Patrick Müller, Werner Lehnert, Detlef Stolten
Design and experimental validation of an HT-PEFC stack with metallic BPP
Int. J. Hydrogen Energy 43 (2018) 18488-18497

M. Andersson, A. Mularczyk, J. Eller, S.B. Beale, A. Lamibrac, W. Lehnert, F. Büchi
Modeling and synchrotron imaging of droplet detachment in gas channels of polymer electrolyte fuel cells
J. Power Sources 404 (2018) 159-171

Dieter Froning, Junliang Yu, Uwe Reimer, Werner Lehnert
Stochastic Analysis of the Gas Flow at the Gas Diffusion Layer/ Channel Interface of a High-Temperature Polymer Electrolyte Fuel Cell
Appl. Sci. 8 (2018), 2536

Doctoral theses

Cao, Q.
Modelling of High Temperature Polymer Electrolyte Fuel Cells
Schriften des Forschungszentrums Jülich, Reihe Energie & Umwelt, Band 389, 2017, ISBN 978-3-95806-263-4

Yu, J.
Lattice Boltzmann Simulations in Components of Polymer Electrolyte Fuel Cell
Schriften des Forschungszentrums Jülich, Reihe Energie & Umwelt, Band 438, 2018, 978-3-95806-360-0

Lin, Y.
Characterization of Polybenzimidazole Membranes
Schriften des Forschungszentrums Jülich, Reihe Energie & Umwelt, Band 440, 2018, ISBN 978-3-95806-364-8

Rahim, Y.
Characterization of High Temperature Polymer Electrolyte Fuel Cells
Schriften des Forschungszentrums Jülich, Reihe Energie & Umwelt, Band 440, 2018, 978-3-95806-364-8

Important Patents

Patents granted:

Principal inventor	**PT**	**Description**
Dr. A.A. Kulikovsky	1.2601	Methods for characterizing the catalyst structure in a fuel cell, and fuel cell design suitable for said method
Dr. A. A. Kulikovky	1.2644	Direct alcohol fuel cell and direct alcohol fuel cell stack with effective CO2 removal, and method for operating such a direct alcohol fuel cell

3.4 Direct Methanol Fuel Cells

3.4.1 Objectives and fields of activity

Thanks to its high energy density and simple handling, the liquid energy carrier methanol offers advantages for fuel cell systems in which high energy densities and permanent operation without refueling are more important than a particularly high power density. Therefore, the main fields of application for direct methanol fuel cell (DMFC) technology which IEK-3 focuses on are small mobile applications such as the field of material handling or uninterruptible power supplies (UPS), particularly at remote locations where frequent refueling is impracticable. The fact that methanol is liquid can be attributed to its intermolecular interactions due to its slightly complex chemical structure. However, this also means that methanol cannot be electrochemically converted as quickly as hydrogen. Direct methanol fuel cells therefore require a larger catalyst volume, which in turn increases costs. To counteract this, it is crucial to develop highly reactive catalysts that require smaller amounts of the noble metal platinum. The structure of a DMFC system is relatively simple due to the liquid fuel methanol. However, in the interest of long lifetimes, a sophisticated operation management strategy is necessary to achieve and maintain maximum electrical efficiency during the gradual degradation of the cells. In addition, operation management is designed so that operating states are prevalent, achieving the smallest possible aging rate for the DMFC and preventing irreversible damage.

3.4.2 Important Results

3.4.2.1 New catalysts for DMFC and electrolysis

As part of a collaborative project[9] funded by the Federal Ministry for Economic Affairs and Energy (BMWi) between Universität Hamburg, Fraunhofer CAN, and SFC Energy, cathode catalysts developed by Universität Hamburg and manufactured by Fraunhofer CAN in a continuous process in a flow reactor are processed into cathodes for DMFCs and tested in DMFC operation. Furthermore, hierarchically structured composite nanoparticle systems are produced in which carbon nanotubes grown on a stainless steel lattice are used as catalyst substrates. Since these systems were initially only available with dimensions of 25 x 25 mm², it was necessary to develop an adapted flow distributor structure. It is not sufficient, however, to simply reduce the size of the existing flow distributor structure (42 x 42 mm²). Reducing the channel depths and widths to less than the current size (1 mm) is not recommended, since gas bubbles on the anode and water droplets on the cathode would no longer be removed, meaning the cell would be insufficiently supplied. In the checkerboard structure (Fig. 45 left), such obstacles lead to the temporary deactivation of an area of a few mm². In a smaller flow field, however, this would represent a larger proportion of the entire area and should therefore be avoided. Instead, a meandering flow field (Fig. 45 center) was selected. Due to the small cell surface area, the meanders are so small that no significant pressure drop is to be expected.

---

[9] Hierarchische Kompositnanopartikelsysteme zur Anwendung in Brennstoffzellen – Entwicklung und kontinuierliche Herstellung (HiKAB), FKZ 03ET1435C

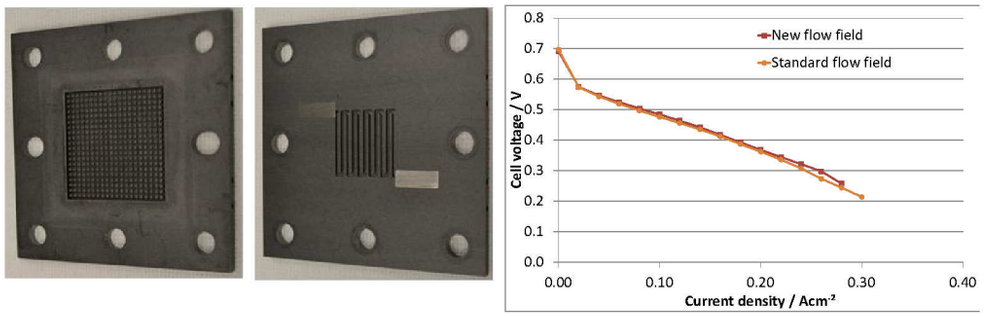

Fig. 45: **Checkerboard flow field 42 x 42 mm² (left) and meandering flow field 25 x 25 mm² (center), as well as characteristic curves of standard MEAs with the different flow fields (right); T = 70 °C, c(methanol) = 0.75 mol/l, air volume flow rate = 0.037 l/cm²min**

This was not possible in the larger flow distributor due to the considerably longer channel. Measuring the pressure drop showed that the pressure decreases by up to 10 mbar with the maximum required volume flows, while the pressure drop in the previous flow field was up to 5 mbar. In comparison with pressure drops due to weather changes of several 10 mbar, this difference is negligible. As expected, the characteristic curves for both flow fields were thus nearly identical (Fig. 45 right).

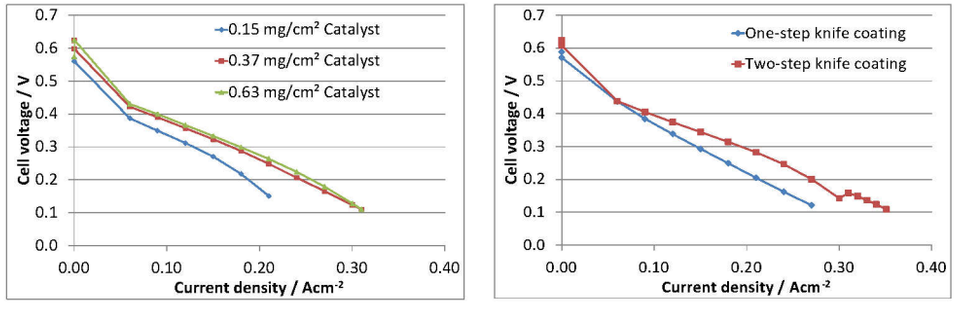

Fig. 46: **Characteristic curves with different cathode loading (left) and different blade coating techniques (right); T = 70 °C, c(methanol) = 0.75 mol/l, air volume flow rate = 0.037 l/cm²min**

Fraunhofer CAN first supplied PtNi alloy catalysts with 25–30 % metal on the carbon carrier XC72. This was applied to a decal substrate using the blade coating technique established for commercial catalysts by IEK-3 and then transferred to the Nafion 115 membrane by means of pressing. A standard anode was subsequently pressed onto this, resulting in the MEA. The catalyst loading required for optimal performance first needed to be determined. As shown in Fig. 46 (left), the increase in cathode loading from 0.15 mg/cm² to 0.37 mg/cm² led to a considerable performance improvement, while a further increase to 0.63 mg/cm² had no considerable effect. Loading in the range of 0.4–0.6 mg/cm² was thus targeted for further MEAs. At this loading, the catalyst layer develops large cracks during drying ,and parts of the catalyst layer frequently fall onto the membrane before the transfer is complete. For this

reason, a double dispersion technique was developed: the catalyst ink was first blade coated and then scratched off the substrate using a rubber spatula before once more dispersing it. The new ink thus obtained from the rougher particles dried with fewer cracks and Fig. 46 (right) shows that the electrodes produced in this way were also more powerful.

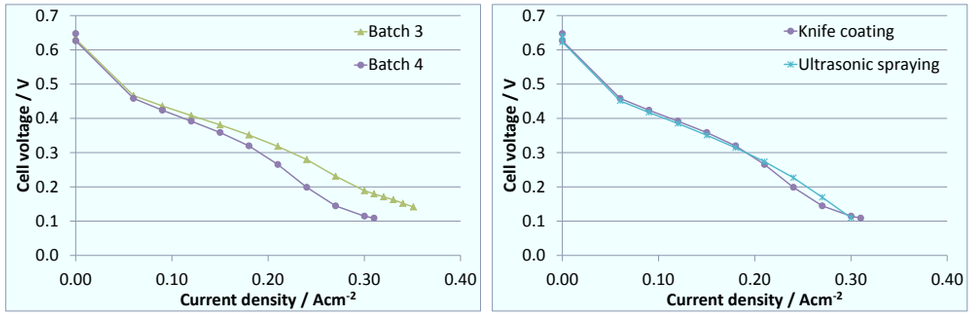

Fig. 47: Characteristic curves using different catalyst batches (left) and different transfer methods (right); T = 70 °C, c(methanol) = 0.75 mol/l, air volume flow rate = 0.037 l/cm²min

Fig. 47 (left) shows that there was a considerable difference in performance between the two larger batches received from CAN. Batch 3, which was the better batch, was produced in a flow reactor in one coating and then transferred to the XC72 substrate, while batch 4, which was of slightly poorer quality, was produced in several coatings and then jointly transferred. In future, uniform quality must be ensured. The previously observed cracking of the catalyst layer can be prevented entirely by applying the catalyst ink on a heated substrate through ultrasonic spraying. With this method, several thin layers are applied and dried immediately until the desired loading is achieved. Fig. 47 (right) shows that the same performance can be achieved using ultrasonic spraying as blade coating.

Cathodes for DMFCs and cathodes for PEM electrolysis have many similarities. It is therefore to be expected that the catalysts developed within the scope of this project might then also be used for PEM electrolysis with minor adaptations. An initial experiment showed that the performance of an MEA with alloy catalysts from CAN is comparable with the performance of an MEA with a commercial cathode catalyst (Fig. 48). However, the CAN catalyst loading on the cathode was considerably higher than the loading of the cathode with the commercial catalyst, since a cathode produced for DMFC with the appropriate loading was used. However, it is usually relatively straightforward to reduce the loading for use in electrolysis. It is thus likely that the catalysts developed within the scope of this project can also be used for electrolysis.

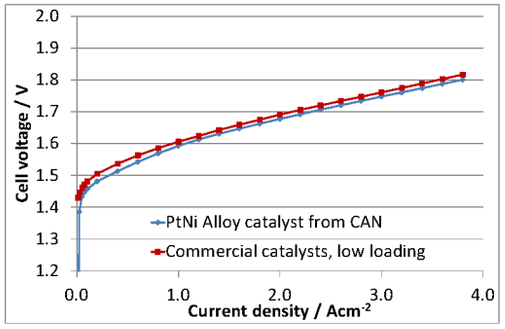

Fig. 48: Characteristic curves of MEAs with alloy catalyst from CAN and commercial catalyst on the cathode in PEM electrolysis operation

3.4.2.2 Control strategies for efficiency-optimized operation of DMFCs

Im As part of a doctoral thesis, an efficiency-optimized operation management concept was developed which concerns the aspects of efficiency maximization as well as error and aging tolerance within the context of long-term stability. Model predictive control (MPC) was used as a basis of operation management, with a model of the entire DMFC developed for this purpose. Practical tests showed that limit values of process parameters to be controlled – stack temperature and cell voltage – are adhered to within the DMFC system. The resulting advantage is particularly crucial in the field of DMFCs, since it prevents low cell voltages and high temperatures, which accelerate the degradation of cells.

In order to maximize efficiency, the input power – determined by the dosage of methanol – was minimized. In this context, a model was created that describes the input power through the controllable process values, i.e. stack temperature, cell voltage, and methanol concentration. By means of statically economic optimization, the minimum input power was detected for a given output power.

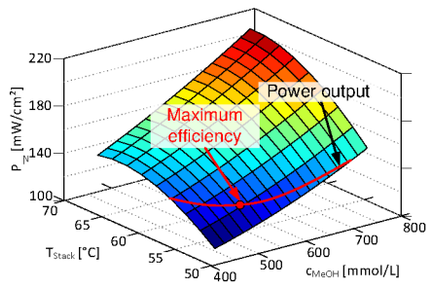

Fig. 49: Minimum specific input power at P_{out} = 53.97 mW/cm²

Fig. 49 shows the input power as a function of the stack temperature and the methanol concentration. The defined output power (53.97 mW/cm²) resulted in a power hyperbola limiting the minimum input power. This showed that the minimum input power is located exactly on this power hyperbola and approaches the function minimum; it denotes the maximum stack efficiency under optimum operating conditions.

In addition, the output power was varied across its range to continuously achieve maximum efficiency at optimum stack temperature and methanol concentration. Fig. 50 a additionally shows the resulting maximum efficiency (red). In contrast to fixed operating parameters, the required output power was provided across the entire operating range. For a direct comparison, Fig. 50 a also shows randomly selected variations of stack temperature and methanol concentration (black).

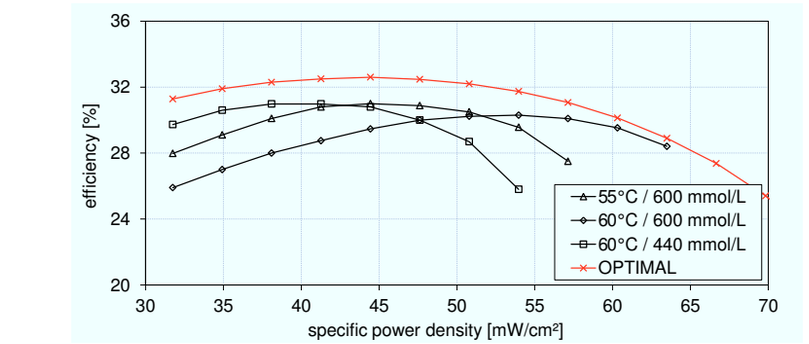

a)

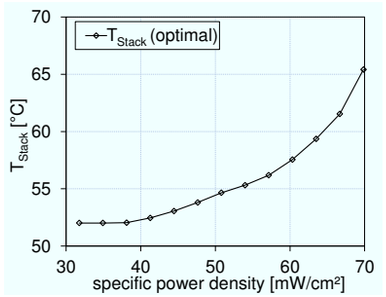

b)

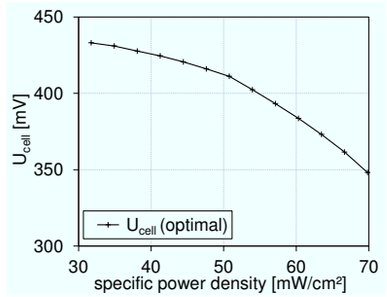

c)

Fig. 50: Comparison of maximum efficiency with varying operating parameters

The maximum efficiency of the DMFC stack (32.6 %) was achieved at an output power density of 44.4 mW/cm². Furthermore, it can be seen that the curve of optimum efficiency for the entire load range was considerably higher than the efficiency curves using fixed operating parameters. The maximum efficiency increase was 7 percentage points. The static economic optimization not only provided the maximum efficiency: through the targeted variation of the individual operating parameters, the minimum stack temperature and maximum cell voltage were set, thus preventing accelerated degradation and critical operating states. The change in stack temperature and methanol concentration are shown in Fig. 50 b and Fig. 50 c.

In terms of long-term stability and the associated degradation phenomena, the measurement data of a 25,000 h DMFC experiment were analyzed with the aim of generating a degradation-dependent cell model. In this context, the initial model of DMFC input power was maintained and expanded to include the characteristic aspect of the degradation degree. Using this degradation-dependent model, the degradation was evaluated in terms of the previously defined operating management aspects. Fig. 51 shows the maximum efficiency and the cell voltage throughout the entire operating time with continuous minimization of the

input power and adaptation to the degradation degree (black) and without continuous minimization of the input power (red).

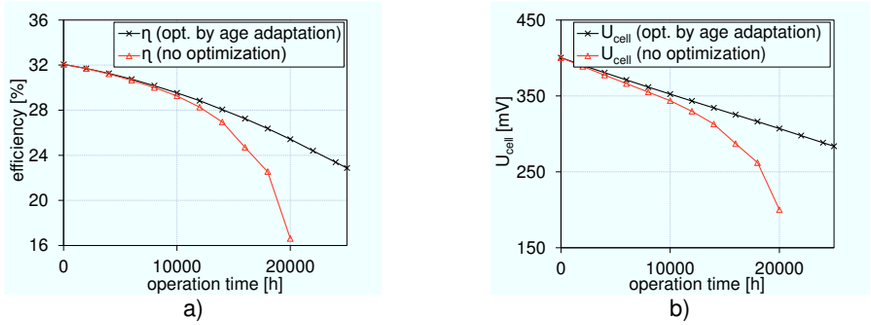

Fig. 51: η **and** U_{Zelle} **at 0…25,000 operating hours**

This showed that when actively minimizing the input power and taking into consideration the current degradation degree, the maximum efficiency decreases by only 9 percentage points over 25,000 operating hours and there are no critical operating points concerning the cell voltage distribution. Inactive minimization over 20,000 operating hours resulted in an additional decrease of efficiency by 10 percentage points. In addition, the cell voltage achieved critical values after 20,000 operating hours, resulting in a considerable reduction in long-term stability.

Based on these results, an active degradation-tolerant operation management strategy was conceived. In doing so, error diagnostics were first developed that unambiguously identify the current degradation degree. Once this was achieved, operation management was reconfigured in relation to the degradation level, so that the maximum efficiency could continuously be achieved and the long-term stability criteria fulfilled. Fig. 52 shows the efficiency and the cell voltage during practical application in a 5-cell DMFC stack. It highlights how the reconfiguration of operation management at 1200 s increased the efficiency even at advanced degradation.

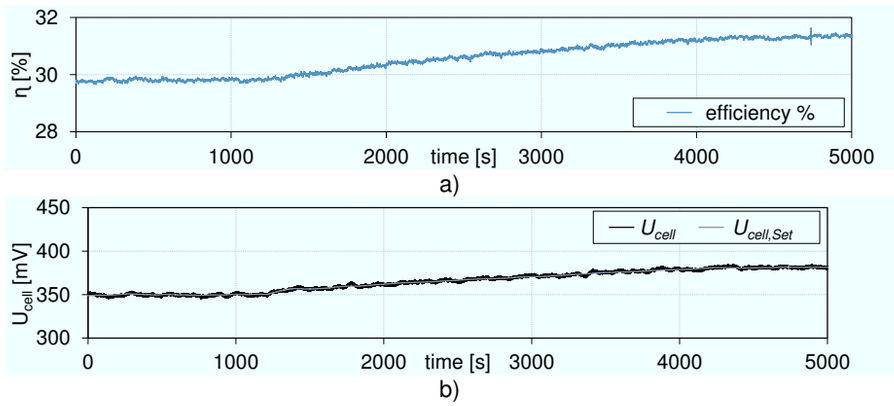

Fig. 52: η **and** U_{Zelle} **during practical application in a 5-cell DMFC stack**

The operation management strategy proved effective: at a degradation of 660 operating hours, stack efficiency increased by 1.5 percentage points (Fig. 52 a). Long-term stability – with a focus on the achievable cell voltage – was also demonstrated experimentally through a maximum increase of $\Delta U_{\mathrm{Zelle}}$ = 30 mV (see Fig. 52 b).

3.4.3 Staff members and fields of activity

Name	Tel. (02461-61-) Email	Field of activity
Dr. M. Müller	1859 mar.mueller@fz-juelich.de	Head/coordinator
Dr. A. Glüsen	5171 a.glüsen@fz-juelich.de	MEA development
M. Hehemann	5431 m.hehemann@fz-juelich.de	Stack and stack manufacture
R. Keller	4124 r.keller@fz-juelich.de	Control development
W. Zwaygardt	2103 w.zwaygardt@fz-juelich.de	Stack and stack manufacture

3.4.4 Important publications, doctoral theses, and patents

Publications

Ince, A. C.; Karaoglan, M. U.; Glüsen, A.; Colpan, C. O.; Müller, M.; Stolten, D.,
Semiempirical Thermodynamic Modeling of a Direct Methanol Fuel Cell System. ***International***
Journal of Energy Research 2019, 0, 1-15. DOI: 10.1002/er.4508

Glüsen, A.; Dionigi, F.; Paciok, P.; Heggen, M.; Müller, M.; Gan, L.; Strasser, P.; Dunin-Borkowski, R. E.; Stolten, D.,
Dealloyed Ptni-Core–Shell Nanocatalysts Enable Significant Lowering of Pt Electrode Content in Direct Methanol Fuel Cells
ACS Catalysis 2019, 9, 3764-3772. DOI: 10.1021/acscatal.8b04883

Karaoğlan, M. U.; İnce, A. C.; Colpan, C. O.; Glüsen, A.; Kuralay, N. S.; Müller, M.; Stolten, D.,
Simulation of a Hybrid Vehicle Powertrain Having Direct Methanol Fuel Cell System through a Semi-Theoretical Approach
Int. J. Hydrogen Energy 2018. DOI: 10.1016/j.ijhydene.2018.11.039

Colpan, C. O.; Ouellette, D.; Glüsen, A.; Müller, M.; Stolten, D.,
Reduction of Methanol Crossover in a Flowing Electrolyte-Direct Methanol Fuel Cell
Int. J. Hydrogen Energy 2017, 42, 21530-21545. DOI: 10.1016/j.ijhydene.2017.01.004

Important patents

Patent applications:

Principal inventor	**PT**	**Description**
Dr. A. A. Kulikovsky	1.2601	Methods for characterizing the catalyst structure in a fuel cell, and fuel cell design suitable for said method
Dr. A. A. Kulikovsky	1.2644	Direct alcohol fuel cell and direct alcohol fuel cell stack with effective CO_2 removal and methods of operating such a direct alcohol fuel cell

3.5 Water electrolysis

3.5.1 Objectives and fields of activity

The Electrochemistry Electrolysis (EEL) and Process Engineering Electrolysis (VEL) departments' work focuses on the development of commercially viable electrolysis systems and components. The priority here is the issue of cost reduction, which is achieved by increasing the lifetime and power density. Yet improving efficiency is also key to being able to make practical use of electrolysis on a large scale in the future.

Major progress with regard to increased power density and efficiency has been achieved by reducing the membrane thickness and thus increasing ionic conductivity. This work has mainly been directed at PEM electrolysis in the past and will be expanded to include alkaline electrolysis in the future.

In the long term, the focus of development is on the storage of large quantities of energy produced from renewable sources. The use of electrolysis on a scale of gigawatts is necessary for this. In order to improve its economic viability, the proportion of platinum group metals must be kept as low as possible, and simultaneously the lifetime of the electrodes must be increased to 40,000 hours or more. One approach for achieving this involves developing suitable catalyst and electrode structures. The nanostructured catalysts developed at the institute in particular may be a key technology in this effort.

Another priority is running electrolysis at high temperatures. By increasing the temperature to values of up to approx. 200 °C, it is expected that the reaction kinetics will be improved and it will simultaneously be made technically feasible to extract waste heat. As outlined below, we take a holistic approach to low-temperature water electrolysis, which ranges from electrochemistry to the overall functioning system. This makes it possible to identify the often complicated interactions between the cell and system components, and to achieve development that is in line with the stated goals.

3.5.2 Important results

3.5.2.1 Nanocatalysts for Water Electrolysis

The sluggish kinetics of the oxygen evolution reaction (OER) leads researchers to continue to develop more active and stable electrocatalysts for water electrolysis. Currently, the most active OER catalysts in acidic solutions are IrO_2 or RuO_2, but these catalysts suffer from the scarcity and high cost of precious metals. Intense research efforts have been dedicated to obtain high surface areas, maximum atomic utilization and low-cost electrocatalysts such as first-row transition metal oxides and perovskites[10,11]. Doping with non-noble metals can reduce the Ir content of electrocatalysts and meanwhile increase their intrinsic activity owing to the synergistic effects between different metals[12]. A very promising approach is the

[10] Koper, M. T. M. Thermodynamic Theory of Multi-Electron Transfer Reactions: Implications for Electrocatalysis. J. Electroanal. Chem. 2011, 660 (2), 254–260.
[11] Wang, H.; Dai, H. Strongly Coupled Inorganic-Nano-Carbon Hybrid Materials for Energy Storage. Chem. Soc. Rev. 2013, 42 (7), 3088–3113.
[12] Chen, C., Y. et al. Directions at low temperature in the Present Classical Theory without Randomness, S. Science (80-.). 2014, 343 (March), 1339–1343.

bimetallic framework nanostructures which can achieve excellent catalytic activity compared to bulk materials. The three dimensional geometry and exposed corners and edges will have a positive role as the active sites. Here we report on a synthetic strategy for one pot preparation of Ni-Ir core shell nanostructures which further etched to form a nanoframe structure. Since thermodynamic calculations suggest that iridium does not favor the formation of binary alloy phase with Ni due to the negative segregation energies of IrNi phases, these data predict that Ir-based multimetallic nanocrystals can serve as desired model systems for core–shell structures. As presented in Fig. 53 the morphology of as-prepared Ni-Ir which was characterized by scanning transmission electron microscopy (STEM) and EDX map has a core shell structure.

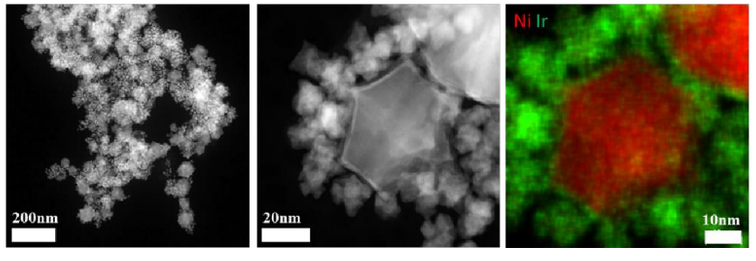

Fig. 53: **(a) high-angle annular dark field scanning TEM (HAADF-STEM) overview image of as-prepared Ni-Ir nanostructures. (b) High resolution HAADF STEM image of a single Ni-Ir nanostructure, (c) corresponding EDX maps showing Ni (red) and Ir (green).**

As large amount of Ni in the structure for the OER in acidic condition is not beneficial for the stability of the electrocatalysts, the next step was to remove the Ni from the core and stay with a nanoframe structure. Forming the nanoframe is done by choosing the selective etching of the leachable component from phase-segregated solid alloy nanoparticles. In our case Ni is more favorable to leach out to form the Ni-Ir nanoframe by using acid treatment. As presented in Fig. 54 the HAADF-STEM images shows Ni-Ir nanoframe after the etching process.

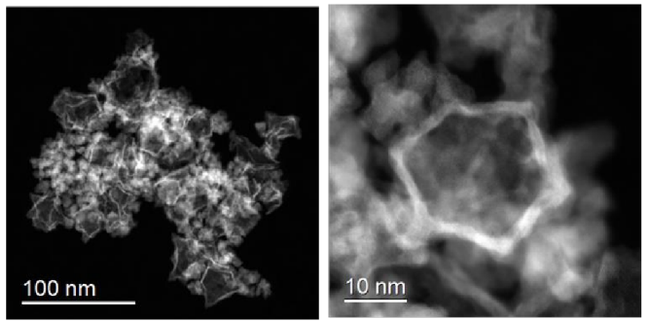

Fig. 54: **(a) HAADF-STEM image of Ni-Ir nanoframes after etching.**
(b) High resolution HAADF STEM image of a single Ni-Ir nanoframe.

As the next step we will study those nanoframes as electrocatalysts for the OER in acid solution. We believe that this investigation will open up alternative route for the assembly of alloyed bimetallic nanostructures and also provide prospective OER catalysts for potential energy conversion in the future.

3.5.2.2 MEA Manufacturing

The manufacture of membrane electrode assemblies (MEAs) for PEM water electrolysis is faced with the challenge of increasing the electrochemical efficiency of the MEAs and of structuring the processes used for this in such a way that they are scalable and can be used for mass production. The electrochemical efficiency (eta) of the MEAs heavily depends on the thickness of the membrane used (Fig. 55), because the protons flowing through the membrane during cell operation cause ohmic losses, which heat up the membrane.

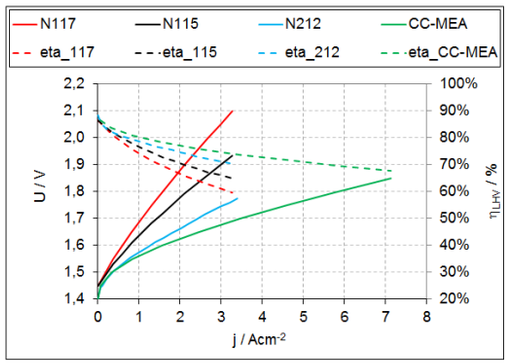

Fig. 55: Effect of membrane thickness on the polarization curve and efficiency (relative to the lower heating value LHV) of an MEA for PEM water electrolysis. N117: membrane thickness of 178 µm, N115: membrane thickness of 127 µm, and N212: membrane thickness of 50 µm. The results for a CC-MEA with equal catalyst loading are shown in green. The membrane thickness is 20 µm.

If using very thin membranes to build PEM MEAs proves successful, these loss processes can be greatly reduced and the efficiency can be increased. However, the disadvantage of just a few membranes with thicknesses of 10 µm is that they are difficult to manufacture and tear easily, especially in the manufacturing process of large-area MEAs. Furthermore, the small membrane thickness leads to increased hydrogen permeation through the membrane during cell operation, causing higher hydrogen concentrations on the anode, which may form hazardous explosive mixtures of hydrogen and oxygen.

In order to solve the mechanical problem involved in working with the thin membranes, a new method was developed at IEK-3. In this method, the MEA is produced using only a coating process and without using a separate membrane. The most important steps in such a CC-MEA (completely coated MEA) manufacture are shown in Fig. 56.

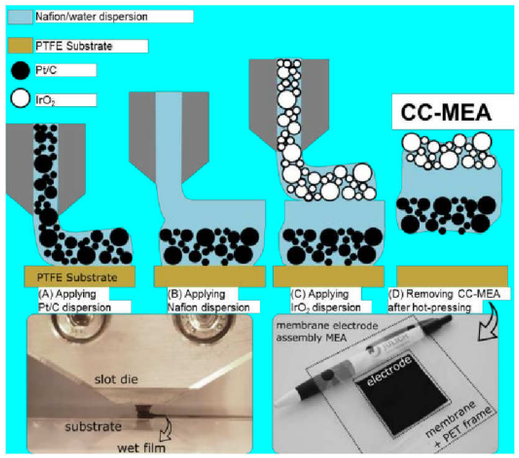

Fig. 56: **A–C: The CC-MEA is manufactured by successively applying coatings of the cathode, the membrane, and the anode. D: After a hot-pressing process, the CC-MEA is removed from the carrier film (PTFE). Bottom left: Side view of the slot nozzle during coating. Bottom right: CC-MEA including a PET frame stabilization (the dotted line indicates the PET frame).**

The cathode dispersion is first applied to a PTFE substrate using a slot nozzle and then dried for the manufacture of the CC-MEA. In order to ensure better stability for the later MEA, a PET frame is then placed around the active surface area of the electrode, and an ionomer solution (Nafion D2021) is poured over both the frame and the electrode. The dried membrane is coated with the anode dispersion in a final coating step. After the anode has been dried and the hot-pressing process is finished, the CC-MEA can be removed from the PTFE. The PET frame gives the CC-MEA sufficient mechanical stability despite its low membrane thickness of 20 µm, meaning that it can be characterized easily in single-cell measurements.

Further work is necessary in order to identify why the processes responsible for the permeation occur and thus to reduce the high hydrogen permeation that occurs with the thin membranes. One factor influencing the permeation is the cathode's electrode structure, which forms during the manufacture of the electrode, specifically as it is being dried. In order to understand the correlations between drying and structure formation in the electrode, a drying analysis technique developed at IEK-3 was used to understand the causes of cracking and their dependence on manufacturing parameters.

In this technique, layers of catalyst-free dummy dispersions containing aqueous propanol were produced using a slot nozzle with different wet layer thicknesses. A clear increase in the number and width of cracks was found both when the layer thickness increased and when the amount of propanol in the dispersion decreased (see Fig. 57). The results illustrate the possibility of targeted control of the macroscopic layer formation process with only a slight modification of the original system. Other possibilities for designing the layer formation process so as to be controllable will be reviewed in future. This allowed for a study of the correlation of cracks, electrode performance, and H_2 permeation.

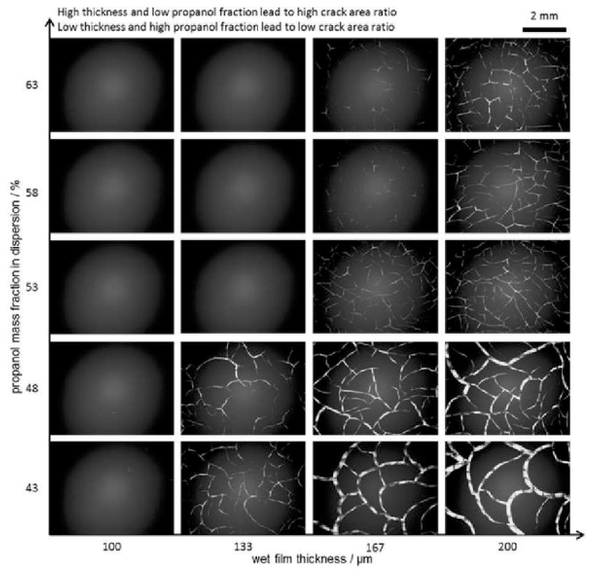

Fig. 57: Effect of layer thickness and propanol mass fraction in the original dispersion on the formation of cracks in the dried layer.

The correlation between hydrogen permeation and electrode structure will be studied further in future work, so as to reduce permeation to the point that no safety-critical aspects occur. The goal is to use the CC-MEA method for large-scale MEA manufacture and their safe operation.

3.5.2.3 Alkaline water electrolysis

In close collaberation with the Frauenhofer Institute IMWS and the company Kumatec GmbH, intensive investigation of electrode development for the hydrogen evolution reaction in alkaline electrolysers is now underway. The aim of the ELKE (Entwicklung leistungsoptimierter und kostengünstiger Elektrodenstrukturen für die alkalische Elektrolyse) project is to design new electrodes which are high in performance (1 A cm^{-2} at 2 V), low in fabrication cost and, most importantly, highly durable. Raney-Nickel and various Ni/Mo alloys have therefore been chosen as electro-catalyst materials due to their high stability in strongly alkaline environments. The preferred deposition method is blade-coating due to its adaptability to the roll-to-roll method by which electro-catalysts can be deposited onto substrates continuously and on large scales, which reduces the cost significantly. To achieve these goals a new laboratory has in the past year (2018) been set up at IEK-3 to allow the simultaneous operation of eight single alkaline electrolysis cells. One of the four test-rigs can be seen in Fig. 58, which shows a pre-heater cell which heats the electrolyte before it flows into the two measurement cells. Two of the test-rigs are used for short-term measurements such as polarization curves to quickly provide an initial insight into the newly designed electrodes. The remaining two rigs are set aside for long-term durability studies.

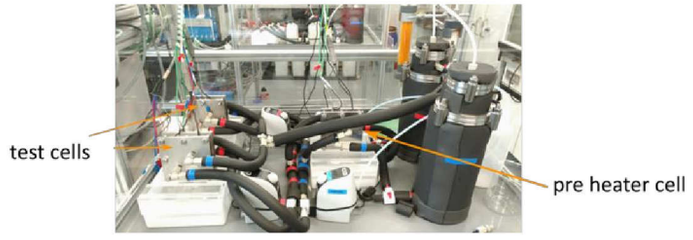

Fig. 58: Photograph of an alkaline test-rig in the newly established laboratory

The new electrodes developed during the course of the ELKE project will need to be compared to a stable benchmark electrode, for which nickel foam is an obvious choice. A sketch of the employed cell design can be seen in Fig. 59 Only the cathode side will be modified with the new electro-catalysts. On the anode side a pre-heated Ni foam is welded onto the flow field to ensure the anode is the same in each measurement. The temperature of the cells is maintained at 80 °C, and a KOH concentration of 32.5 wt% is used.

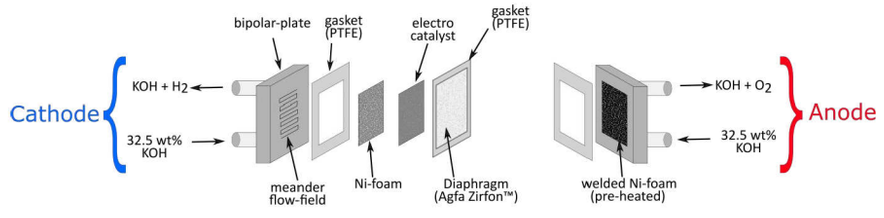

Fig. 59: Sketch of the cell design used in IEK-3 studies of alkaline electrolysis

To ensure the newly constructed test-rigs can reproducibly and interchangeably characterise the benchmark cell, the latter was assembled ten times and the performance was measured each time using two different test-rigs. The results obtained are illustrated in Fig. 60, and it can be seen there is reasonable agreement between the two rigs. Average voltages and standard deviations are represented by data points and error-bars, respectively. The baseline voltage at 200 mA/cm² of one test rig is 2.00 ± 0.04 V and for the other is 2.01 ± 0.03 V.

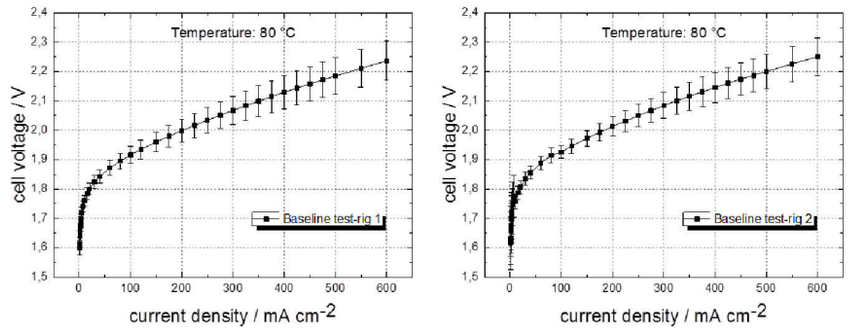

Fig. 60 Polarisation curves obtained using the baseline arrangement in both of the short-term test-rigs.

A long-term test was also performed using the benchmark cell, by which a voltage of 2 V was applied for 1000 h to determine how the nickel foam degraded over time. The result in Fig. 61 shows after 200 h it was found that the cell had attained a stable condition, and subsequently no further degradation was observed.

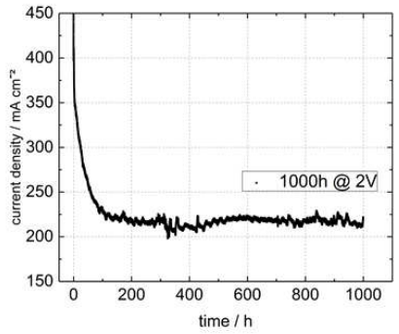

Fig. 61: Long-term measurement of the benchmark cell for 1000 h at 2 V

3.5.3 Staff members and fields of activity

Name	Tel. (02461-61-) Email	Field of activity
Dr. M. Müller	1859 mar.mueller@fz-juelich.de	Head of Process Engineering Electrolysis
Dr. M. Carmo	5590 m.carmo@fz-juelich.de	Head of Electrochemistry Electrolysis
Dr. M. Stähler	2775 m.staehler@fz-juelich.de	Head of MEA Manufacturing Technology
D. Borah	6365 d.borah@fz-juelich.de	Flow simulation
E. Borgardt	3079 e.borgardt@fz-juelich.de	Stack development, stack mechanics
A. Burdzik	2574 a.burdzik@fz-juelich.de	MEA Manufacturing
S. Cheriyan	2094 s.cheriyan@fz-juelich.de	Analytics
N. Commerscheidt	3464 n.commerscheidt@fz-juelich.de	Stack manufacture, cell tests
S. Fischer	4478	MEA Development

	st.fischer@fz-juelich.de	
I. Friedrich	1948 i.friedrich@fz-juelich.de	MEA Manufacturing
Dr. A. Glüsen	5171 a.gluesen@fz-juelich.de	Use of polymeric materials
D. Günther	2378 d.guenther@fz-juelich.de	Electrochemical characterization, quality assurance of processes
M. Hehemann	5431 m.hehemann@fz-juelich.de	Safety engineering of test stands
D. Holtz	2956 d.holtz@fz-juelich.de	MEA Development
R. Lambertz	6695 r.lambertz@fz-juelich.de	Flow visualization, modeling, 3D topography
Dr. M. Langemann	9759 m.langemann@fz-juelich.de	Development and evaluation of suitable substrates and coatings for metallic bipolar plates
O. Panchenko	3079 o.panchenko@fz-juelich.de	Development and characterization of porous layers
L. Ritz	5725 l.ritz@fz-juelich.de	Mechanics
S. Saba	9568 s.saba@fz-juelich.de	Economic viability of electrolysis systems
F. Scheepers	2177 f.scheepers@fz-juelich.de	MEA manufacturing
A. Schulz	8965 a.schulz@fz-juelich.de	MEA manufacturing
R. Wegner	4832 r.wegner@fz-juelich.de	Mechanical assembly of stacks and systems
W. Zwaygardt	2103 w.zwaygardt@fz-juelich.de	Stack development and characterization

3.5.4 Important publications, doctoral theses, and patents

Publications

Borgardt, E., Panchenko, O., Hackemüller, F. J., Giffin, J., Bram M., Müller, M., Lehnert, W., Stolten, D.

Mechanical characterization and durability of sintered porous transport layers for polymer electrolyte membrane electrolysis
Journal of Power Sources 374, Pages 84-91 {2018}

Saba, S. M., Müller, M., Robinius, M., Stolten, D.
The investment costs of electrolysis--a comparison of cost studies from the past 30 years
International Journal of Hydrogen Energy 43, Pages 1209-1223, 2018

Tjarks, G., Gibelhaus, A., Lanzerath, F., Müller, M., Bardow, A., Stolten, D.
Energetically-optimal PEM electrolyzer pressure in power-to-gas plants
Applied Energy 218, Pages 192-198, 2018

Panchenko, O., Borgardt, E., Zwaygardt, W., Hackemüller, F. J., Bram, M., Kardjilov, N., Arlt, T., Manke, I., Müller, M., Stolten, D., Lehnert, W.
In-situ two-phase flow investigation of different porous transport layer for a polymer electrolyte membrane (PEM) electrolyzer with neutron spectroscopy
Journal of Power Sources 390, Pages 108-115, 2018

Carmo, M., Keeley, Gareth P., Holtz, D., Grube, T., Robinius, M., Müller, M., Stolten, D.
PEM water electrolysis: Innovative approaches towards catalyst separation, recovery and recycling,
International Journal of Hydrogen Energy 44 (7), Pages 3450-3455, 2019

Panchenko, O., Giesenberg, L., Borgardt, E., Zwaygardt, W., Kardjilov, N., Markotter, H., Arlt, T., Manke, I., Müller, M., Stolten, D., Lehnert, W.
Influence of Stoichiometry on the Two-Phase Flow Behavior of Proton Exchange Membrane Electrolyzers
Energies 12, 2019

Müller, M., Carmo, M., Glüsen, A., Hehemann, M., Saba, S., Zwaygardt, W., Stolten, D.
Water management in membrane electrolysis and options for advanced plants
International Journal of Hydrogen Energy (44), Pages 10147-10155, 2019

Bender, G., Carmo, M., Smolinka, T., Gago, A., Danilovic, N., Mueller, M., Ganci, F., Fallisch, A., Lettenmeier, P., Friedrich, K. A., Stolten, D.
Initial approaches in benchmarking and round robin testing for proton exchange membrane water electrolyzers
International Journal of Hydrogen Energy, 2019

Important patents:

Patenet applications:

Principal inventor	**PT**	**Description**
Dr. M. Müller	1.2770	Electrolysis cell and technique for operating the same

3.6 Rocess and Systems Analysis

3.6.1 Objectives and fields of activity

The process and systems analysis department (VSA) underwent considerable change during the period under review. In particular, new and innovative topics were included in the research portfolio (see examples below). This led to a considerable increase in current personnel to approx. 35 scientists, doctoral researchers, and master's and bachelor's students (see Fig. 62). Within the department (head: Dr. Martin Robinius), these new topics were integrated in the groups Stationary Energy Systems (head: Dr. Peter Markewitz), Transportation (head: Dr. Thomas Grube), and Sector Coupling and Infrastructures (head: Dr. Jochen Linßen).

Fig. 62: Process and systems analysis group

The new topics lead to a considerable expansion of techno-economic analyses of hydrogen-based supply pathways towards analyses of entire systems. The department uses energy system models to analyze transformation processes related to the supply and use of energy in Germany and beyond in accordance with the political framework conditions. One major objective is to provide policymakers and industry with the expertise required to take action with respect to the energy transition.

Furthermore, the VSA department's clear aim is to lead the modeling community as well as society towards energy system models. In addition to a series of studies and papers, the VSA department is providing a number of models in an open source format (see below). This means that the entire source code is freely accessible for anyone.

The work conducted at the VSA department was awarded several accolades during the period under review, for example the paper by Welder et al.[13], which, among 444 entries, received the best paper award at the SDEWES conference in Dubrovnik. A paper by

[13] L. Welder, D.S. Ryberg, L. Kotzur, T. Grube, M. Robinius, D. Stolten, Spatio-temporal optimization of a future energy system for power-to-hydrogen applications in Germany, Energy 158 (2018) 1130-1149.

Robinius et al.[14] was awarded the Third Research Paper prize of 2017 by the open access journal *Energies*.

Thanks to current research efforts, the VSA department was able to attract funding for a range of projects and is currently heading two of the Federal Ministry for Economic Affairs and Energy's large-scale projects (MODEX-NET and METIS).

The aim of METIS is to further increase the accuracy of energy system models for operating and dimensioning optimizations as well as to expand their frame of reference within the scope of sector coupling. At the same time, user requirements must be met in terms of clarity and short computing times. In order to reconcile the, at times, adverse demands of modeling, methods are being developed to reduce systematic complexity with a focus on maintaining the accuracy of the models. Furthermore, new data aggregation methods will be developed with a particular emphasis on big data. In addition, various mathematical decomposition algorithms are being tested in order to reduce the computing time of linear and mixed-integer optimization problems as well as to benefit from a higher degree of parallelized computing resources. One- and multi-node models are used for model validation, with both myopic and hard-coupling approaches, in order to optimize the operation of existing systems and the dimensioning of planned systems in equal measure. The software tools developed are made available open source to guarantee the clarity and quality of the methods and models, and to ensure openness and transparency.

The overarching aim of the research project MODEX-NET is a comparison of existing power grid models that represent both the national and the European transmission grid. Using defined case studies (model experiments), the differences between models are identified and analyzed. This comprises a comparison of methodological principles, model architectures, and data from the transmission grid models involved. A particular focus is on the flexibility of supply and demand. On the basis of the insights gained, proposals will be derived for the further development of transmission grid models to increase their significance for the *Energiewende*.

As mentioned above, the developments in the VSA department reflect the stronger orientation towards techno-economic energy systems analysis and away from concrete process analyses. To reflect this reorientation, the department has been renamed from Process and Systems Analysis (VSA) into Techno-Economic Energy Systems Analysis (TSA). In addition, the increase in personnel will be further pursued. This may require the research topics to be subdivided into further groups.

3.6.2 Important results

This chapter will present selected research results from the groups Stationary Energy Systems (head: Dr. Peter Markewitz), Transportation (head: Dr. Thomas Grube), and Sector Coupling and Infrastructures (head: Dr. Jochen Linßen).

[14] M. Robinius, A. Otto, P. Heuser, L. Welder, K. Syranidis, D. Ryberg, T. Grube, P. Markewitz, R. Peters, D. Stolten, Linking the Power and Transport Sectors—Part 1: The Principle of Sector Coupling, Energies 10(7) (2017) 956.

3.6.2.1 Stationary Energy Systems

Lifetimes of fossil ower plants

In many energy scenarios, the assumption of power plant lifetimes plays a central role, since it is often used to project the existing fleet of power plants or as a criterion for decommissioning. The results of such analyses are power plant capacity retirement graphs, which are then used to determine the replacement demand. Many studies refer to empirical values for the assumption of lifetimes without specifying them in greater detail. Against this backdrop, an ex post analysis was conducted – accurate to each individual unit – of German power plants that have been decommissioned since 1990. This analysis shows that the lifetime of fossil-fired power plants has extended considerably over the decades. While the real lifetimes of coal-fired power plants were in a range of 30 to 35 years in the 1990s, they today last for 40 to 45 years. This ex post analysis presents the first reliable lifetime analysis for decommissioned German plants, which can serve as a solid basis for future power plant fleet projections. Particularly within the scope of current discussion regarding the phase-out of coal-fired power generation and the correlating premature decommissioning of coal-fired power plants, the lifetimes determined represent a good basis for evaluation[15].

Cost uncertainties in energy systems models

In order to create energy and greenhouse gas reduction scenarios, optimization models are frequently used which are generally based on a linear optimization approach with a cost-reducing target function. The assumption of input data (e.g. future investments in a technology) by nature correlates with considerable uncertainties. One major objective of optimization calculations is to identify robust solutions. For this purpose, a quadratic approach (quadratic programming) was developed that describes the investments as a function of the capacity of a technology. The approach was integrated in IEK-3's existing national energy systems model. The results reveal that compared to conventional optimization approaches, the new approach selects a larger range of technologies and prevents penny-switching effects. Compared to alternative methods, such as stochastic approaches or Monte Carlo simulations, the computation times are only slightly longer. The approach can also be integrated into existing solvers such as Gurobi, CPLEX, or XPRESS.

Using PV battery storage systems to supply emergency power to single-family houses during blackouts

The combination of battery storage systems with photovoltaic cells in residential buildings in Germany has developed to become state of the art and an established market. Alongside the aim of increasing internal consumption from photovoltaic cells, the option of having an emergency power supply plays a role in decisions to purchase battery storage systems. The emergency power functionality of photovoltaic battery energy storage systems (PV-BESS) was evaluated on the basis of a case study comprising a single-family house in Germany with a defined power load profile and installed PV-BESS. Important factors influencing the emergency power functionality include the beginning and duration of the blackout, the power load and PV production profile during the blackout, and the state of charge of the BESS at

[15] P. Markewitz, M. Robinius, D. Stolten, The Future of Fossil Fired Power Plants in Germany - A Lifetime Analysis, energies 11(6) (2018) 1616.

the beginning of the blackout. The backup functionality particularly depends on the available power generated from the PV cells and therefore has a strong seasonal dependence. In the event of a blackout, a PV-BESS generally provides power that would not be available to a household without a PV-BESS. The complete coverage of longer blackout periods by means of PV-BESS – assuming a normal load profile (100 % independent system operation) – is, however, limited to a few periods of high PV production during the year. In this context, load reduction and load shift through adapted user behavior during a blackout have significant potential to increase the backup supply functionality by extending the period over which the reduced household power load can be covered by PV-BESS[16].

Analysis and evaluation of suitable future energy supply concepts for the reduction of greenhouse gas emissions in urban areas

The urban energy transition requires new greenhouse gas reduction strategies due to the limited availability of land for the construction of energy generation units, on the one hand, and the high population density and the associated high demand for energy, on the other hand. Potential new strategies were considered in a real urban area (neighborhood) in a cluster of residential buildings. To determine the strategies, a mixed-integer optimization approach was selected. The aim of the study is to investigate local sector coupling effects as well as to determine future requirements of operating facilities (e.g. local grid transformers) in a specific urban area under various techno-economic framework conditions. Due to the large number of buildings and technology options, neighborhoods pose a complex optimization problem whose solution is associated with long computing times. To this end, a new two-level approach was developed for the mixed-integer optimization problem in order to reduce complexity and computing time while maintaining a high quality solution[17].

Hydrogen reconversion into electric power

In einer Studie wurden Wasserstoff-Strom-Umwandlungspfade zur Deckung von positiven In one study[18], hydrogen-to-power conversion pathways were techno-economically analyzed in terms of covering positive residual loads from renewable power that is otherwise unusable in the system. The investigations are based on an energy scenario for North Rhine-Westphalia (NRW) for the investigated year 2050, in which otherwise unusable power from northern Germany is converted into hydrogen and stored. In times of low renewable feed-in, the hydrogen can be reconverted into electric power in order to cover demand. The analysis was conducted by means of the cost-optimized energy system model FINE. One key result from the pathway analysis is that the power requirements in NRW can be covered completely by renewable energy sources in this scenario. The reduction in CO_2 amounts to 44.4 million t/ compared to a system in which residual load demand is covered by the conventional power

---

[16] P. Stenzel, T. Kannengießer, L. Kotzur, P. Markewitz, M. Robinius, D. Stolten, Emergency power supply from photovoltaic battery systems in private households in case of a blackout – A scenario analysis, Energy Procedia 155 (2018) 165-178.

[17] T. Kannengiesser, M. Hoffmann, L. Kotzur, P. Markewitz, M. Robinius, D. Stolten, Optimization of Urban Energy Supply Systems with 2-Level Approach, (In Preperation).

[18] L. Welder, P. Stenzel, M. Robinius, D. Stolten, Design and Evaluation of Hydrogen Electricity Reconversion Pathways in National Energy Systems Using Spatially and Temporally Resolved Energy System Optimization, Submited to International Journal of Hydrogen Energy 2018-11-18 (2018).

plant fleet in NRW. The pathway analysis reveals that the most cost-effective option is the use of gas and steam turbines to reconvert hydrogen into electric power, with power generation costs of € 176/MWh (including costs of power procurement, electrolysis, storage, and infrastructure for reconversion). The structure of this pathway is shown in Fig. 63.

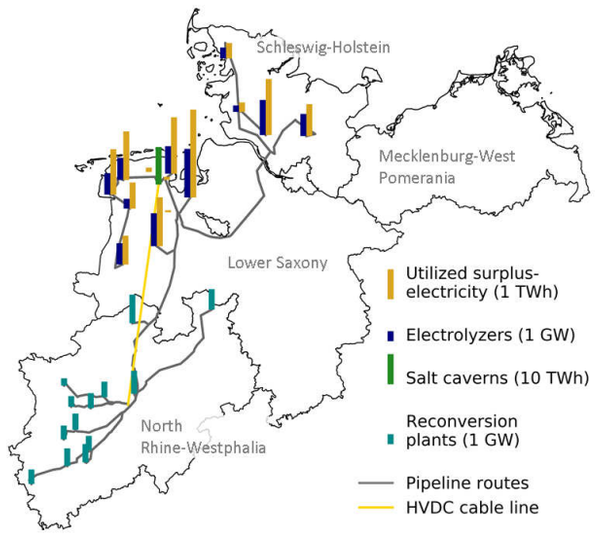

Fig. 63: Surplus power, installed capacities of electrolysis and power plants, and necessary transmission infrastructures of the most cost-effective reconversion pathway

An extensive hydrogen storage and conversion system as well as the use of a dedicated hydrogen infrastructure can thus help to relieve the load on the power grid. In addition, the evaluated hydrogen conversion pathways, including seasonal storage in salt caverns, make a considerable contribution to increasing the supply security of a mostly renewable energy system.

3.6.2.2 Sector coupling and infrastructures

The transformation of the energy system requires a reorganization of the existing energy system with a considerable increase in renewable energy and energy efficiencies, and the defossilization of the end energy demand . These developments frequently require considerable adaptations as well as the expansion and also dismantling of existing infrastructures for the conversion, transport, and distribution of energy carriers. Sector coupling permits the expanded use of renewable energy in all end energy sectors. The developed set of models permit the analysis and evaluation of individual technology pathways and entire energy systems. Within the scope of scenario analyses, it is possible to conduct system simulations and optimization calculations as well as to analyze and evaluate efficiencies, dynamics, emissions, and costs of future energy systems. The aim of the analyses is to quantify the potential contributions of innovative technologies, concepts, and system designs to strategies aiming to reduce greenhouse gas emissions as well as to define techno-economic requirements of infrastructures in the energy supply system.

Power generation from onshore wind power makes an important contribution to the reduction of global greenhouse gas emissions. Evaluating possible wind power generation potentials in Europe is the subject of numerous research activities. These potential evaluations are based on numerous assumptions on the distribution of the wind turbines, their current design, and performance values as well as the local wind conditions. Potential wind turbine designs that are adapted to wind conditions are given hardly any consideration in currently published potential evaluations. To account for future turbine designs and resulting power generation costs in the potential analyses for Europe, an existing cost model was expanded to include future turbine designs and considered in the potential analyses. Based on the GLAES model and data on land availability in Europe from[19], the inclusion of an adapted wind turbine design results in a maximum installable generation capacity of onshore wind power generation of 13.5 TW in Europe for the year 2050. Taking into account the spatially resolved wind speed developments of various weather years results in a technical power generation potential of 34.4 PWh. The power generation costs of the relevant generation sites differ considerably in some cases, depending on the wind speed and the turbine design, with power generation costs increasing with the total capacities of a region. This is due to the fact that wind sites of poorer quality also have to be exploited in order to achieve high regional generation potentials. Fig. 64 shows the behavior of the average power generation costs of onshore wind energy facilities as a function of the desired onshore wind energy generation capacities in a European country. The relevant cost increase is strongly dependent on the local wind situation and the available land with good wind yield situations. The UK, France, Spain, Norway, Austria, Ireland, Denmark, Sweden, Finland, and Greece all offer power production potential with generation costs of less than 3 ct/kWh. Norway has the highest capacity potentials and does not exceed the threshold of 3 ct/kWh until the installed capacity reaches almost 50 GW. According to this potential evaluation, Germany has a wind energy facility capacity of just over 100 GW at power generation costs of less than 5 ct/kWh.

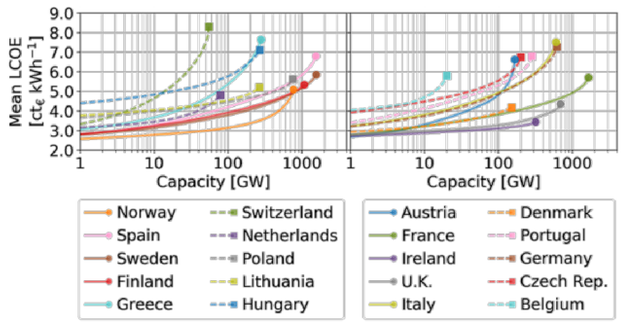

Fig. 64: Development of average power generation costs of onshore wind energy facilities as a function of the total capacity of a region [20]

The significant increase of supply-dependent power generation from renewable energy sources (primarily wind and PV) in Europe requires a considerable expansion of flexibility in

[19] S. Ryberg, M. Robinius, D. Stolten, Methodological Framework for Determining the Land Eligibility of Renewable Energy Sources, arXiv, 2017.

[20] Ryberg, D.S.; Caglayan, D.G.; Schmitt, S.; Linßen, J.; Stolten, D..; Robinius, M. The Future of European Onshore Wind Energy Potential: Detailed Distribution and Simulation of Advanced Turbine Designs. Preprints 2018, doi: 10.20944/preprints201812.0196.v1.

power demand. Based on the high-resolution temporal and spatial power grid model EUROPOWER, the influence of demand flexibility options in the form of storage systems or controllable consumers was analyzed in terms of the integrability of renewable energy in Europe's future power supply system[21].. In order to investigate the high market penetration of renewable energy in future, a scenario was developed for the power supply of Europe in the year 2050. A variation of the proportion of flexible power demand shows that both surplus power and load coverage deficit can be reduced all over Europe through increased flexibility. However, this effect is considerably limited by the shift period of the flexible loads. With an assumed flexible power demand of 10 % of the entire power demand and a 24 h load shift period, only a 7 % reduction of renewable surplus power and a 12.1 % reduction of the load coverage deficit can be achieved. Further reductions of surplus energy and load coverage require seasonal energy storage systems and further grid expansions.

As part of an analysis of future energy systems designs, potential power-to-hydrogen pathways for Germany were investigated, taking into consideration spatially and temporally resolved data[22]. The FINE model generator was used for the optimization of the energy system. The investigated energy system represents renewable power generation based on onshore wind turbines for the production of hydrogen via electrolysis, which is used to supply passenger cars and industry. A 75 % penetration of the passenger car fleet with fuel cell drives is assumed as well as the industrial use of hydrogen in ammonia, methanol, and blast-furnace steel production processes, and in refinement processes in the year 2050. In total, this results in an annual hydrogen demand of approx. 4.1 million t/a The energy supply system is optimized both with and without the option of geological hydrogen storage in salt caverns. The resulting system designs are shown in Fig. 65.

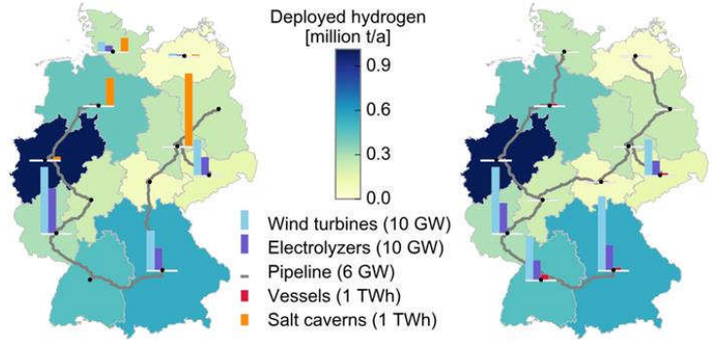

Fig. 65: Result of the energy system optimization (left: with salt caverns as a geological storage option; right: without salt cavern storage)

In the first scenario, salt caverns are calculated with a capacity of 10 TWh (relative to the heating value of the stored hydrogen) and onshore wind turbines with a capacity of 79 GW_{el}. The geological storage systems are used for seasonal storage as well as to soften the

[21] K. Syranidis, P. Markowitz, J. Linssen, M. Robinius, D. Stolten, Flexible Demand for Higher Integration of Renewables into the European Power System, 2018 15th International Conference on the European Energy Market (EEM), 2018, pp. 1-6.

[22] L. Welder, D.S. Ryberg, L. Kotzur, T. Grube, M. Robinius, D. Stolten, Spatio-temporal opti optimization of a future energy system for power-to-hydrogen applications in Germany. In: Energy 158 (2018), pp. 1130-1149.

impact of fluctuations in demand. In the scenario without salt caverns, technical storage systems with considerably higher specific storage costs must be constructed. The cost optimization leads to a significant reduction of the storage capacity of technical storage systems (0.8 TWh_{H2}) and a simultaneously considerable increase of installed onshore wind energy capacities (116 GW_{el}). This in turn leads to considerably stronger curtailment of wind power compared to the scenario with salt caverns. The comparison of the resulting hydrogen generation costs is shown in Fig. 66.

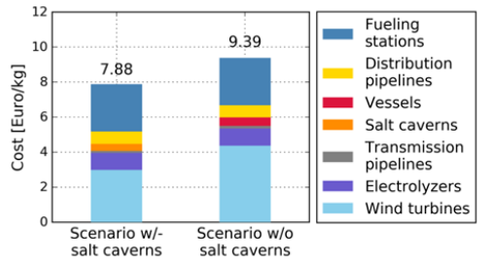

Fig. 66: Specific hydrogen generation costs in the 2050 scenario

The specific hydrogen generation costs were calculated at below € 10/kg_{H2} in both scenarios. A comparison of the two supply systems shows that the availability of salt caverns for the geological storage of hydrogen leads to a reduction in costs of approx. € 1.5/kg_{H2}, thus highlighting the value of salt caverns in hydrogen supply systems.

3.6.2.3 Transportation

Analysis of the contribution of various drive strategies to achieving climate protection goals

In terms of the national targets for reducing greenhouse gas emissions, the transportation sector in particular is required to make substantial contributions alongside the energy sector. For the investigations conducted in this context, a Python-based model was first developed that permits a description of the various drive options and the associated fuels in passenger transport. Modeling was oriented according to the methodology of well-to-wheel (WTW) balancing. The result of the scenario-based analysis includes primary and end energy consumption, greenhouse gas emissions, and costs in temporal resolution until the year 2050. Input parameters of the simulation include the temporal penetration rates of alternative drive concepts as well as assumptions regarding the primary energy basis of the fuels used over time. The analysis shows that radical changes are required in the structure of the drive mix for passenger cars in order to achieve the greenhouse gas reduction targets, for example in terms of the market penetration of battery electric drives as well as fuel cell drives. Fig. 67 shows that – assuming a sharp rise in the proportion of fuel cell vehicles and a simultaneous shift from hydrogen generation towards renewable energy – sufficient reductions in greenhouse gas emissions are possible in the example scenario. The model also offers a basis for the investigation of additional transport carriers and thus serves as a starting point for associated further developments in terms of the fleet or cost model

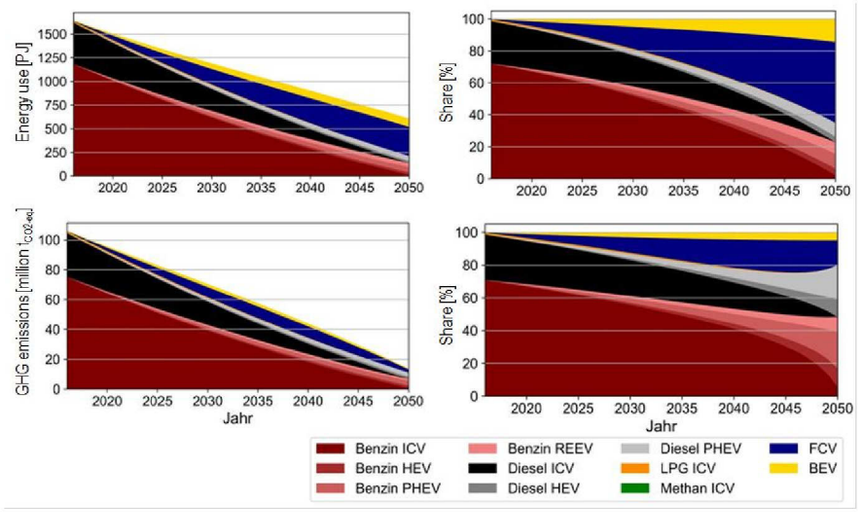

Fig. 67: WTW results in the hydrogen scenario; author's depiction

Development of infrastructures

The technological supremacy of the present carbon-based fuel system is partly due to the limited availability of alternative fuel infrastructures. In the case of hydrogen, the high infrastructure investment requirements and a simultaneously low level of utilization represent one of the biggest challenges for the introduction of hydrogen technologies. In previous studies conducted at IEK-3, Robinius et al. and Reuß et al. demonstrated the economic viability of the hydrogen supply at high market proportions[23] [24] . Building on this work, it is now crucial to investigate the pathway from today's low turnover towards high market penetration levels as well as to develop strategies for the economic introduction of a hydrogen infrastructure. To this end, detailed systems will be modeled of the nationwide development of the hydrogen infrastructure for a low to medium hydrogen demand, corresponding to the demand of an introductory phase. A discrete point-to-point supply chain analysis spanning the years 2023–2050 will be used to investigate promising infrastructure development scenarios and the associated hydrogen distribution costs. The supply chain pathways include hydrogen transport via trucks and pipelines as well as seasonal storage to balance out variable H_2 production due to fluctuating renewable power generation. Our current investigations design and analyze various penetration scenarios for fuel-cell-based transportation applications such as buses, trains, industrial trucks, and passenger cars, as well as further hydrogen uses in industry.

[23] M. Robinius, A. Otto, K. Syranidis, D.S. Ryberg, P. Heuser, L. Welder, T. Grube, P. Markewitz, V. Tietze, D. Stolten, Linking the Power and Transport Sectors—Part 2: Modelling a Sector Coupling Scenario for Germany, Energies 10(7) (2017) 957.

[24] M. Reuß, T. Grube, M. Robinius, P. Preuster, P. Wasserscheid, D. Stolten, Seasonal storage and alternative carriers: A flexible hydrogen supply chain model, Applied Energy 200 (2017) 290-302.

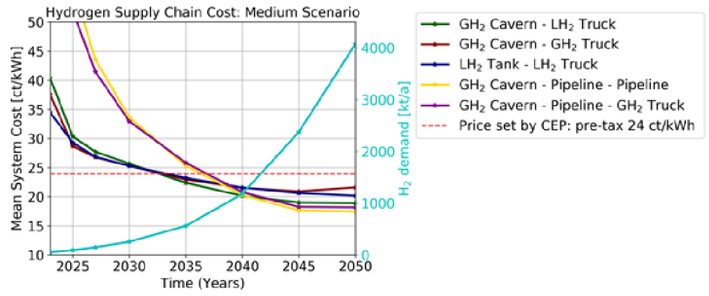

Fig. 68: Average hydrogen supply costs for various time periods

Initial results indicate significant cost degression of 40–50 % during the introductory phase of the investigated renewable hydrogen supply paths. These reductions in cost can be achieved at an annual total demand of 400 kt (13.3 TWh), which corresponds to approx. 20 % of today's annual hydrogen turnover in Germany[25]. In the selected hydrogen demand scenario, all investigated supply paths reach an economically viable price zone in the years 2033–2037. This leads us to the conclusion that economically viable costs can be achieved for entirely renewable, nationwide hydrogen supply chains within a decade.

Techno-economic analysis of global provision of hydrogen based on renewable energy

The electrolytic production of hydrogen (power to gas) lends itself to harnessing the energy potential of international regions that are advantageous for solar and wind power in a technologically and economically reasonable manner. Within the scope of the techno-economic analysis conducted at IEK-3 for a global hydrogen supply infrastructure based on renewable energy, selected regions in the world are initially investigated in terms of their wind or PV potential. Patagonia, Chile, Canada, and Iceland were identified as having the highest wind energy yields[26]. The following analysis encompasses the placement of wind energy facilities, taking into consideration land availability, the dimensioning of the electrolyzers, the compressors, and the transportation pipelines to ports, as well as the liquidization or bonding of the hydrogen to organic carrier materials (liquid organic hydrogen carriers, LOHCs). A 30-day reserve is included for storage at ports. To derive region-specific cost functions of hydrogen provision, the minimum number of full-load hours and therefore the degree of RE development is varied. Fig. 69 summarizes the elements of the hydrogen supply infrastructure and the example of a cost curve for hydrogen based on wind energy in Argentina.

[25] Roads2HyCom, European Hydrogen Infrastructure Atlas and Industrial Excess Hydrogen Analysis. 2007. p. 55-86.

[26] P.-M. Heuser, D.S. Ryberg, T. Grube, M. Robinius, D. Stolten, Techno-economic analysis of a potential energy trading link between Patagonia and Japan based on CO2 free hydrogen, International Journal of Hydrogen Energy (2019).

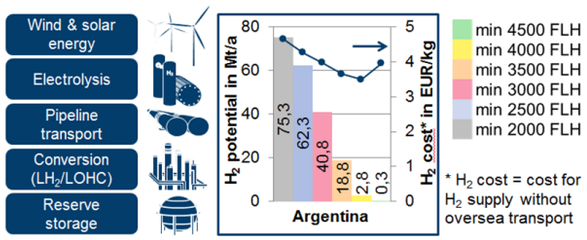

Fig. 69: Infrastructure elements and example of a supply cost curve for Argentina

Based on the hydrogen supply determined in this way, the associated supply cost curves, and the corresponding naval transport costs, an assumed global hydrogen demand, broken down according to individual regions, is covered – on the condition of a global supply cost minimum. Fig. 70 shows the coverage of a hydrogen demand based on the current number of passenger cars in selected import regions. A fuel cell vehicle proportion of 75 % of the entire fleet was assumed here. Taking naval transportation into consideration, preliminary import costs of 4.34 – 4.81 €/kg are incurred, depending on the distance between the trading partners.

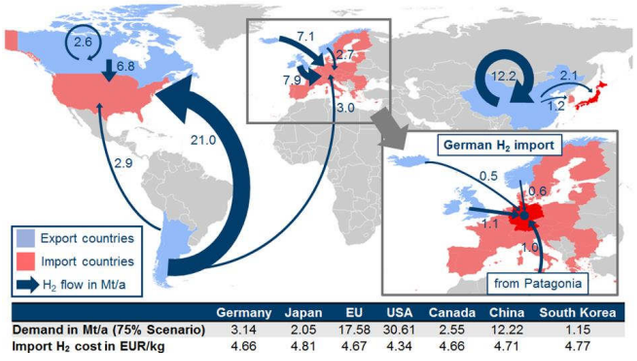

	Germany	Japan	EU	USA	Canada	China	South Korea
Demand in Mt/a (75% Scenario)	3.14	2.05	17.58	30.61	2.55	12.22	1.15
Import H_2 cost in EUR/kg	4.66	4.81	4.67	4.34	4.66	4.71	4.77

Fig. 70: Coverage of an assumed regional hydrogen demand and associated import costs

The distribution result clearly indicates that the hydrogen transport is primarily regional (America, Europe, Asia) and that import costs are heavily dependent on global demand. Using various distribution ratios for the assumed global hydrogen demand, and taking into consideration a planned integration of hydrogen supply from solar power generation, the option of an emission-free energy import for various scenarios can be defined in more detail from a technological and economic perspective.

3.6.2.4 Open source models from the VSA department

The FINE Python package developed at IEK-3 (published on GitHub https://github.com/FZJ-IEK3-VSA/FINE in July 2018) is a model generator for the mapping, optimization, and evaluation of energy systems. With this framework, systems with several regions/sites, raw materials, and

time intervals can be modeled. One criterion for optimization is the minimization of total annual costs, taking into consideration technical framework conditions and additional target criteria such as reductions of CO_2 emissions. Furthermore, the model has the option of aggregating time series with continuous temporal resolution into combined time periods in order to reduce the complexity of the optimization problem and thus also the computing time of the model. The versatile model generator is currently used for the optimization of both individual neighborhoods and for national and international energy systems, including their supply infrastructures.

The open source tool GLAES (geospatial land availability for energy systems; https://github.com/FZJ-IEK3-VSA/glaes) developed at IEK-3 can be used to conduct scenario analyses for the placement of renewable-energy-based power generating plants and taking into consideration potential land use criteria. Building on this, additional tools can be used to conduct potential analyses for Europe and the the world. The tool enables the combination and analysis of various georeferenced data from different sources. GLAES is based on the Geospatial Data Abstraction Library (GDAL) and can use information from any geodata set that GDAL is able to interpret. The selected structure of the model thus offers a high degree of flexibility in addition to the consistent processing and application of data.

3.6.3 Staff members and fields of activity

Name	Tell. (02461-61-) Email	Field of activity
Dr. M. Robinius	3077 m.robinius@fz-juelich.de	Head of Process and Systems Analysis
Dr. T. Grube	5398 th.grube@fz-juelich.de	Group leader Mobility
Dr. P. Markewitz	6119 p.markewitz@fz-juelich.de	Scientific responsibility for the field of stationary energy systems
Dr. J. Linßen	3581 j.lilnssen@fz-juelich.de	Scientific responsibility for the field of Sector Coupling and Infrastructures
R. Beer	85447 r.beer@fz-juelich.de	Spatial aggregation for energy systems analysis
D. Caglayan	5396 d.caglayan@fz-juelich.de	Pan-European solution for sector coupling via hydrogen
S. Cerniauskas	9154 s.cerniauskas@fz-juelich.de	Introduction strategy for hydrogen infrastructure
T. Groß	96995 t.gross@fz-juelich.de	Infrastructure analysis in a multi-node energy system model
Dr. H. Heinrichs	9166 h.heinrichs@fz-juelich.de	Global energy and resource flows

P. Heuser	9742 p.heuser@fz-juelich.de	Techno-economic analysis of a global hydrogen infrastructure
M. Hoffmann	85402 max.hoffmann@fz-juelich.de	Complexity reduction of energy system models through time series aggregation
T. Kannengießer	8732 t.kannengiesser@fz-juelich.de	Cost-optimal supply systems for neighborhoods
L. Kotzur	6689 l.kotzur@fz-juelich.de	Cost-optimal supply systems for houses
P. Kuckertz	1822 p.kuckertz@fz-juelich.de	Research data management and technical model coupling
F. Kullmann	85446 f.kullmann@fz-juelich.de	Modeling of industrial processes and recycling pathways in Germany
P. Lopion	1923 p.lopion@fz-juelich.de	Sector-coupling potential analyses for Germany
M. Reuss	9153 m.reuss@fz-juelich.de	Techno-economic analysis of hydrogen supply pathways
S. Ryberg	4064 s.ryberg@fz-juelich.de	Modeling of the European residual load at different development degrees of renewable energies
Dr. P. Stenzel	6556 p.stenzel@fz-juelich.de	Urban and Industrial energy systems
K. Syranidis	9156 k.syranidis@fz-juelich.de	Techno-economic analyses of electricity generation and transmission in the European context
Y. Wang	3742 yu.wang@fz-juelich.de	Membrane-based gas separation processes in energy technology
L. Welder	96992 l.welder@fz-juelich.de	Development of a multi-node energy system model with high spatial and temporal resolution
Dr. L. Zhao	4064 l.zhao@fz-juelich.de	Membrane-based gas separation processes in energy technology

3.6.4 Importants publications, docoral theses, and patents

Publications

Robinius, M., Otto, A., Stolten, D., Heuser, P., Welder, L., Syranidis, K., Peters, R.
Linking the power and transport sectors - Part 1: The prinicple of sector coupling
Energies 10(7), 956 doi:10.3390/en10070956

Reuss, M., Grube, T., Robinius, M., Preuster, P., Wasserscheid, P., Stolten, D
Seasonal storage and alternative carriers: A flexible hydrogen supply chain architecture model
Applied Energy, 200, 290 - 302. doi:10.1016/j.apenergy.2017.05.050

Lopion, P., Markewitz, P., Robinius, M., Stolten, D.
A Review of Current Challenges and Trends in Energy Systems Modeling. Renewable & sustainable energy reviews
96, 156 - 166. doi:10.1016/j.rser.2018.07.045

Welder, L., Ryberg, S. D., Kotzur, L., Grube, T., Robinius, M., Stolten, D.
Spatio-temporal optimization of a future energy system for power-to-hydrogen applications in Germany
Energy, 158, 1130 - 1149. doi:10.1016/j.energy.2018.05.059

Ryberg, S. D., Robinius, M., & Stolten, D.
Evaluating Land Eligibility Constraints of Renewable Energy Sources in Europe
Energies, 11(5), 1246 -. doi:10.3390/en11051246

Robinius, M., Raje, T., Nykamp, S., Rott, T., Müller, M., Grube, T., Stolten, D
Power-to-Gas Electrolyzers as an Alternative to Network Expansion - An Example from a Distribution System Operator
Applied Energy, 210, 182 - 197. doi:10.1016/j.apenergy.2017.10.117

Syranidis, K., Robinius, M., Stolten, D.
Control Techniques and the Modeling of Electrical Power Flow across Transmission Networks
Renewable & sustainable energy reviews, 82(3), 3452 - 3467. doi:10.1016/j.rser.2017.10.110

Kotzur, L., Markewitz, P., Robinius, M., Stolten, D.
Impact of Different Time Series Aggregation Methods on Optimal Energy System Design
Renewable energy, 117, 474 - 487. doi:10.1016/j.renene.2017.10.017

Kotzur, L., Markewitz, P., Robinius, M., Stolten, D.
Time Series Aggregation for Energy Systems Design: Modeling of Seasonal Storage
Applied Energy, 213, 123 - 135. doi:10.1016/j.apenergy.2018.01.023

Otto, A., Robinius, M., Grube, T., Schiebahn, S., Stolten, D., Praktiknjo, A.
Power-to-Steel: Reducing CO2 through the integration of renewable energy into the German steel industry
Energies, 10(4), 451 doi:10.3390/en10040451

Doctoral theses

Kotzur, L.
Future Grid Load oft he Residential Building Sector
Schriften des Forschungszentrums Jülich, Reihe Energie & Umwelt, Band 442, 2018
ISBN 978-3-95806-370-9

Important patents

Patents granted:

Pricipal inventor	PT	Description
S. Schiebahn	1.2584	Method for operating two sub-processes with different steam requirements in an overall process
S. Schiebahn	1.2585	Method for operating a subprocess in an overall process that requires steam

3.7 Physicochemical principles/electrochemistry

3.7.1 Objectives and fields of activity

The Physicochemical Laboratory (PCL) department investigates fundamental physicochemical and electrochemical issues in the field of polymer fuel cells, proton-conducting, non-aqueous electrolytes, electrode and electrolyte materials for Li battery applications, and ceramic solid oxide cells. In addition to electrode redox kinetics and ionic bulk transport, PLC also focuses on ion transfer kinetics across interfaces between various electrolytes and on conduction processes along these interfaces. The basic structure–activity relationships of complex processes are analyzed to contribute new functional materials as well as optimized cell assemblies and operating parameters for improving electrochemical transducers and storage. Various in situ and ex situ methods are used:

- Imaging techniques
  - Scanning electron microscopy (SEM/EDX)
  - Optical microscopy
  - X-ray tomography (n-CT)
  - Atomic force microscopy (AFM)
- Materials analysis, chemical analysis
  - Raman spectroscopy
  - IR spectroscopy/ATR
  - X-ray diffraction (XRD), X-ray reflectometry (XRR)
- Thermochemical and mechanical analysis techniques
  - Thermogravimetry and calorimetry (TGA/DSC)
  - Elasticity/expansion measurements
  - Determination of the inner surface area (BET), densitometry (gas pycnometer)
- Electrochemical analysis techniques
  - Impedance spectroscopy (EIS)
  - Cyclic voltammetry (CV), cycling of battery cells/differential capacity
  - Microelectrode measurements/rotating disk electrode

Existing methods are adapted depending on the tasks at hand and new methods are established as required.

3.7.2 Important results

3.7.2.1 Ionic liquids as non-aqueous, proton-conducting electrolytes used in polymer electrolyte fuel cells (PEFCs) at operating temperatures of around 120 °C

An operating temperature of over 100 °C would enable a much simpler PEFC system setup: i) no wetting of the fuel gas or the added air and, therefore, no recirculation of water; ii) a more efficient cooling system or the production of usable waste heat; and iii) higher tolerance to fuel gas and air contaminants. At present, high-temperature (HT) PEFCs based on phosphoric-acid-doped polybenzimidazole (PBI) membranes, which are suited to operating temperatures of 160–180 °C, are unable to compete with the power density of NAFION®-based PEFCs. The presence of H_3PO_4 inhibits the oxygen reduction reaction (ORR) at the cathode. There is therefore a need for new, non-aqueous proton-conducting electrolytes which allow the fuel cell to operate at a temperature in the 100–120 °C range. Proton-conducting ionic liquids (PILs) with acidic cations are promising candidates for future applications as non-aqueous electrolytes at operating temperatures above 100 °C.

Electrode kinetics PIL/water

All electrochemical processes that are relevant for fuel cells occur at the interface between the (platinum) catalyst and the electrolyte, for example an ionic liquid. Knowledge of the structure and properties of this electrolytic double layer can help in influencing the electrochemical reactions and is therefore crucial for optimizing these processes. Even at 120 °C, there is pronounced residual water activity during fuel cell operation, which is why it must be considered an important influencing parameter. The water content in a HT PEFC increases with increasing operating current density and decreasing temperature.

Initial work investigated the double-layer properties of the platinum/2-sulfoethylmethylammonium triflate ([2-Sema][TfO]) interface were investigated by means of impedance spectroscopy (EIS) and the results were published.27 In addition to looking at electrode potential and temperature, this work also focused on the influence of the water content (0.7–6.1 wt.%) in the ionic liquid on double-layer capacitance. This is an important parameter, since water in its protonated form acts as a proton source for electrode processes, such as oxygen reduction and the underpotential deposition of hydrogen (HUPD), and considerably accelerates these processes. In addition, water is essential for the formation of platinum hydroxides and oxides, which in turn influences the double-layer properties and electrode processes.

[27] K. Wippermann, J. Giffin, S. Kuhri, W. Lehnert and C. Korte, Phys. Chem. Chem. Phys. 19 (2017) 24706-24723

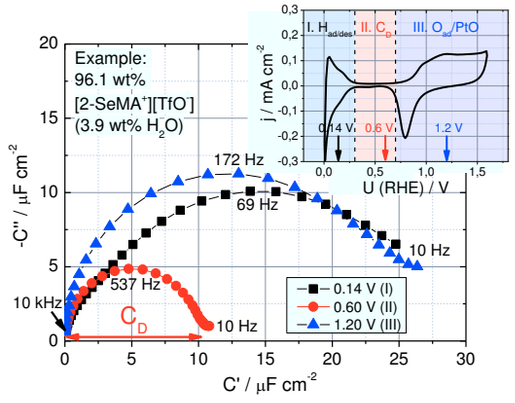

Fig. 71: Impedance spectra represented as complex capacitance for 3 potentials in 3 potential regions: I. H_{UPD}; II. double-layer area; III. platinum oxide formation.

An analysis of impedance spectra (Fig. 71) in the form of complex impedances revealed the following important findings: (i) up to four capacitive processes occur in the entire frequency range of the spectra; (ii) the double-layer capacitance of the high-frequency (fast) processes increases with increasing water content and is explained by the stronger adsorption of water on the platinum surface; (iii) the high-frequency capacities can be linked to ion transport in the double layer; the low-frequency capacities – as pseudocapacities – with electrochemical processes.

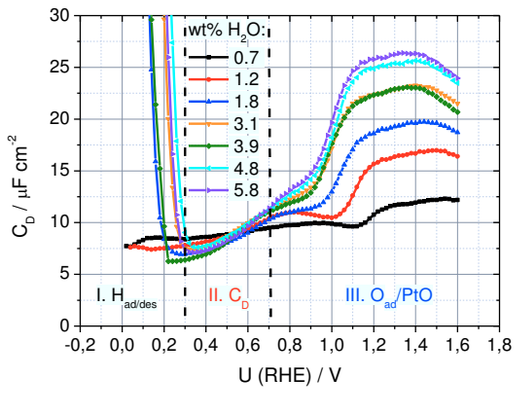

Fig. 72: Differential double-layer capacitance at the platinum/[2-Sema][TfO] interface for various water contents.

During electrochemical experiments, it is difficult to maintain a constant water content of the ionic liquids over a long period of time, since open systems are mostly used, through which gas flows. It is therefore all the more important to determine the water content as accurately as possible over the duration of the experiment. In another published study, four electrochemical methods were tested on two ionic liquids with very different acidic and hygroscopic properties, namely [2-Sema][TfO] and diethylmethylammonium triflate

([Dema][TfO])[28]. The methods concern conductivity measurements, the underpotential deposition of hydrogen, platinum oxide reduction, and the starting potential of platinum oxidation. The measured parameters, i.e. the specific conductivity, the HUPD and reduction charges, and the starting potential, were applied and calibration curves were generated as a function of water content (Fig. 72).

A comparison of the four methods revealed that the measurement of specific conductivity is the simplest and most accurate method. Furthermore, it is an important reference method, since it can be performed without gas purging under highly contained conditions. However, this method is not suitable for small water contents, since conductivity is almost constant here. Under these conditions, platinum oxide reduction charge is the method of choice, as it is also sensitive to changes at low water contents. A combination of this and other methods increases the accuracy further.

In a comparison of both investigated ILs, the less acidic PIL, [DEMA][TfO], exhibited much smaller reduction charges at low water contents, and therefore less accuracy in determining the water content. Precision in determining the water content therefore also depends on the type of PIL. For both PILs, an extrapolation of the HUPD charges to a water content equal to zero only results in very small charges close to zero. This result is important, since it shows that in the absence of water, PILs only play a secondary role as a proton source during electrochemical reactions, irrespective of their acidity. In contrast, even small amounts of water – or after the H_3O^+ protolytic reaction – appear to significantly accelerate electrochemical processes.

Two test stands were also set up for electrochemical measurements using microelectrodes. Microelectrodes can be used to determine the bulk properties of ILs, such as the diffusion coefficient and the solubility of gases such as oxygen, as well as to investigate the kinetics and mechanisms of electrochemical processes, such as the oxygen reduction reaction.

Interaction of PILs/ionogenic polymers

In addition to electrochemical behavior, the investigation of (proton) conductivity, charge transport mechanisms, and intermolecular interaction with a host polymer is of major importance. In order to be used as an electrolyte in a PEFC, the PIL must be immobilized in a suitable polymer matrix.

Various acidic PILs, each based on the triflate anion, were investigated in terms of their conductivity and their dependence on water content. [DEMA][TfO], 1-ethylimidazolium triflate [EIm][TfO], and [2-SEMA][TfO] were selected, with their cation acidities varying by many orders of magnitude (p^K_A values of -1, 7, and 10, respectively). In this range, the concentrations of H_3O^+ in the protolytic equilibrium with water span several decades, i.e. from almost neutral for [DEMA][TFO] to highly acidic for [2-SEMA][TFO].

In comparison, the conductivity of [2-SEMA][TfO] shows the biggest increase in water content (Fig. 73 and Fig. 74). The associated protolytic and exchange processes were also investigated by means of Raman and 1H-NMR spectroscopy (DOSY). In the case of [2-SEMA][TfO], a transition was observed from a pure vehicle mechanism for the low-water state to a cooperative mechanism with fast proton exchange with increasing water content. For the less acidic PILs, the increase in conductivity with increasing water content is

[28] K. Wippermann, J. Giffin and C. Korte, J. Electrochem. Soc. 165(5) (2018) H263-H270

predominantly associated with a decrease in viscosity. The acidic proton is localized on the cations.

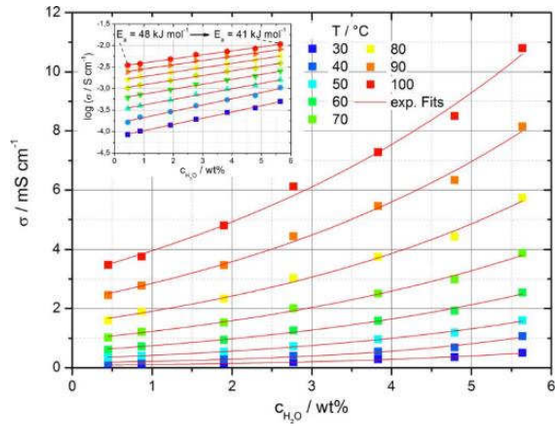

Fig. 73: (Total) conductivity of [2-SEMA][TfO] as a function of water content and temperature

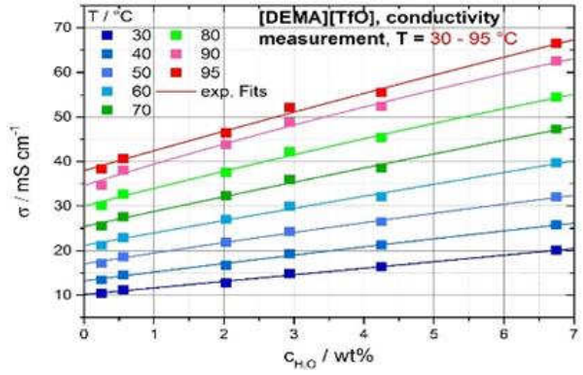

Fig. 74: (Total) conductivity of [DEMA][TfO] as a function of water content and temperature

Another aspect is the immobilization/absorption of the PIL in a polymer matrix for use as a membrane electrolyte in a fuel cell. A gradual uptake of [SEMA][TfO] in the m-PBI was determined here. The diffusion coefficient was measured at around $4.4 \cdot 10^{-11}$ cm/s, which is roughly three orders of magnitude smaller than for phosphoric acid. The molar doping level (PIL formula units per polymer repeat unit) is also rather small at roughly 135 %. Investigations are therefore being conducted into alternative membrane production processes, such as solution casting, to achieve higher doping levels and thus also higher conductivity data as well as into alternative membrane materials such as sulfonated polyetheretherketone (sPEEK).

3.7.2.2 Investigation of the degradation phenomena of high-voltage cathode materials in lithium batteries by operando Raman spectroscopy

Due to the growing significance of electromobility and the ranges that this requires, attention is increasingly being devoted to high-voltage cathode materials which enable cell voltages of over 4.5 V (Li anode) and their resulting high power densities. A promising candidate is $LiNi_{0.5}Mn_{1.5}O_4$ (LNMO), with a redox potential of 4.75 V (Li anode). In comparison to conventional cathode materials such as $LiCoO_2$ and $LiFePO_4$, the energy density of LNMO is 20–30 % higher. LNMO crystallizes in two different cubic crystal structures. The Ni and Mn ions are found in an octahedrally coordinated lattice position, the Li ions in tetrahedrally coordinated, interlattice positions, and the oxide ions in a cubic close-packed lattice. A statistical distribution of Ni and Mn ions results in a spinel-type cathode (Fd-3m), while an ordered arrangement of Ni and Mn ions produces a $LiFe_5O_8$ cathode (P4332).

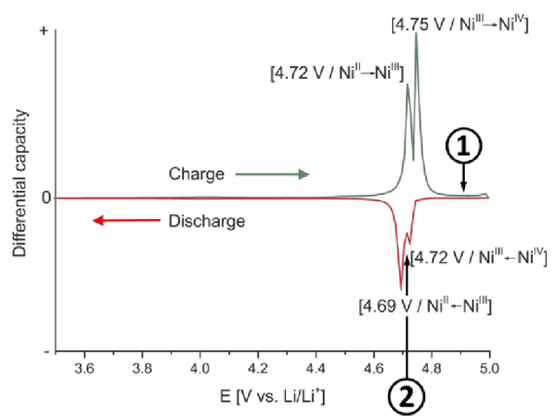

Fig. 75: Differential capacity of a half-cell with an o-LNMO cathode (Li anode). The conversion of $Li_{0.5}Ni_{0.5}Mn_{1.5}O_4$ to $Ni_{0.5}Mn_{1.5}O_4$ is denoted by the symbols ① and ②

The electrochemical stability window of a conventional electrolyte based on alkyl carbonates is between 0.7 V and 4.4 V (Li anode). A solid electrolyte interface (SEI) thus forms on the Li/intercalated graphite anode due to the electrolyte reduction. This anode SEI prevents further reduction of the electrolyte, since it completely covers the surface and is conductive to Li ions. However, with a redox potential of close to 5 V, the high-voltage cathode materials also exceed the oxidative stability of the electrolyte. Using high-voltage cathode materials, it is not currently possible to construct cells with sufficient cycle stability for technical applications. The redox potential of LNMO at 4.75 V in a delithiated (i.e. charged) state likely leads to fast oxidative degradation processes between the cathode and the electrolyte. The possible formation of a degradation layer, its composition, stability, porosity, and thickness compared to known anode SEIs, as well as the possible irreversible degradation of the cathode material have not yet been fully explained. Only a precise understanding of these processes will enable a substantial improvement in the cyclic stability of cells using high-voltage cathode materials.

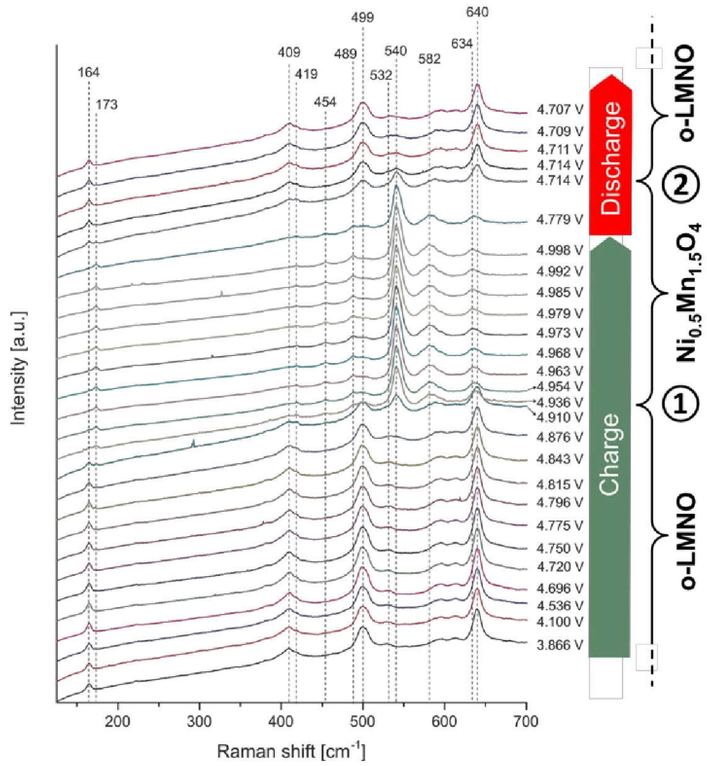

Fig. 76: Raman spectra – staggered according to cell potential – for a half-cell with an o-LNMO cathode (Li anode). The conversion of $Li_{0.5}Ni_{0.5}Mn_{1.5}O_4$ to $Ni_{0.5}Mn_{1.5}O_4$, detected by Raman spectroscopy, is denoted by the symbols ① and ②

To study these degradation phenomena, operando Raman investigations were conducted on full cells with a $Li_4Ti_5O_{12}$ anode and half-cells with a Li anode. In particular, the cycling behavior of differently balanced full cells was investigated in terms of anode and cathode capacity.29 The obtained Raman spectra provide information on the cathode material and electrolyte phase. The material changes occurring during cycling can thus be correlated with electrochemical measurements (Fig. 75 and Fig. 76).

Investigations were conducted with cathodes from the ordered LNMO phase (o-LNMO) and the disordered LNMO phase (d-LNMO). The phase transition between the fully lithiated phase ($Li_{0.5}Ni_{0.5}Mn_{1.5}O_4$), the half-lithiated phase ($Li_{0.5}Ni_{0.5}Mn_{1.5}O_4$), and the (almost) fully delithiated phase ($Ni_{0.5}Mn_{1.5}O_4$, λ-MnO_2 type) can be well distinguished by Raman spectroscopy. It should be noted that the phase transition detected by Raman spectroscopy occurs at higher cell potentials than the electrochemically detected phase transition (see ① in Fig. 75 and Fig. 76). The phase transitions during delithiation (charging) appear to continue in the cathode from the current collector to the surface, where they can be detected by Raman spectroscopy. Similar observations are found in the literature in operando XRD

[29] P. Jehnichen, K. Wedlich and C. Korte, Sci. Technol. Adv. Mater. 20(1) (2019) 1-9

studies. The phase transitions during lithiation (discharging) show no such unusual delays (see ② in Fig. 75 and Fig. 76).

After approx. 300 cycles, the operando half-cells can no longer be cycled due to degradation processes. The cathode material remains in the delithiated state. In addition to the signals of the cathode material and electrolyte, new Raman signals also occur. Depending on their location, these signals can be traced back to the formation of (open-chain) esters and ketones. The Raman signals of ethylene carbonate tail off significantly in relation to the dimethyl carbonate signals (LP30 components). The signal intensity of the PF6- anion drops below the detection limit. SEM investigations reveal no compact top coat on the surface. Deposits of degradation products can also be found on the separator between the anode and cathode.

At potentials above 4.5 V, the LP30 solvent is oxidatively decomposed at the charged cathode. Ethylene carbonate appears to be primarily consumed. During this process, the Li ions dissolved as LiPF6 in the electrolyte are immobilized and are therefore no longer available for cycling the cell. The cathode material can no longer be relithiated; its capacity collapses. Li ions and PF6- are either incorporated into poorly soluble compounds or begin to decompose. The degradation products of the electrolyte do not form a compact top layer on the cathode; they detach from the cathode (as detected on the separator). Irreversible degradation of the cathode material also occurs. Mn and Ni can also be detected on the anode. This is not, however, the limiting process for the strong degradation of the cell.

3.7.3 Staff members and fields of activity

Name	Tel. (02461-61-) Email	Field of activity
PD. Dr. C. Korte	9035 c.korte@fz-juelich.de	Head of the Physicochemical Laboratory
A. Everwand	8710 a.everwand@fz-juelich.de	Scanning electron microscopy/EDX, XRD, n-CT
Dr. J. Giffin	6228 j.giffin@fz-juelich.de	Physical properties: DSC, TGA, mechanical properties, conductivity
Fr. H. Hou	85360 h.hou@fz-juelich.de	Electrochemical and physical characterization of new PILs (HIFI-PEFC)
P. Jehnichen	1891 p.jehnichen@fz-juelich.de	Aging processes in LiMn1.5Ni0.5O4 high-voltage cathode materials for Li batteries
Fr. K. Klafki	1895 k.klafki@fz-juelich.de	Sample preparation for scanning electron microscopy and optical microscopy
Fr. J. Lin	9804 j.lin@fz-juelich.de	Conduction mechanism in PILs, interaction of PILs with ionogenic/polar polymers

Dr. Chr. Rodenbücher	6142 c.rodenbücher@fz-juelich.de	Physical investigations of interfaces: XRD, n-CT, Raman/IR spectroscopy, atomic force microscopy (AFM)
J. Sanarov	85356 j.sanarov@fz-juelich.de	Construction and testing of PEFCs with new membrane materials, PIL/polymer and POLY-ILs (HIFI-PEFC)
Y. Suo	1579 y.suo@fz-juelich.de	Basic research into the redox kinetics (ORR, HUPD, PtOx) of PILs
Dr. K. Wippermann	2572 k.wippermann@fz-juelich.de	Electrochemical investigations: double-layer behavior, electrochemical kinetics, spatially resolved measurements, aging processes
T. Wekking	1891 t.wekking@fz-juelich.de	Charge transfer between solid and liquid Li electrolytes

3.7.4 Importants publications, doctoral theses, and patents

Publications

M. Schleutker, J. Bahner, C.-L. Tsai, D. Stolten und C.Korte
On the interfacial charge transfer between solid and liquid Li^+ electrolytes
*Phys. Chem. Chem. Phys.**19** (2017) 26596-26605*

K. Wippermann, J. Giffin, S. Kuhri, W. Lehnert und C. Korte
The influence of water content in a proton-conducting ionic liquid on the double layer properties of the Pt/PIL interface
*Phys. Chem. Chem. Phys. **19** (2017) 24706-24723*

J. Keppner, J. Schubert, M. Ziegner, B. Mogwitz, J. Janek und C. Korte
Influence of texture and grain misorientation on the ionic conduction in multilayered solid electrolytes – interface strain effects in competition with blocking grain boundaries
*Phys. Chem. Chem. Phys. **20** (2018) 9269-9280*

K. Wippermann, J. Giffin und C. Korte
In Situ Determination of the Water Content of Ionic Liquids
*J. Electrochem. Soc. **165(5)** (2018) H263-H270*

P. Jehnichen, K. Wedlich und C. Korte
Degradation of high-voltage cathodes for advanced lithium-ion batteries – differential capacity study on differently balanced cells
*Sci. Technol. Adv. Mater. **20(1)** (2019) 1-9*

Important patents

Patents granted:

Principal inventor	**PT**	**Description**
T. Bergholz	1.2660	Electrolyte system for application in electrochemical components

4

Results

Selected Results

- Jülich high-temperature fuel cell passes lifetime test of more than ten years
- Reduction of noble metal loading
- Infrastructural study

4.1 Jülich high-temperature fuel cell passes lifetime test of more than ten years

As previously reported, a world record was achieved in October 2015 during an SOFC lifetime test. A short stack achieved 70,000 h of operation under load. The stack went on to achieve a lifetime of 11.5 years during which time it was operated under load for 93,138 operating hours, with an overall voltage degradation of 0.5 %/kh (see Fig. 77). The increase in area-specific resistance (ASR) during the first 40,000 h was approx. 16 mΩcm²/kh (3.7 %). During the subsequent 50,000 h, the ASR rate of increase declined to approx. 3 mΩcm²/kh (0.3 %/kh). Due to an error in the test rig, the stack was mostly idled during the last six months (with regular impedance measurements). After 100,000 h at operating temperature, the stack was switched off in January 2019 and is currently being investigated further.

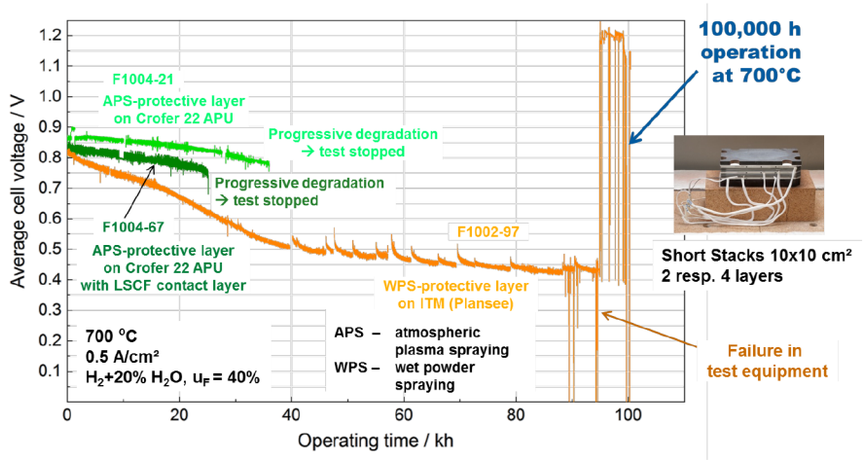

Fig. 77: Long-term operation of the 2-level short stack F1002-97 and the 4-level short stack F1004-67

A second short stack (F1004-21) with an improved chromium protective layer had to be shut down after 34,500 operating hours due to a sudden and unexpectedly sharp voltage drop on one level. A post-test analysis revealed that Mn diffusion from the contact layer to the anode destroyed the electrolyte.

Another short stack (F1004-67) without Mn in the contact layer exhibited an average voltage drop of 0.25 %/kh over 23,500 operating hours, corresponding to an ASR increase of approx. 5 mΩcm²/kh (1.2 %). After approx. 25,000 operating hours, it also exhibited a sudden voltage drop on one level, requiring the stack to be shut down prematurely. Preliminary post-test examination results in this case indicate that, again, the problem was the Mn at the anode–electrolyte interface. In this case, however, the Mn appears to have originated in the oxide layer of the steel on the anode side. Further analyses are required.

4.2 Reduction of noble metal loading

Loading began with the standard loading of 2.25 mg/cm² IrO_2 (AAe) and was reduced to 0.6 and 0.3 mg/cm² IrO_2 (AAe). The polarization curves of the three loadings are shown in Fig. 78.

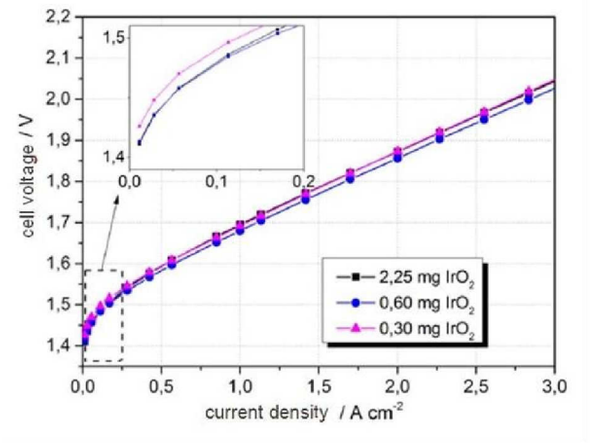

Fig. 78: Long-term operation of the 2-level short stack F1002-97 and the 4-level short stack F1004-67

A comparison of the polarization curves of the three different loadings in Fig. 78 shows that all three loadings have a comparable polarization curve after a run-in time of 74 h. At 2 A/cm², the CCMs with anode loadings of 2.25 mg/cm² and 0.3 mg/cm² both had a voltage of 1.872 V and the CCM with an anode loading of 0.6 mg/cm² had a cell voltage of 1.856 V. The lowest current density $U_{j0.01}$ increases with decreasing loading by a total of 13 mV to 1.426 V. The polarization curves show that it is possible to reduce the loading of the anode by 87 % to 0.3 mg/cm² without impacting on cell performance. This in turn reduces the amount of iridium required for the installation of 84 GW of PEM electrolysis capacity from 117 tonnes to 14 tonnes. This corresponds to only slightly more than twice the annual amount currently mined. For the same performance, the amount of iridium saved is therefore almost twice the amount saved when the new catalyst “Kat. A” is used. The literature also indicates that the iridium loading of the anode only has a small impact on the polarization curve of the CCMs.

Long-term stability under reduced loading of the anode

The cells with anode loadings of 0.6 and 0.3 A/cm² were operated at 80 °C and 2 A/cm² over a period of 1077 h. The single potentials were measured by means of a Nafion bridge. The time curves of the cell voltage as well as the single potentials of anode (red) and cathode (green) are shown in Fig. 79 for the CCM at 0.6 mg/cm². In addition, the cell voltages U_{j2} from the polarization curve are shown as grey triangles.

In the case of the cell with an anode loading of 0.6 mg/cm² shown in Fig. 79, the cell voltage at 1077 h is only 3 mV higher than at the beginning of the test at 0 h. However, periods with decreasing and increasing cell voltage can be distinguished so that an averaging of the degradation rates permits no conclusions about the occurring voltage change. Therefore the

test period for the cell with standard loading is divided into shorter periods. Two such periods are defined: The time period from 0 to 74 h is designated as the run-in period (0) and the remaining period from 74 h to 1077 h is designated as period (I).

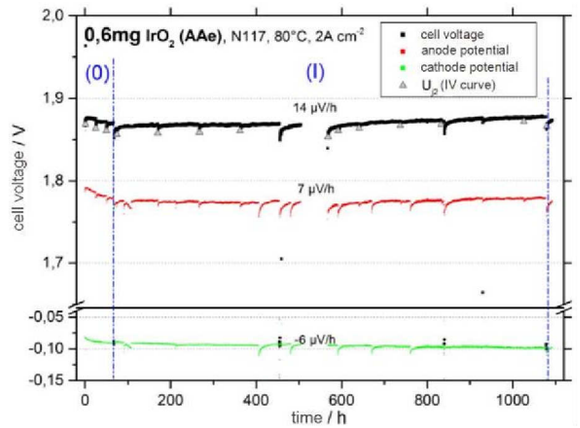

Fig. 79: Reduced anode loading with 0.6 mg/cm² IrO_2 (AAe). Cell voltage and single potentials over time.

The cell voltage first decreases during period (0) and then, during period (I) increases at a rate of 14 µV/h. The single potentials measured at the bipolar plates also change. The anodic potential increases at a rate of 7 µV/h while the potential of the cathodic bipolar plate decreases by 6 µV/h. The single potential measurement reveals that the overpotentials at the cathode and anode sides increase approximately equally. The cell voltage U_{j2}, which was determined from the polarization curve at a reference current density of 2 A/cm², exhibits a time curve comparable to the cell voltage in the long-term experiment. While the cell voltage in the long-term experiment increases by a total of 15 mV during period (I), the polarization curve exhibits an increase in cell voltage U_{j2} by 13 mV. It can thus be used to evaluate the cell performance. U_{j2} is roughly 8 mV lower than the voltage in the long-term test. The cell voltage curve for anode loading of 0.3 mg/cm² is shown in Fig. 80 and is also divided into two periods (0) and (I). In period (I), the cell voltage increases at a rate of 39 µV/h. The anode potential increases in the same time frame at a rate of 40 µV/h and the cathode potential rises by 1 µV/h. The increase in cell voltage in this period can therefore by fully attributed to the anode.

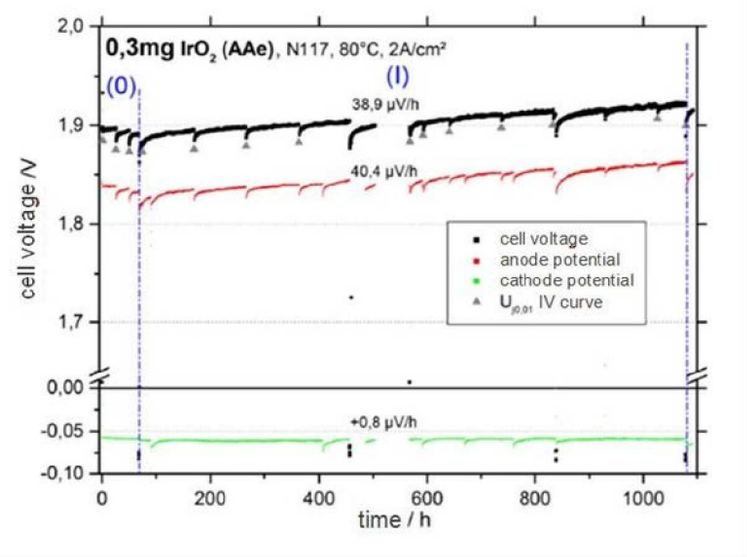

Fig. 80: Reduced anode loading with 0.3 mg/cm² IrO_2 (AAe). Cell voltage and single potentials over time.

4.3 Infrastructural study

A Electrical drives are the key to climate-smart traffic based on renewable energy. Local zero-emission traffic is an important prerequisite for improving the future quality of life, particularly in conurbations. Both battery and fuel cell electric vehicles fulfil these important criteria. However, both technology pathways require new infrastructural concepts.

Objectives and approach

The objective of the analysis was a detailed dimensioning and investigation of the necessary infrastructures for various levels of market penetration of battery electric vehicles as well as hydrogen fuel cell electric vehicles in Germany. The study provides information on the investments, costs, efficiencies, and emissions of the relevant infrastructures for supplying electric power or hydrogen to vehicles ranging in number from several hundreds of thousands up to several million. Both technologies are currently at the beginning of market development and the dimensioning and adaptation of the necessary infrastructure to the respective market penetration of the vehicles has yet to be clarified. Furthermore, these infrastructures also need to offer options for integrating excess power that will in future be generated by energy systems dominated by renewable sources. The present study contains detailed dimensioning of the infrastructures and their components (Fig. 81) and clarifies the underlying assumptions. A transparent factual basis is thus created that can be adapted using newly gained empirical values, permitting a fact-based discussion.

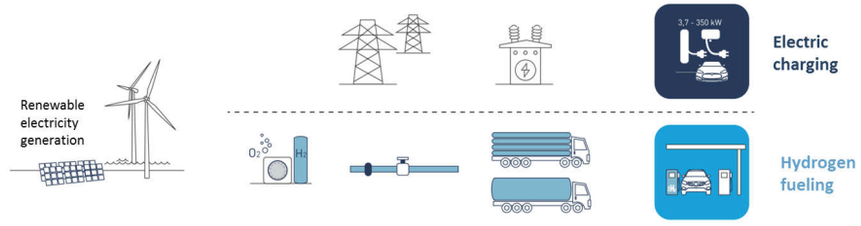

Fig. 81: Schematic of the supply infrastructures investigated

One important part of the study is a comprehensive meta-analysis of existing studies with information on the infrastructure development of both technologies. Based on the insight that existing studies are insufficient for high market penetration and that the data basis is not always transparent, detailed scenario calculations and techno-economic analyses were performed.

Results

The analysis of the scenarios shows that the investments for infrastructural development are almost the same for both technology pathways for small fleets of up to several hundreds of thousands of vehicles. During the transition phase, hydrogen generation will shift towards the exclusive use of excess renewable power paired with the construction of seasonal hydrogen storage systems capable of bridging 60 days. The concept permits the supply of green hydrogen. During the initial phase, higher investments will be required than for a charging infrastructure. The study does not cover seasonal power storage for a charging

infrastructure, which would be necessary for a secure supply of 100 % renewable power. A comparison of the cumulative investments of both concepts for a high market penetration of 20 million vehicles shows that investment costs for a charging infrastructure would be considerably higher at € 51 billion than those for a hydrogen infrastructure at approximately € 40 billion (Fig. 82)

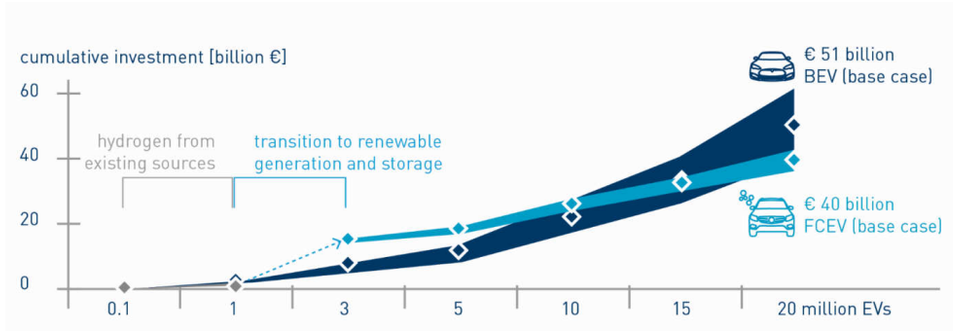

Fig. 82: Comparison of cumulative investment costs for the necessary infrastructure development

The resulting kilometer-specific costs will be almost the same for both supply systems at high market penetration: the electric charging system would cost approximately 4.5 €c/km and the hydrogen system roughly 4.6 €c/km. The fact that electrical generation and storage of hydrogen permits the use of otherwise unusable renewable power directly on site approximately balances out the lower energetic efficiency of the hydrogen pathway due to the lower costs of using excess energy.

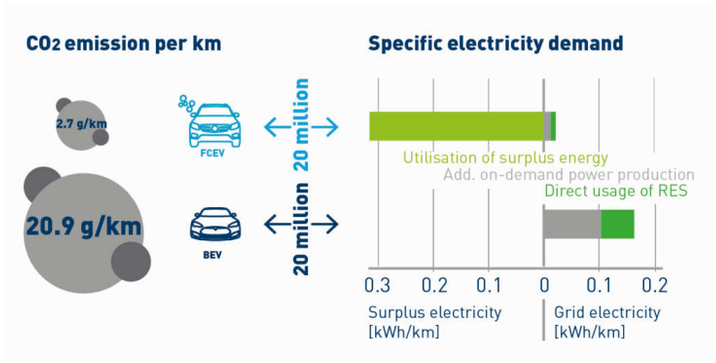

Fig. 83: Comparison of the kilometer-dependent CO_2 emissions and power demands for 20 million vehicles

The scenario with 20 million fuel cell electric vehicles requires 87 TWh of excess power for electrolysis and an additional 6 TWh of power from the grid (transport and distribution of hydrogen). Charging 20 million battery electric vehicles requires 46 TWh from the distribution grid. The efficiency of the charging infrastructure and vehicles is higher but the flexibility of power demand is limited to shorter periods of time. The amount of excess power in the

assumed energy supply scenario with large proportions of renewable energy exceeds the supply demand of 20 million vehicles in both infrastructural pathways by a factor of three to six.

Thanks to the use of excess renewable power and grid power with high proportions of renewable energy, the kilometer-specific CO_2 emissions of both supply options are low in comparison with those of fossil fuels. The hydrogen infrastructure with inherent seasonal storage can integrate larger proportions of excess renewable energy and is thus advantageous for CO_2 reduction (Fig. 83). However, a charging strategy for battery electric vehicles oriented towards the availability of renewable power could also further reduce their CO_2 emissions.

Conclusion

In conclusion, both infrastructures are important components for realizing climate-friendly, clean, and renewable traffic concepts.

A smart and complementary combination of both infrastructures could combine the strengths of the hydrogen infrastructure with those of electric charging and avoid less sustainable individual solutions with low system capability or efficiency. For system solutions, it may be advantageous to focus on the more easily achievable objective of overnight charging of battery electric vehicles for short trips and to address the challenges of long-distance and heavy-goods transport by means of hydrogen. A hybrid strategy to develop both infrastructures could thus permit a considerable increase in the use of renewable energy and in efficiency as well as a significant reduction in CO_2 emissions across as many transport sectors and uses as possible. The investments necessary to realize either infrastructure are low in comparison with other infrastructures (e.g. the expansion of renewable power generation or the maintenance and expansion of road infrastructures).

Although a charging infrastructure would have a higher energy efficiency than the hydrogen pathway, a hydrogen infrastructure is also viewed as a key element for the expanded use of seasonal power excesses in other energy sectors such as industry. Considering the system as a whole, hydrogen thus offers the potential of also realizing cross-sector energy supply concepts (sector coupling).

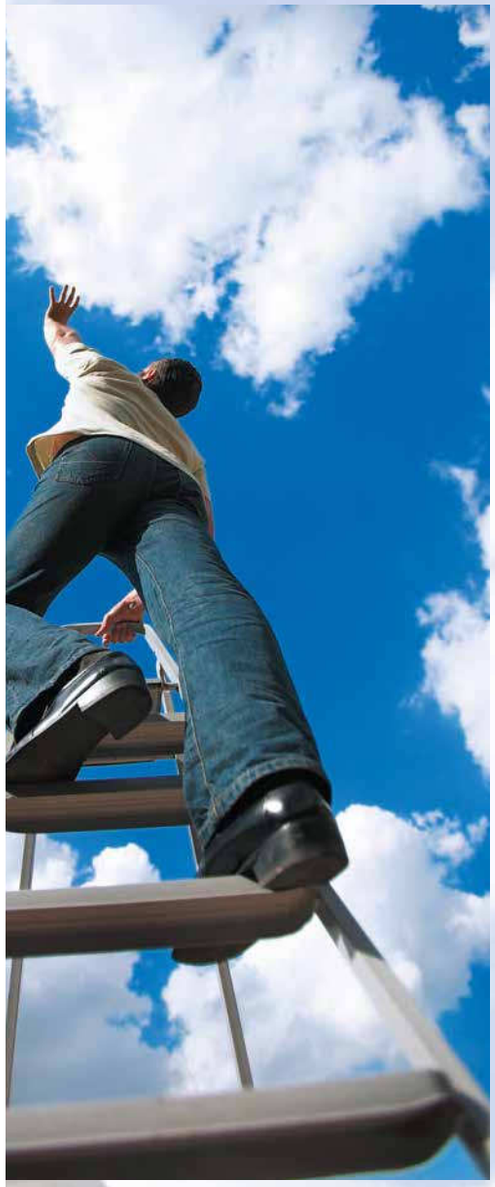

5

Outlook

Outlook for New R&D Projects

- Solid oxide cells for reduced operating temperatures from 400 bis 600 °C
- In-Situ TEM study of electrocatalysts
- Approaches to developing medium-temperature cells and systems
- Supply systems for alternative fuels
- Evaluative research on sustainable energy systems

5.1 Solid oxide cells for reduced operating temperatures from 400 to 600 °C

Fuel cells can be operated at temperatures ranging from approx. 80 °C to approx. 900 °C. Polymer electrolyte membrane fuel cells (PEFCs) cover the lower temperature range and solid oxide fuel cells (SOFCs) the upper temperature range. Both types have already achieved high power densities and market-ready long-term stability. Many tests with a multitude of fuel cell types have been conducted in the past to achieve similar power densities and long-term stabilities in the intermediate temperature range. However, none of the types tested (HT-PEFC, PAFC, MCFC) achieved this. They did not exhibit sufficient power densities or long-term stability. There are plans to close this gap in the coming years on the basis of SOFC research expertise that Forschungszentrum Jülich has acquired over the years in the fields of materials development, microstructure design, and interface design. SOCs based on oxygen ions or proton conductors offer the fundamental potential for high performance and long lifetimes since they build on previous development work on HT-SOCs.

These medium temperatures permit new, expanded application options such as range extenders in road- or rail-bound vehicles as well as ships, and in areas with frequent on/off cycles (faster power provision). For electrolysis purposes, the technology of these systems can more easily be coupled to existing industrial plants where usable waste heat in the medium range occurs. Due to better waste-heat coupling, the system can be operated more efficiently. The lower operating temperature also does not significantly impact on the typical fuel flexibility of SOFCs, since it is only internal reforming directly on the cell that is no longer possible under approx. 650 °C.

The efficiency of the electrolyzer is largely independent of the operating temperature, so that no major disadvantages are to be expected here. Electrolysis operation with oxygen ion conductors also permits the co-electrolysis of steam and carbon dioxide, and electrolysis via proton-conducting electrolytes permits both the production of very pure hydrogen (without steam content) and the electrolysis of, for example, steam and carbon dioxide in separate gas chambers (anode/cathode side). This means that the operation of a SOFC or SOEC (and/or PCFC, PCEC) at medium operating temperatures would both considerably expand the application portfolio and make it possible to determine the resulting usable product gases in a targeted manner.

For the first development stage, it is above all material issues that must be clarified:

In addition to a cell (thin CGO electrolyte; varied fuel gas electrode; improved air electrodes; proton-conducting cell), contact layers adapted in parallel, a new interconnect material, an alternative joining concept (material type), and adequate operating strategies (joining/reduction procedures, thermal/redox cycles…) must be developed.

5.2 In-Situ TEM study of electrocatalysts

Designing new materials as stable electrocatalysts require the understanding of them during working conditions[30]. In-situ transmission electron microscopy (TEM) is a powerful technique which allows this study. By using in-Situ TEM one can learn on the morphology evolution and elemental distribution in the metallic nanostructures together with their interaction with the support in reducing and oxidizing treatments at the atomic scale[31].

Recently we applied the in-situ electrochemical "liquid cell" technique together with the group of Martial Duchamp in Nanyang Technological University in Singapore to observe the structural evolution of individual Pt−Ni nanocatalysts in real-time, under electrochemical bias, and inside alkaline liquid electrolyte environment using a Scanning TEM (STEM). Pt−Ni nanocatalysts study here as potential electrocatalysts for alkaline water electrolysis which can offer higher durability and activity. The ultimate goal was to be able to maintain the atomic-level resolution (0.1-0.2 nanometers) in a liquid as is possible inside a vacuum environment, and to conduct a high signal to noise ratio electrochemical test at high current values. In this way, it would be possible to observe the details of the degradation of the Pt-Ni octahedral nanostructures while precisely controlling the potential applied and to quantitatively analyze the relationship between the potential and the degradation mode. Using the TEM specimen holder and commercially available MEMS chips made by Protochips an observation of the PtNi octahedral was conduct first without flow of alkaline solution inside the cell, as presented in Fig. 84

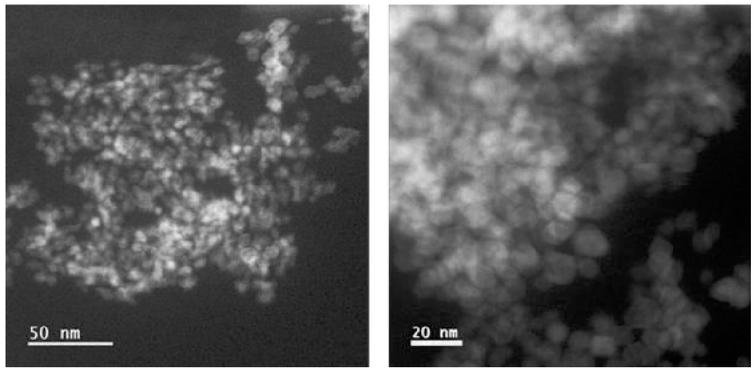

Fig. 84: STEM dark field images of Pt Ni octahedral coated on MEMS chip

Then the next step was to flow the liquid inside the cell, the real-time observation results showed low resolution and unclear images as presented in Fig. 85.

[30] Zhu, G. Z.; Prabhudev, S.; Yang, J.; Gabardo, C. M.; Botton, G. A.; Soleymani, L. In Situ Liquid Cell TEM Study of Morphological Evolution and Degradation of Pt-Fe Nanocatalysts during Potential Cycling. J. Phys. Chem. C 2014, 118 (38), 22111–22119.

[31] Shviro, M.; Gocyla, M.; Schierholz, R.; Tempel, H.; Kungl, H.; Eichel, R. A.; Dunin-Borkowski, R. E. Transformation of Carbon-Supported Pt-Ni Octahedral Electrocatalysts into Cubes: Toward Stable Electrocatalysis. Nanoscale 2018, 10 (45), 21353–21362.

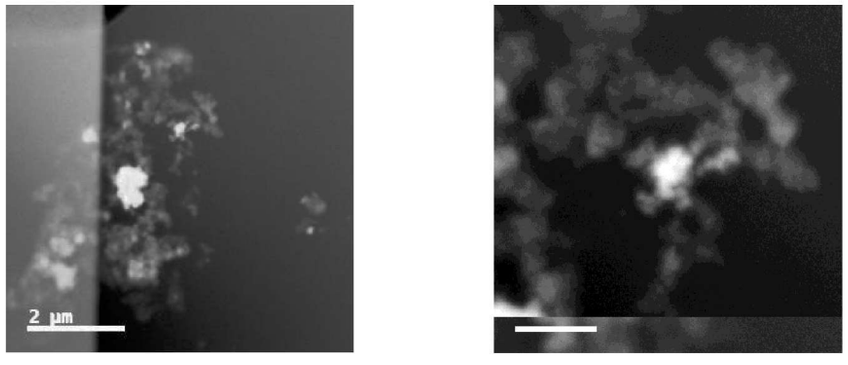

Fig. 85: STEM dark field images of Pt Ni octahedral coated on MEMS chip under flow of alkaline solution.

While applying voltage to the Pt-Ni octahedral, the real-time observation results showed again the same low resolution and unclear images as showed in Fig. 85. However, because the results of cyclic voltammetry showed that the current value was small and the changes in Pt-Ni octahedral nanostructures could not be clearly seen. It was learned that a commercially available MEMS chip could not produce the desired resolution and therefore, could not be used in the required electrochemical test. In order to study those materials in the liquid cell, new MEMS chip will be developed.

5.3 Approaches to developing medium-temperature cells and systems

High efficiency in energy conversion will be crucial for the widespread application of electrolysis when it comes to storing electric energy in the form of hydrogen in future. Operation at high temperatures, in particular, offers the opportunity of considerably improving efficiency in comparison with conventional systems. The range between 100 °C and 250 °C is especially attractive since the kinetics in this “medium-temperature” range is significantly accelerated in comparison to low-temperature systems. In addition, higher-value waste heat is generated and temperature control is easier. In contrast to high-temperature electrolysis, however, cost-effective conventional materials such as polymers can be used.

Due to the stronger corrosion of acidic electrolytes, this temperature range is particularly challenging. Work on alkaline medium-temperature electrolysis conducted at the Technical University of Denmark (DTU) has already shown a reduction in overpotentials and improved efficiency (Allebrod2014).

In spite of considerable advances, polymer-based alkaline electrolyte membranes are not yet stable enough for applications above 100 °C. Inorganic hydroxide ion conductors such as layered double hydroxides are therefore currently the most promising electrolyte materials for medium-temperature electrolysis. Membranes with sufficient mechanical stability can be maintained through processing into polymer composites. The general suitability of the material as an electrolyzer membrane as well as the production of thin membranes and conductivity at increased temperatures have already been demonstrated (Zeng2012, He2018, Kim2010).

The next step is the development of composite membranes for the medium-temperature range. Based on IEK-3’s years of experience in producing thin films, the material and production parameters will be modified in order to achieve membranes with high stability and conductivity. In this regard, understanding the underlying processes will be essential for targeted improvements.

An alkaline medium-temperature electrolyzer poses special requirements concerning the peripherals due to the medium as well as the higher pressure and temperature. To a certain degree, experiences with HT-PEM fuel cells can likely be taken advantage of here. The stability of the materials used, however, must be investigated under application conditions. A new test rig with an integrated analytics system is being set up for this purpose. It will permit in operando investigations of the gases produced as well as of the liquid medium. Material stability and electrolysis performance can thus be observed as a function of operation management. The medium can be fed into the cells in liquid or gaseous form. The latter permits operation at lower pressures and avoids the circulation of alkaline solutions. This is advantageous in terms of safety and corrosion risk. The reactants and products remain in the same phase, which simplifies the flow in the electrodes but complicates product separation.

Tests will first be conducted on the scale of individual cells. Using established catalysts permits a comparison of electrolysis performance with conventional systems. On this scale, further promising catalysts from current research can also be tested for alkaline low-temperature electrolysis. Building on this, experiments will be conducted on the short-stack scale. Such experiments will permit a better understanding of the overall system, including its heat balance and expansive analytics during operation.

5.4 Supply systems for alternative fuels

According to current projections, the global demand for liquid fuels will grow considerably by 2050. Alternatives to fossil fuels include liquid synthetic fuels produced from biomass (BTL) or in power-to-fuel (PTF) processes using carbon dioxide and hydrogen, methane from biomass fermentation (bio CH_4), and hydrogen and methane from power-to-gas (PTG) processes.

5.4.1 PTF fuels

Whether a fuel produced by PTF processes will prevail on the market depends on two fundamental conditions: it must harmonize with current fuels and their infrastructure and technologically viable, economic production must be possible. The fuel must require no significant changes to infrastructure or existing vehicles. Furthermore, suitable non-fossil and non-biological fuels should be available for the various applications in the transportation sector. As is currently the case for the fossil-dominated market, a diversification of the fuels available is necessary.

IEK-3 is working on a comparative overview of various alternative fuels and their production, including Fischer–Tropsch hydrocarbons and polyoxymethylene dimethyl ethers (PODE). Both of these products can be blended with conventional diesel. Commercial usage is therefore conceivable. Despite having the same application, the processes and products differ considerably. Fig. 86 summarizes the major properties of both fuel types.

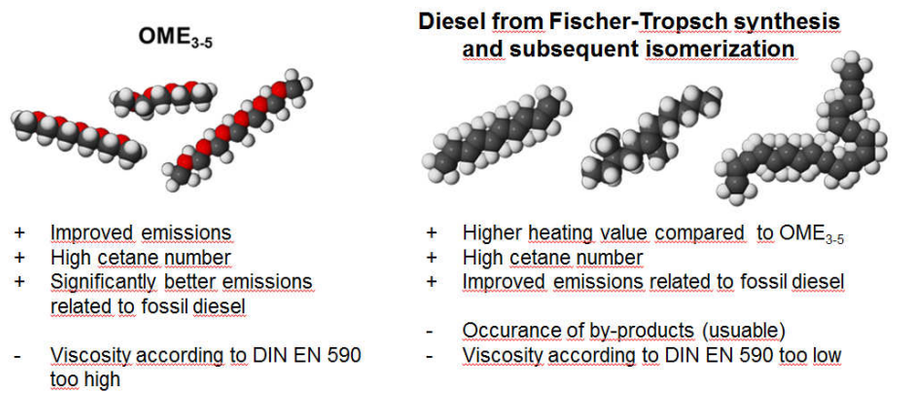

Fig. 86: Comparison of the power-to-fuel routes PODE synthesis and Fischer–Tropsch

On a molecular level, Fischer–Tropsch hydrocarbons are very similar to fossil diesel. This does not apply to ethers such as PODE. Although PODE has a lower heating value, it has outstanding potential for improving exhaust-gas values since the usual trade-off between the formation of soot and nitrous oxide does not apply. Industrial-scale Fischer–Tropsch processes have been state of the art for decades. This does not apply to PODE processes since the demand for these products is low. In terms of system design, there are different fundamental options for both processes. System design and process parameters influence

educt and energy demand as well as product quality, co-products, and by-products. The challenges of product processing differ for Fischer–Tropsch and $PODE_{3–5}$ synthesis. The difficulty with hydrocarbons, for example, is in the broad product distribution. The difficulty with $PODE_{3–5}$ synthesis is the liquid–liquid separation due to diverse miscibility gaps and azeotropes. Just like the product specification analysis, the techno-economic analysis of the production processes plays an important role in the strategy aiming to implement a climate-neutral transportation sector.

In addition to technical aspects, the comparative evaluation comprises the economic potential and ecological impacts. Fig. 87 provides an overview of the research approach at IEK-3. In addition to ethers and Fischer–Tropsch products, methanol-based processes are also investigated in the BmWi-funded C³ Mobility project. Based on an initial process design, the processes are being optimized to increase yield and efficiency, for example by installing additional heat exchangers or further chemical reactors. Ultimately, this will be followed by an economic analysis, determining the investment costs of setting up fuel synthesis and estimating operating costs.

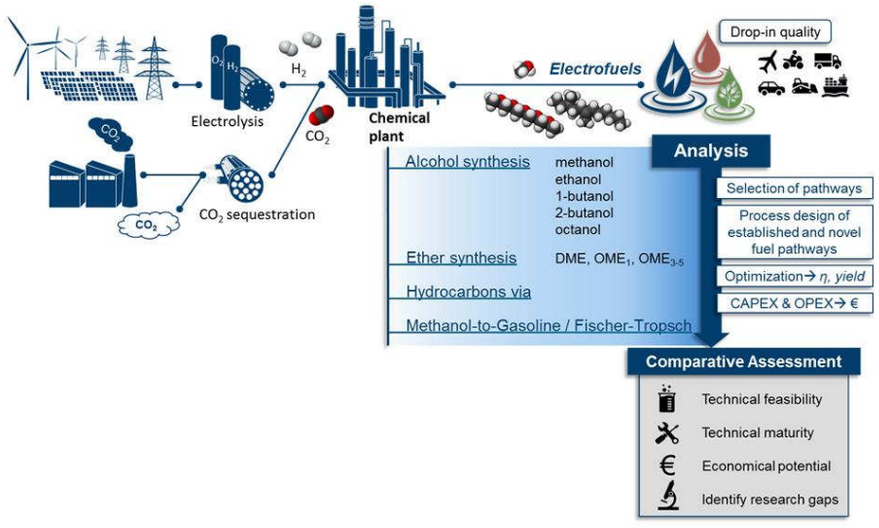

Fig. 87: Power-to-fuel research approach for methanol-based processes

5.4.2 Thermodynamic modeling

A special challenge for formaldehyde synthesis (route A of PODE production) is the description of phase equilibria. In mixtures of water/methanol and formaldehyde, oligomerization reactions occur that lead to the formation of unstable intermediate products such as methylene glycols (MG_n) and hemiformals (HF_n). The reaction network shown in Fig. 88 shows the relations in the gas and liquid phases. Only the shortest oligomers (chain length: 1) are assumed to contribute to the vapor pressure. Longer chains are disregarded in the gas phase and primarily form in the liquid phase.

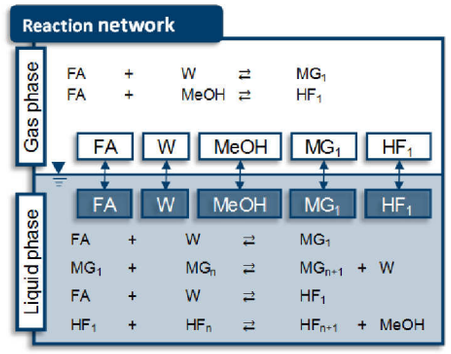

Fig. 88: Equilibrium model for mixtures of formaldehyde, water, methanol taken from Maurer et al.[32]

The implementation in Aspen Plus® utilized the existing UNIFAC model. The individual species were split into functional groups in order to derive the dimensions required. The correlation parameters were optimized based on experimental data. The optimization aimed to minimize the error squares between the simulated and experimental boiling and dew curves of the various mixtures. The results show a successful representation of the phase equilibria across almost the entire mixture and temperature range. An example of this successful implementation is shown in Fig. 89.

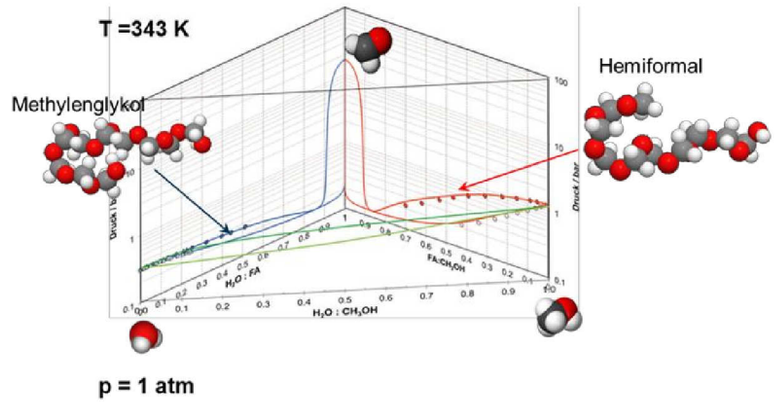

Fig. 89: Three-dimensional representation of the phase behavior of a formaldehyde-methanol-water mixture; simulation using Aspen Plus® and experimental data from Mauer et al.[30] for 343 K and 1 bar.

[32] Maurer, G., Vapor-liquid equilibrium of formaldehyde-and water-containing multicomponent mixtures. AIChE Journal, 1986. 32(6): p. 932–948.

The simulated boiling and dew curves show good agreement with the experimentally determined points. For higher fractions of formaldehyde from approx. 80 % up to the azeotrope of the mixture at 90 %, no experimental comparison was possible. The steep progression of the boiling and dew point curves from the azeotrope up to pure formaldehyde is due to the high boiling pressures of formaldehyde. However, these ranges are not important for the following simulations.

The thermodynamic models are used in Aspen Plus® for column design. Fig. 90 shows the process design of the distillation columns during methylal synthesis. A particular difficulty is posed by the phase equilibria resulting from the occurrence of formaldehyde; each stage of the distillation column is characterized by a different reaction equilibrium of methylene glycols, hemiformals, water, and methanol. Molecular formaldehyde no longer occurs in such mixtures. The column designs were verified using measurement data from the thermal separation process.

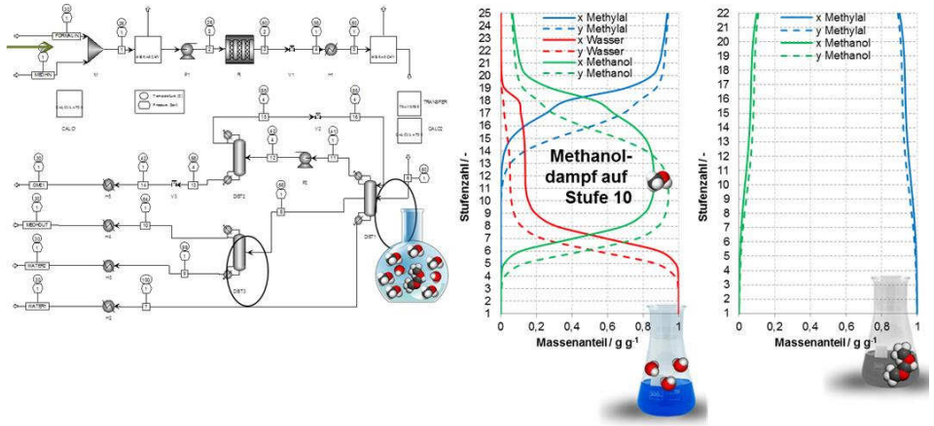

Fig. 90: Process design of the distillation columns during methylal synthesis

The column designs were verified using measurement data from the thermal separation process for all intermediate products of PODE synthesis.

Trioxane is also an important intermediate product for the production of $PODE_{3-5}$. Trioxane is used for the synthesis of $PODE_{3-5}$ according to routes B and C in Burger[33]. On an industrial scale, trioxane is produced using an extraction method developed by BASF. The process simulation here, however, was developed using the process design in Grützner et al.[34] as a basis. This process developed by Grützner promises a higher energy efficiency than the typical BASF process. In his paper, Grützner describes convergence problems for simulations with Aspen Plus®. However, the selected, special modeling approach (see

[33] Burger, J. A novel process for the production of diesel fuel additives by hierarchical design. PhD, Kaiserslautern, Kaiserslautern, 2012.

[34] Grützner, T., et al., Development of a new industrial process for trioxane production. Chemical Engineering Science, 2007. 62(18-20): p. 5613–5620.

above) made it possible to transfer the trioxane process to Aspen Plus® in a converged state. The total energy consumption of the columns in the shown trioxane process was determined by Grützner as 65.2–65.5 MJ/kg trioxane. From the modeling shown, a value of 65.3 MJ/kg trioxane was calculated, which is in good agreement with Grützner's value. The model was further validated by the correct prediction of the azeotropes. Both the synthesis of trioxane and the synthesis of formaldehyde are additionally heat integrated, which means that much less heat is required than the shown by the values above.

5.4.3 Economic analysis

The techno-economic analysis was based on the methodology of production costs. First, the investment costs and the operating costs have to be determined for the respective systems. The operating costs are determined using the values from the process simulation and the corresponding cost factors for the individual operating resources. The investment costs depend on the costs of system components. The component costs are calculated individually according to the module costing technique in R. Turton[4]. This technique has an accuracy of +50 % to -30 %. The general methodology of this analysis is shown in Fig. 91.

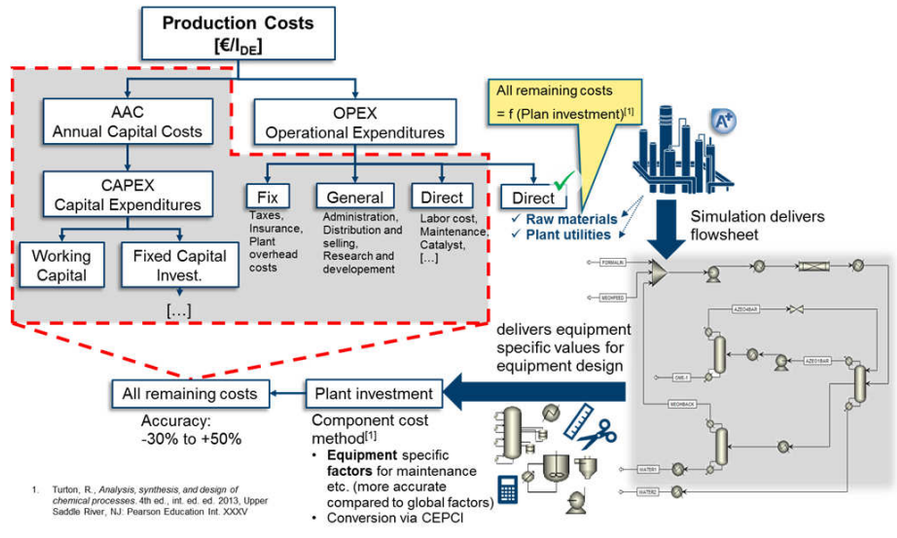

Fig. 91: General methodology of the economic analysis according to Turton[35].

At the present point in time, the processes of methanol synthesis, the two-stage DME synthesis, and the methylal synthesis have been techno-economically analyzed as described. A sensitivity analysis is advisable for such an analysis. The system size is constant in the following (300 MW_{th}). The reference value for the specific production costs is the energy contained in one liter of diesel (34.7 MJ), i.e., the production costs are determined

[35] Turton, R., Analysis, synthesis, and design of chemical processes. 4th ed., int. ed. ed. 2013, Upper Saddle River, NJ: Pearson Education Int. XXXV

for a selected fuel containing the same amount of energy in total as contained in one liter of diesel. The variations in limiting factors are summarized in Table 1.

Using these basic values, production costs of € 1.99/l_{DE} were calculated for methanol. In agreement with the process analysis, the provision of hydrogen via electrolysis is the greatest factor influencing the production costs of methanol. If the cost of hydrogen varies between € 3/kg and € 6/kg, then the costs of methanol fluctuate between € 1.34/l_{DE} and € 2.37/l_{DE}. Another strong influence involves the costs associated with the provision of CO_2. All remaining variables are of secondary significance, i.e., mainly the investment and operating costs of the systems.

Unit	Unit	Lower limit	Base value	Upper limit
H_2 costs	€/kg	3	4,6	6
CO_2 costs	€/kg	0,02	0,07	0,17
FCI (investment costs)	%	-30	-	+50
Interest rate	%	2	8	12
Steam	€/t	16	32	48
Cooling water	€/t	0,01	0,1	1
Operating current	€.ct./kWh	4	9,76	14,7

Table 3: Overview of the most important limiting factors on the economic analysis of electrofuels

Assuming the base values and a system size of 200 MW_{th}, production costs of € 1.85/l_{DE} can be achieved for DME, i.e., the costs are slightly lower than those for methanol. In general, the situation here is very similar to the analysis of methanol. The educts have the greatest influence on the costs, followed by investment costs, interest rates, and electricity. Since the process of DME synthesis (similar to methanol synthesis) was determined to be exothermic, no costs arise for process steam. The cooling water has an extremely small influence in this consideration.

These analyses will be fundamentally different for the $PODE_{3-5}$ synthesis routes because the following aspects will be more important:

- Investment costs will be higher due to the greater system complexity, which also means a greater influence of the effective interest rate.
- Additional costs will be incurred due to the provision of process steam for the operation of separation columns (cf. trioxane process).

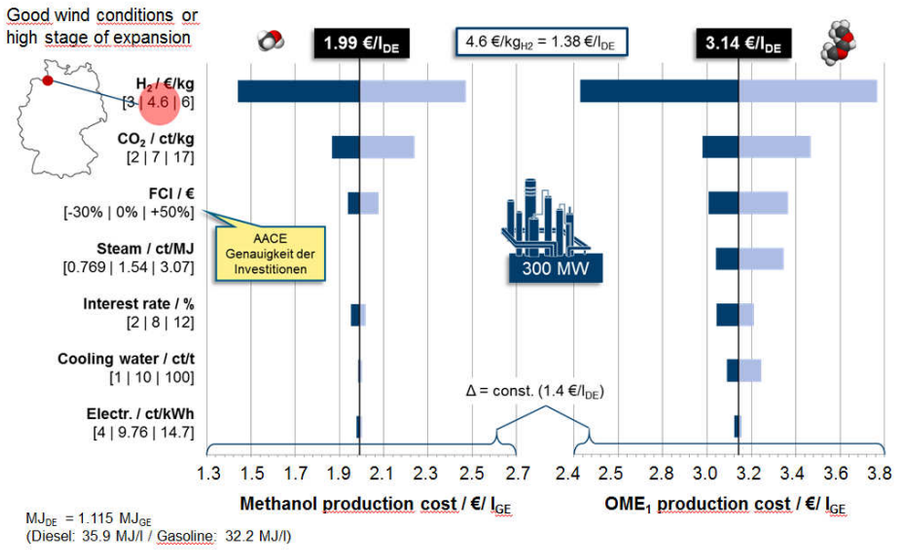

Fig. 92: Economic analysis of the methanol and methylal production costs based on system sizes of 300 MW$_{th}$.

Fig. 92 shows that in the case of PODE$_1$ production, operating costs of € 3.14/l$_{DE}$ are significantly higher than those of methanol. For long-chain PODE compounds, the formation of trioxane is necessary, depending on the route used. The energy demand is particularly high for trioxane production. For this reason, routes that avoid trioxane as an intermediate product are preferable.

5.5 Evaluative research on sustainable energy systems

5.5.1 Implementation strategies for greenhouse-gas-free transportation by 2050

Current political objectives, social trends, and progress in the field of transportation technology are pointing towards a major change in the manner in which people and goods will be transported in future. Significant changes are expected regarding the provision of energy sources for the transportation sector, particularly due to an altered end energy mix, which – within in the context of sector coupling – will shift towards charging current for battery electric vehicles, hydrogen for fuel cell vehicles, and synthetic liquid hydrocarbons. However, the extent to which individual solutions can be implemented in practice and will help to achieve objectives remains uncertain. A detailed analysis and evaluation requires the development of suitable models and the definition of scenarios which can be used to calculate the spectrum of expected changes in the transportation sector in terms of the quantity and structure of transportation services for passengers and goods. In addition, results of a disruptive nature, for example the exclusion of specific transport technologies, must be suitably depicted.

Within this context, there are new topics in the field of transport and mobility which concern the potential development of transportation demand, on the one hand, and the evaluation of available technical options over time, on the other. Key elements include the development of scenarios and models, the inclusion of sociological analyses and findings, and the integration of the overall model to be created with an existing energy system model above the level of the system, which directly uses the model results of the transportation sector for the purposes of energy system optimization at national level. To this end, impacts caused by sector coupling, for example due to an altered power demand in the transportation sector, can be directly investigated and evaluated.

The analysis of future mobility requirements and transport demand is the starting point for scenario development. Building on this, techno-economic models are developed to describe the system elements. It is also expected that subtasks will be performed with the aid of dynamic and static models, ensuring that one or several model environments can be used and suitably integrated. This includes, for example, refined analyses of vehicle fuel consumption in high temporal resolution (at least in the seconds range for light-duty vehicles) and investigations of overarching infrastructures and supply systems that are conducted in spatial (at least NUTS 3 level) and temporal (hourly) resolution. Furthermore, potential options derived from findings for the target period 2050 should be implemented for the necessary roadmapping over time.

5.5.2 Stationary energy systems

One of the aims of the planned work is to project and specify in detail IEK-3's energy and greenhouse gas reduction scenarios. To this end, the overall energy system model FINE-NESTOR, which was developed at IEK-3, will be used for the first time to model the national energy system – from primary energy production right up to the end energy sectors. In contrast to conventional models, the major advantage of this model is its ability to generate consistent scenarios. Using this myopic model, the aim is to develop transformation strategies for the energy transition (*Energiewende*). Many of the existing models at IEK-3 will

also be used within this framework. One of the aims here is to create reliable data input (e.g. wind power time series) for the NESTOR model. In addition, the aggregated results will be analyzed with the detailed models (e.g. required H_2 infrastructure). This requires an iterative approach, which is being tested for the first time. The work will provide an indication as to which coupled models can be hard-linked in future.

The realization of various PtX technologies requires the use of CO_2. However, it is currently unclear how much CO_2 might be available. It is crucially important to determine how much CO_2 will be available and in what areas. These localized amounts of CO_2 must be brought in line with localized amounts of hydrogen. To meet this objective, the development of a national CO_2 register is planned.

In terms of energy strategies for buildings and districts, the FINE.Building (optimization of building energy systems) and FINE.District (optimization of district energy systems) models, which were developed at IEK-3, will be developed further. One particular focus is the implementation of additional energy conversion and storage technologies (e.g. small wind turbines, CHP fuel cell systems, building-integrated PV, hydrogen storage systems). The FINE.District model will be extended for a specific district in order to depict a local grid transformer with all connected local grids. In addition, the FINE.District model will be coupled with a downstream load flow calculation.

These models will be used to investigate various issues relating to transformation strategies for buildings and districts. On the buildings level, the techno-economic analysis and evaluation of CHP fuel cell systems in combination with battery storage systems will be one of the priorities. The focus here will be on optimal system design and systems operation. Furthermore, the direct integration of conversion and storage technologies in building façades will be investigated on the basis of a case study. On the district level, various modernization rates in the building stock will be considered. Building on this, different sector coupling options will be investigated and the effects of a changed supply structure on grid operating systems (local grid transformer) will be determined. Another aim is to investigate the extent to which a self-sufficient district with a microgrid could represent an alternative to a conventional local grid structure with a transformer.

5.5.3 Sector coupling and infrastructures

The transformation of the energy system poses major challenges for all infrastructures dedicated to the transportation and distribution of energy, not only in terms of financing and planning, but also the realization of infrastructures in the fields of electricity, gases, and fuels. With the aid of spatially and temporally resolved energy system models, the aim is therefore to investigate how energy infrastructures with long planning horizons can be efficiently adapted to new and changing structures for energy generation and demand. The respective energy infrastructures will be analyzed with a view to Europe.

Possible sector coupling options, for example electromobility or power-to-hydrogen, will offer the possibility of coupling the relevant infrastructures in future and enable the potential relocation of energy transport pathways. For instance, the burden on the power transmission grid can be alleviated by the targeted production of hydrogen during grid bottlenecks, while energy can be transported and/or stored by a gas infrastructure. In terms of energy transport infrastructures for the target year 2050, development strategies must not be optimized in

isolation, but instead require multimodal, integrated modeling. The flexibility and storage capability of energy infrastructures must also be considered.

The plan is to expand the FINE model generator – which depicts, optimizes, and evaluates energy systems – to also incorporate multimodal infrastructure considerations. In order to analyze strategies for the construction and redesign of infrastructures, multiple time periods will be considered using various approaches. These developments will enable an integrated consideration of consistent scenarios for infrastructure expansion and, based on this, cost analyses and evaluations.

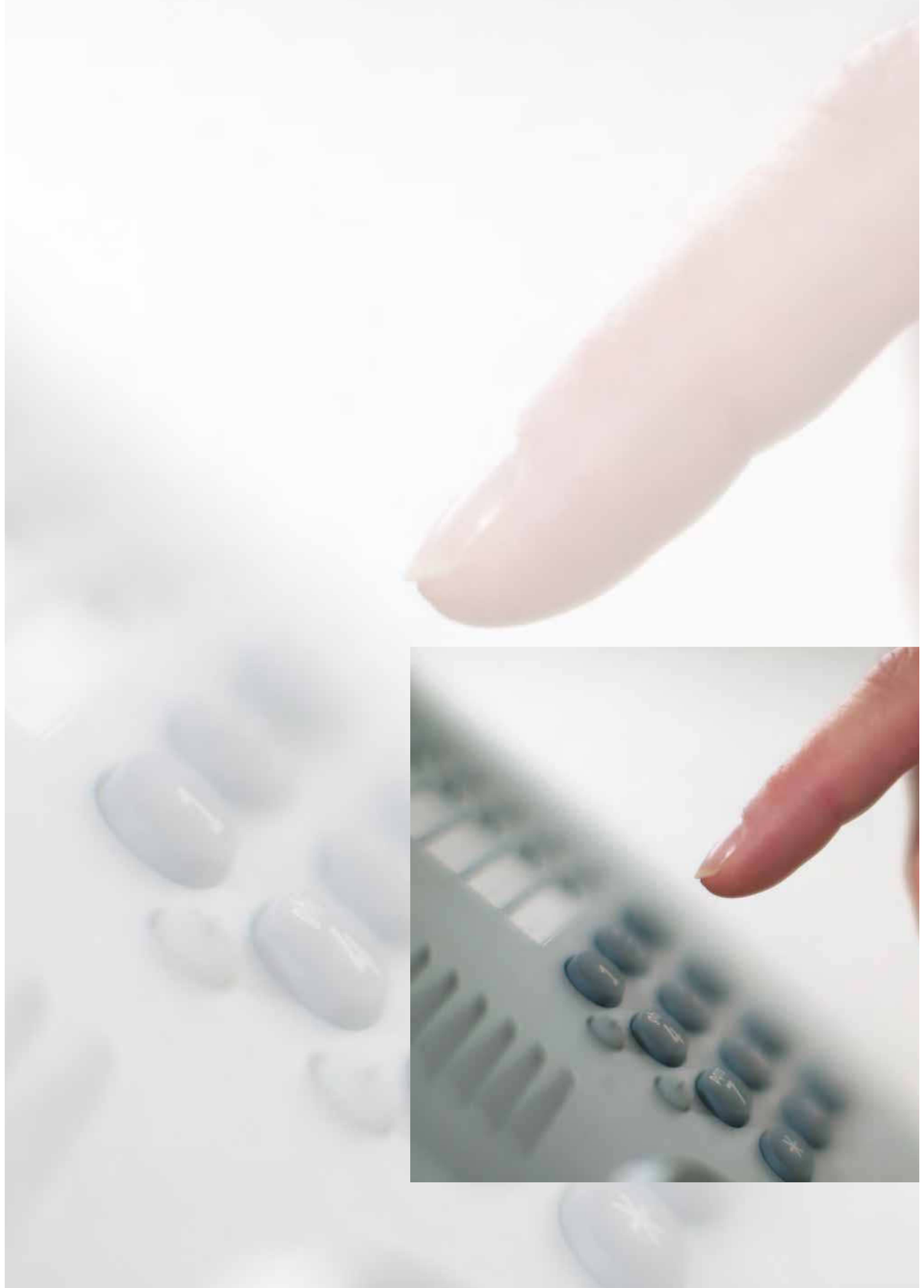

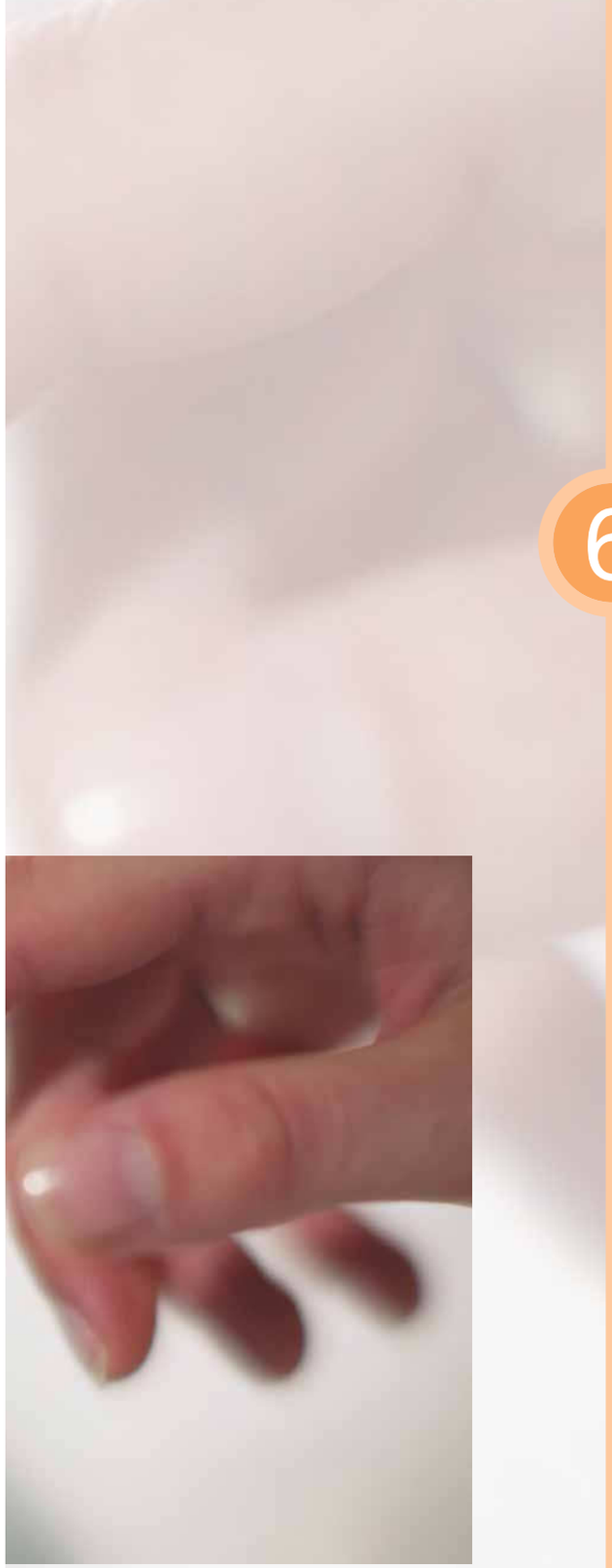

6

Data

Data, Facts and Figures

- The Institute of Energy and Climate Research – Electrochemical Process Engineering (IEK-3)
- Overview of department expertise
- Publications, technology transfer, and resources
- Prizes and awards
- Committee work
- Contributions to trade fairs and exhibitions
- How to reach us
- List of abbreviations

6.1 The Institute of Energy and Climate Research – Electrochemical Process Engineering (IEK-3)

Developments at IEK-3 during the period under review (2017–2018) involved intense work on targeted results for the key R&D issues handled by IEK-3 (fuel cells, electrolysis, and future fuels) in the newly established HGF programme “Storage and Cross-Linked Infrastructures”, in an attempt to provide plausible solutions to the major issues of the *Energiewende*. The thematic priority of systems for auxiliary power units is to develop – based on cell stacks from commercial providers – a fuel cell for a hydrogen-rich fuel gas from the system’s own fuel supply. The work on high-temperature polymer electrolyte fuel cells (HT-PEFCs) will be concluded during a transitional phase and expertise will be transferred to other IEK-3 activities that are also based on polymer electrolyte membranes.

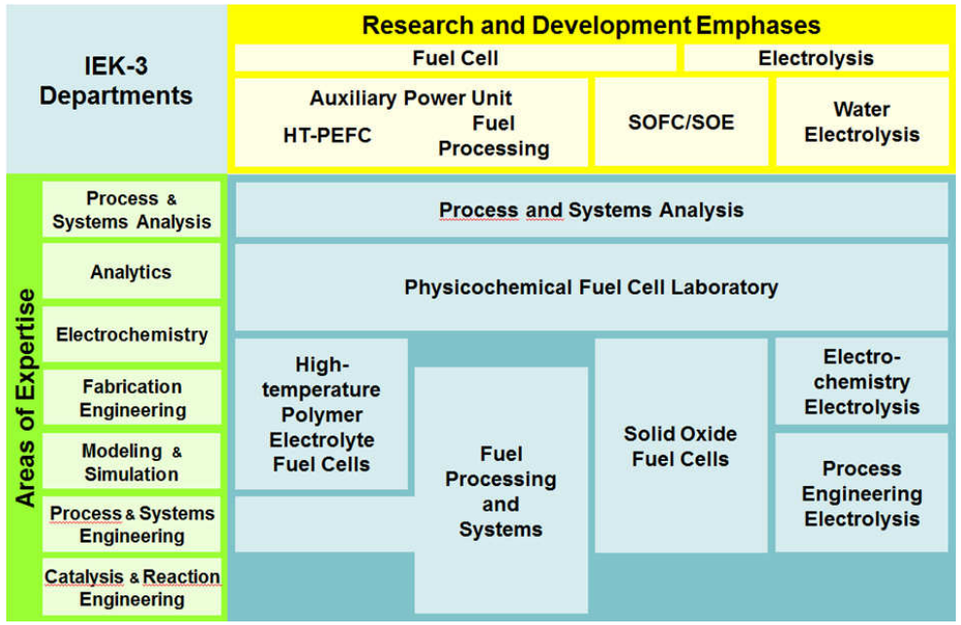

Fig. 93: Departments, areas of expertise, and R&D priorities

Additional topics at IEK-3 include ceramic high-temperature fuel and electrolysis cells (SOFC/SOE) as well as low-temperature electrolysis (shown in Fig. 93 with the corresponding competence fields). Focusing more closely on concrete areas of application enables IEK-3 to work on all aspects of each of these R&D topics from the basic phenomena up to process engineering for entire systems with teams of supercritical size and in research facilities of up to pilot-plant scale. Synergies between the scientific disciplines are exploited. The analysis and study results of technology-based process and systems analysis serve as a strategic orientation for the technology-based departments of IEK-3 responsible for analyzing, conceiving, designing, evaluating, and comparing future-oriented processes and energy systems. The approach used here accounts for technical, economic, and ecological aspects, and permits quantitative conclusions to be drawn on the performance efficiency and sustainability of an energy system. Application-oriented R&D activities are also accompanied by basic research aiming to clarify structure–activity relationships using selected advanced

analysis methods. These activities are pooled in the physicochemical fuel cell laboratory, which works together with the technology-oriented departments within the institute.

The first phase of the Power-to-X (P2X) Kopernikus project was successfully launched and concluded – with the help of scientific contributions from IEK-3 – resulting in a transition towards the second project phase. Through the focused expansion and consolidation of process and systems analysis (VSA) at IEK-3, the importance and visibility of this topic for the integrated design of sustainable energy supply systems was considerably increased. This benefited the granting of an extensive funding project, the implementation of which is being realized by the VSA group together with scientists from Jülich's IAS/JSC, RWTH Aachen University, and Friedrich-Alexander-Universität Erlangen-Nürnberg. The project concerns the development of extensive methods and models for realizing the *Energiewende* and for integrating energy systems. Within the scope of the HGF initiative Energy System 2050, collaboration was systematically established and intensified with the HGF centres GFZ, HZB, and DLR on the research topic of energy and raw material pathways involving hydrogen, and has already produced its first scientific results in the form of dissertations/theses and publications. Furthermore, IEK-3's commitment to the pioneering topic of energy system integration was expanded from work package 1 ("Multimodal energy system 2050^{+}") to include work package 2 ("Flexibilization of fundamental industrial process chains").

Institute of Energy and Climate Research
IEK-3: Electrochemical Process Engineering
Forschungszentrum Jülich GmbH
52425 Jülich

Head of Institute
Prof. Dr.-Ing. Detlef Stolten
Tel.: 02461-61-3076
e-mail: d.stolten@fz-juelich.de

For 25 years, Jülich has been working on institutional research into fuel cells and electrolyzers. It therefore has one of Europe's largest and most experienced research teams in this field with approximately 150 employees. In addition to IEK-3, three additional institutes with 12 employees for electrochemical process engineering are active in the field of SOFCs/SOEs. IEK-1 is responsible for manufacturing materials, IEK-2 tests the materials and conducts steel research, and IEK-9 focuses on the electrochemical principles. The Central Institute of Engineering, Electronics and Analytics – Engineering and Technology (ZEA-1) is concerned with stack construction. Of the approximately 101 IEK-3 employees (not including visiting scientists, student assistants, or trainees), 86 work on technological developments for low-temperature fuel cells and electrolyzers as well as energy systems analysis. Process and systems analysis has grown substantially to a total of 15 full-time employees due to its increased importance for the *Engergiewende*. A coordinator is responsible for the fields of work at IEK-3, and is also available to deal with overarching topics.

Deputy Head and scientific coordinator
Dr.-Ing. Bernd Emonts
Tel.: 02461-61-3525
e-mail: b.emonts@fz-juelich.de

6.2 Overview of Department Expertise

High-Temperature Polymer Electrolyte Fuel Cells	Fuel Processing Systems

Fields of work, range of services

Work on the HT-PEFC extends from the electrode to the stack and is conducted in cooperation with internal and external partners. New electrode structures and preparation methods are developed. MEAs are manufactured and electrochemically characterized. Structure–activity relationships of MEA components are also investigated. Metallic and graphite-based bipolar plates are developed and tested in cells and stacks. Comprehensive modeling and simulation activities from the component level up to the stack level support their development. In the field of NT-PEFCs, two-phase flow phenomena are investigated experimentally and theoretically.

H^2 produced from commercially available fuels enables the early introduction of fuel cell technology. For this purpose, middle distillates – kerosene, diesel, and heating oil – and diesel-like biofuels are reformed in the power range of 3–50 kWel An auxiliary power unit with an electrical power output of 7.5 kW el is currently being developed in combination with a commercial HT-PEFC as a compact module. PEFC systems will be integrated in cooperation with project partners. In future, the reactors and methods developed will be utilized in components and systems for fuel synthesis.

Facilities, processes, methods

Equipment - Test stands for the electrochemical characterization of MEAs - Test stands for electrochemical studies on stacks up to 5 kW_{el} - Equipment for the fabrication of gas diffusion electrodes Models - Simulation models to describe mass, charge and heat transport processes in cells and stacks - Lattice–Boltzmann simulation tools - CFD simulation tools (OpenFOAM and commercial tools)	Equipment - Test stands for the examination of reactors and whole systems - Test stands for the screening and examination of catalyst activity and selectivity - Analytical devices for the determination of reaction gas concentrations (GC, GC/MS, NDIR, FTIR) - Temporal analysis of products (TAP): Determination of the reaction process and the kinetics of catalyst materials Models - CFD simulation programs for reactor and system design

Contact

Prof. Dr. Werner Lehnert
Tel.: 02461-61-3915
e-mail: w.lehnert@fz-juelich.de

Prof. Dr.-Ing. Ralf Peters
Tel. 0261-61-4260
e-mail: ra.peters@fz-juelich.de

Solid Oxide Fuel Cells	Electrochemical Electrolysis

Fields of work, range of services

A key area of scientific and technical expertise is the development and optimization of cell stacks and systems for high-temperature fuel cells as well as high-temperature electrolysis. Stacks, systems, and system components are devised, designed, constructed, assembled, and tested. To optimize concept evaluation, the experimental studies are accompanied by the development of thermomechanical and process-engineering models. Priorities here are the electrochemical characterization of stacks and the development, testing, and evaluation of new system concepts and control technology concepts in cooperation with industry.

Advanced PEM electrolyzers facilitate the economic production of H_2 from excess renewable electricity. With support from project partners in research and industry, development work concentrates on membrane electrode assemblies (MEAs) in which the platinum group metals required for catalytic reactions are either reduced or completely replaced while retaining comparable performance. New types of membranes aim to ensure that planned large-scale systems are sufficiently stable. Additional topics include the identification of cost-effective materials and the development of replicable fabrication techniques for MEA development and production.

Facilities, processes, methods

Test stands

- Characterization: high-temperature heat exchangers up to 850 °C@ 200 m^3 air/h
- Characterization: reformers and afterburners for stacks up to 5 kW
- Characterization: 5 kW rSOC system
- Electrochemical characterization: 100 W–10 kW stacks in fuel cell and electrolysis operation

Models

- CFD/FEM models to determine flow and voltage distribution in stacks and system components
- Simulation models for the design of fuel cell systems

Equipment

- Test stands for the characterization of electrocatalysts (rotating disk electrode)
- Test stands for the characterization of membranes (gas permeation measurements, fluorine release rate)
- Test stands for the electrochemical characterization of CCMs
- Test stand for electrochemical studies up to 30 kW_{el}
- Coating facility (roll-to-roll) for continuous electrode fabrication

Contacts

Prof. Ludger Blum
Tel.: 02461-61-6709
e-mail: l.blum@fz-juelich.de

Dr. Marcello Carmo
Tel. 0261-61-5590
e-mail: m.carmo@fz-juelich.de

Process Engineering Electrolysis	Physicochemical Fuel Cell Laboratory

Fields of work, range of services

Using ideas for new concepts, electrolysis stacks and systems are developed and modeled. The aim is to improve efficiency, power density, and lifetime while simultaneously reducing the amount of material needed. Work is validated in component tests and by characterizing entire stacks and systems. In cooperation with project partners, coatings, stack components, stacks, and systems are optimized and characterized. Combined with automated fabrication on an industrially relevant scale, this work builds a bridge between science and technology.

As the technical development of new pioneering energy systems progresses, scientific work is becoming increasingly important for understanding basic phenomena. The department therefore focuses on fully elucidating material and structural properties as well as physicochemical and electrochemical processes. Imaging, physical, and spatially resolved analysis techniques are used to determine chemical and structural changes, mechanical and thermodynamic suitability, and fluid dynamic and electrochemical performance.

Facilities, processes, methods

Equipment

- Test stands for electrochemical studies of electrolyzers up to 100 kW_{el} and fuel cells (DMFCs)
- Visualization tests
- Corrosion test stands for the evaluation of coatings
- Analysis of ion-exchange materials with media containing specific impurities
- Laser coating for local modification of surfaces
- Robot facility for the reproducible fabrication of stacks

Models

- Description of mass, charge, and heat transport

Equipment and methods

- Imaging analysis techniques: high-resolution scanning electron microscope (H-SEM) with EDX analysis, optical microscopes, confocal laser scanning microscope
- Spatially resolved analysis techniques: segmented cell technology (SCT), magnetic imaging, and mass spectroscopy (SRMS)
- Physicochemical analysis techniques: thermogravimetric analysis (TG, TGA), differential scanning calorimetry (DSC), contact angle measurement (KF analysis), impedance spectroscopy/CV, RDE, climate cabinet, tensile testing machine with climate chamber, BET and standard porosimeter, particle size measuring unit

Contacts

Dr.-Ing. Martin Müller
Tel.: 02461-61-1859
e-mail: mar.mueller@fz-juelich.de

PD Dr. Carsten Korte
Tel.: 02461-61-9035
e-mail: c.korte@fz-juelich.de

Process and Systems Analysis

Fields of work, range of services

The selection, development, and implementation of future energy systems demands approaches which analyze and evaluate the sustainability and economic viability of entire systems. Techno-economic comparisons of competing technologies for energy conversion and storage are the foundation for this. The broad experimental basis and extensive modeling at IEK-3 make it possible to design energy systems, describe them in models, and compare them with competing technologies under realistic conditions as well as to identify development potential and shortcomings. Studies for industry are also conducted while protecting sensitive information, and policy recommendations are derived on a neutral basis.

Facilities, processes, methods

Methods

- Energy systems modeling using modeling environments such as METIS (models for energy transformation and integration systems), a Python- and database-based environment developed at IEK-3
- Potential analyses of renewable energy in the overall European system, for example
- Dynamic simulations (Python, Matlab/Simulink)
- Well-to-wheel analyses (spreadsheets)
- Technology-based benchmarking
- Economic evaluations (SWOT, WACC, CAPM, Monte Carlo simulations)
- Process analysis and optimization (Fluent, AspenPlus)

Contacts

Dr.-Ing. Martin Robinius
Tel.: 02461-61-3077
e-mail: m.robinius@fz-juelich.de

6.3 Publications, technology transfer, and resources

The results of scientific and technical work carried out at IEK-3 are published in relevant journals and presented to interested specialist audiences at national and international conferences. In 2017 and 2018, scientists from IEK-3 published three articles in journals with great influence, i.e. a high impact factor (9.0 or higher; see Table 4). In addition, other journals were addressed whose thematic orientation largely corresponds to the work priorities of IEK-3. This led to a maximum number of publications in the three favored journals – between 5 and 18 articles per year and journal. The total number of articles published in peer-reviewed journals amounted to 60 in 2017 and 58 in 2018.

Journal	Impact factor	2017	2018
Journal of the American Chemical Society	14,357	1	0
Renewable and Sustainable Energy Reviews	9,184	0	2
Applied Energy	7,900	2	9
Journal of Power Sources*	6,945	9	5
Journal of Membrane Science	6,578	1	0
Energy Conversion and Management	6,377	2	0
Journal of CO2 Utilization	5,503	0	1
Electrochimica Acta	5,116	4	2
Energy	4,968	1	1
Fuel	4,908	1	0
Renewable Energy	4,900	1	0
Electrochemistry Communications	4,660	2	1
International Journal of Hydrogen Energy*	4,229	18	10
APL Materials	4,127	0	1
Physical Chemistry, Chemical Physics	3,906	2	1
Journal of the Electrochemical Society*	3,662	5	8
Journal of Electroanalytical Chemistry	3,235	2	1
The Journal of Chemical Physics	2,843	0	1
Energies	2,676	5	3
Control Engineering Practice	2,616	1	0
Transport in Porous Media	2,211	0	1
Fuel Cells	2,149	1	1
International Journal of Adhesion and Adhesives	2,065	0	1
Applied Sciences	1,689	0	1
Journal of Coatings Technology and Research	1,619	0	1
Journal of Electrochemical Energy Conversion and Storage	1,429	0	2
Review of Scientific Instruments	1,428	0	1
Coatings	1,298	0	1
Materials and Corrosion	1,259	1	0
Bulgarian Chemical Communications	0,242	1	0
Journal of Energy Storage	Not specified	0	2
Sustainable Energy & Fuels	Not specified	0	1

Table 4: Publication performance of IEK-3 in peer-reviewed journals

IEK-3 scientists contributed a total of 44 talks and 10 posters to national and international conferences in 2017, and 61 talks and 19 posters in. The most important conferences with

IEK-3 involvement in 2017 were the 6th European PEFC & Electrolyser Forum in Lucerne/Switzerland with 4 talks, the 232nd ECS Meeting (The Electrochemical Society) in National Harbor/USA with 3 talks, the SOFC-XV – 15th International Symposium on Solid Oxide Fuel Cells in Hollywood/USA with 3 talks; and the MODVAL 2017 – 14th Symposium on Fuel Cell and Battery Modeling and Experimental Validation in Karlsruhe with 3 talks. In 2018, IEK-3 contributed 10 talks to the WHEC 2018 – 22nd World Hydrogen Energy Conference in Rio de Janeiro/Brazil, 3 talks to the 14th International Conference on Greenhouse Gas Control Technologies in Melbourne/Australia, 4 talks to the 69th Annual Meeting of the International Society of Electrochemistry in Bologna/Italy, and 4 talks to the 13th European SOFC & SOE Forum 2018 in Lucerne/Switzerland. The various departments within IEK-3 also contributed to numerous other specialist conferences with papers and presentations both within Germany and abroad.

During the period under review (2017–2018), 11 doctoral theses (Table 5) were completed on SOFCs (1), HT-PEFCs (4), BGS (1), and PEM-EL (4), as well as one doctoral thesis evaluating pioneering energy systems. Furthermore, Professor Stolten assessed 4 successful doctoral projects of external doctoral researchers in 2015.

Year		2017	2018
Publications	Peer-reviewed journals[1)]	60	58
	Books and journals	12	14
	Article in a book	4	8
	Doctoral theses[2)]	3	8
Technology transfer	Ongoing projects with third-party funding	40	37
	HGF initiatives & funds	3	3
	Patent applications	1	2
	Patents granted	5	7
Resources[3)]	Personnel (PoF[4)]/third-party funding)	120 (96/24)	123 (98/25)
Explanatory notes	[1)] according to ISI citation index [2)] internal doctoral researchers [3)] data in PY/a [4)] PoF: Program-oriented funding		

Table 5: IEK-3 core data for 2017 and 2018

In order to guarantee substantial knowledge and technology transfer, IEK-3 is involved in numerous national and international R&D projects (2017: 40; 2018: 37, see Table 5), funded by the European Commission (EC; 2017: 5; 2018: 5), the Federal Ministry for Economic

Affairs and Energy (BMWi; 2017: 12; 2018: 13), the Federal Ministry of Education and Research (BMBF; 2017: 3; 2018: 4), the Federal Ministry of Transport and Digital Infrastructure (BMVI; 2017: 1; 2018: 1), and various ministries of the federal states of North Rhine-Westphalia and Bavaria (2017: 4; 2018: 3), as well as the JARA excellence initiative (JARA; 2017: 2; 2018: 0), or financed by industry (2017: 13; 2018: 11). Some of these projects were headed and coordinated by IEK-3.

With the unlocking of expansion investments made by the Helmholtz Association (HGF) at the end of 2017, IEK-3 was able to begin work on the Energy Lab 2.0 project involving numerous research centres. This concerned the detailed planning of a pilot plant for future hydrogen experiments as well as the specification and awarding of a contract for a MW electrolysis plant as a Jülich component for future power-to-gas processes within the Energy Lab 2.0. In addition, the HGF initiative Energy System 2050, which is carried out by eight HGF centers, presented its first results for the first energy industry assessment in spring 2018. Furthermore, IEK-3 received additional funding for a doctoral project from the Jülich technology transfer fund in order to bolster promising innovations with commercialization prospects. The numerous patent applications (2017: 1, 2018: 2) and patents granted (2017: 5, 2018: 7) during the period under review represent another step towards smooth technology transfer.

During the period under review, the number of employees at IEK-3 fluctuated between 120 (2017) and 123 (2018) (see Table 5). They were financed through the Helmholtz Association's (HGF) program-oriented funding (POF) as well as by third-party funds. In addition to part-time employees, a significant portion of IEK-3 personnel were employed for less than one year during this period, so that the effective personnel capacity amounted to 99 PY/a in 2017 and 106 PY/a in 2018.

6.4 Prizes and awards

Scientists from IEK-3 were awarded a number of important prizes and accolades for their outstanding work on scientific and technical issues during the period under review.

2017

Borchers Badge from RWTH Aachen University
Doctoral thesis: “Reduktion von Edelmetallen in der Wasserstoffelektrode bei der Polymerelektrolyt-Wasserelektrolyse”
Dr. Paul Paciok

Wasserstoff.NRW research prize 2017
Doctoral thesis: “Strom- und Gasmarktdesign zur Versorgung des deutschen Straßenverkehrs mit Wasserstoff”
Dr. Martin Robinius

Wasserstoff.NRW research prize 2017
Master’s dissertation: “Pfadanalyse zur großtechnischen Wasserstoff-Speicherung mit zentraler Rückverstromung”
Natalie Jessica Ebersbach

Wasserstoff.NRW research prize 2017
Master’s dissertation: “Techno-economical potential of reversible Solid Oxide Cells for autarkic Buildings and Districts”
Fritz Thomas Carl Röben

Best Paper Award 12th Conference of Sustainable Development of Energy, Water and Environment Systems – SDEWES
“Spatio-Temporal Optimization of a Future Energy System for Power-to-Hydrogen Applications in Germany”
Lara Welder

2nd Place – Best Paper Award European Fuel Cell Conference & Exhibition in Naples
“Optimized Electrolyzer Operation: Employing Forecasts of Wind Energy Availability, Hydrogen Demand, and Electricity Prices”
Fabian Grüger

2018

Borchers Badge from RWTH Aachen University
Doctoral thesis: “Future Grid Load of the Residential Building Sector”
Dr. Leander Kotzur

Borchers Badge from RWTH Aachen University
Doctoral thesis: “Quantitative Analyse der Trocknungsverläufe von Katalysatordispersionen”
Dr. Fabian Scheepers

Medal of honour from Aachen University of Applied Sciences
Bachelor’s degree with outstanding result
Jennifer Groß

Medal of honour from Aachen University of Applied Sciences
Bachelor’s degree with outstanding result
Joshua Stremme

6.5 Commitee work

IEK-3's national and international reputation in the field of fuel cells and hydrogen technology is reflected in the fact that IEK-3 scientists are members of and collaborate with national and international committees. The impact of numerous scientists from IEK-3 in leading roles for the Technology Collaboration Programme on Advanced Fuel Cells of the International Energy Agency (IEA) provides IEK-3 with great international visibility. On the national level, Prof. Stolten is a member of the Executive Board and Advisory Council of the VDI Society for Process Engineering and Chemical Engineering, Chair of the ProcessNet Subject Division Energy Process Engineering, and member of the advisory council. An overview of committee work performed by IEK-3 employees is listed in detail below.

Technology Collaboration Programme on Advanced Fuel Cells/Advanced Fuel Cells Implementing Agreement of the International Energy Agency
since 2000, Prof. D. Stolten
Head of the German Delegation on the Executive Committee

since 2002, Prof. D. Stolten
Vice-Chairman of the Executive Committee

since 2009, Dr. R.C.Samsun
Member of the Executive Committee

since 2011, Prof. D. Stolten
Chairman of the Executive Committee

since 2011, Prof. D. Stolten
Operating Agent for Annex 36 Systems Analysis

since 2011, Dr. R.C. Samsun
Member of Annex 35 Systems Analysis

since 2013, Prof. L. Blum
Member of Annex 32 Solid Oxide Fuel Cells

since 2014, Prof. S. Beale
Operating Agent for Annex 37 Modeling of Fuel Cell Systems

since 2014, Jürgen Mergel (withdrawal in March 2017)
Operating Agent for Annex 30 "Electrolysis"

since 2014, Prof. D. Stolten, Prof. L. Blum, Dr. M. Carmo, Dr. W. Lüke, Dr. M. Müller
Members of Annex 30 "Electrolysis"

since 2014, Prof. W. Lehnert
Member of Annex 31 Polymer Electrolyte Fuel Cells

since 2014, Dr. T. Grube
Member of Annex 34 "Fuel Cells for Transportation"

since 2014, Dr. M. Müller
Member of Annex 35 "Fuel Cells for Portable Applications"

since 2014, Prof. L. Blum, Dr. D. Fritz, D. Froning, Prof. A. Kulikovsky, Prof. W. Lehnert, Dr. U. Reimer
Members of Annex 37 Modeling of Fuel Cell Systems

since April 2017, Dr. M. Carmo
Operating Agent Annex 30 "Electrolysis"

Institute of Mechanical Engineering (IMechE), UK
since 1980, Prof. Dr. S. Beale
Member

American Society of Mechanical Engineers (ASME), USA
since 1981, Prof. Dr. S. Beale
Member

Professional Engineers Ontario, Canada
since 1985, Prof. Dr. S. Beale
Member

Working Group of Electrochemical Research Facilities (AGEF)
since 1990, Dr. K. Wippermann
Member

since 2000, Prof. D. Stolten
Member

since 2010, J. Mergel
Member of the Board of Directors

German Chemical Society (GDCh)
since 1990, Dr. K. Wippermann
Member of GDCh and of the GDCh Special Interest Group for Applied Electrochemistry

since 1999, Prof. Dr. W. Lehnert
Member

German Physics Society (DPG)
since 1993, Prof. Dr. W. Lehnert
Member

since 2010, Dr. U. Reimer
Member of the Energy Working Group

German Bunsen Society for Physical Chemistry (DBG)
since 1993, PD Dr. C. Korte
Member

Institute of Electrical and Electronics Engineers (IEEE), USA
since 1996, Prof. Dr. S. Beale
Member

International Society of Electrochemistry (ISE), Switzerland
since 1998, Prof. Dr. W. Lehnert
Member

since 2005, Prof. A. Kulikovsky
Member

Electrochemical Society (ECS), USA
since 1999, Prof. Dr. W. Lehnert
Member

since 2005, Prof. A. Kulikovsky
Member

Association of German Engineers (VDI)
since 1999, Prof. Dr. W. Lehnert
Member

since 2013, Dr. T. Grube
Member

since 2015, Dr. P. Stenzel
Personal member

German Informatics Society
since 2002, D. Froning
Member

German Informatics Society – special interest group on numerical simulation
since 2015, D. Froning
Member

ProcessNet Subject Division Energy Process Engineering
since 2003, Prof. D. Stolten
Member

since 2006, Prof. D. Stolten
Vice-Chairman

since 2008, Prof. D. Stolten
Chairman

since 2012, Prof. R. Peters
Member of the Advisory Board

German Hydrogen and Fuel Cell Association (DWV)
since 2004, Prof. Dr. W. Lehnert
Member

since 2011, Prof. D. Stolten
Representative of Forschungszentrum Jülich GmbH as a full member

---

Fuel Cell Qualification Initiative
since 2005, Dr. B. Emonts
Member of the Executive Committee

BREZEL Expert Committee of the Association of German Engineers
since 2005, Prof. L. Blum
Member of the Expert Committee

WILEY-VCH "Fuel Cells" Journal
since 2006, Prof. D. Stolten
Member of the Advisory Board

National Organization for Hydrogen and Fuel Cell Technology (NOW)
2008–2013, 2015–2016, Prof. D. Stolten
Member of the Advisory Board and HGF/BMBF representative for the field

---

N.ERGHY in EU FCH Undertaking
since 2008, Prof. D. Stolten
Representative of Forschungszentrum Jülich GmbH as a full member

2008–2012, Prof. R. Peters
Member of the Working Group for AA Transport and Refuelling Infrastructure

since 2013, Prof. R. Peters
Member of the Working Group Transport Pillar

ProcessNet Section SuPER
since 2008, Prof. D. Stolten
Member of the Steering Committee

ASME K-10 Heat Transfer Technical Committee (heat transfer equipment)
since 2008, Prof. Dr. S. Beale
Member

Computational Thermal Sciences Journal, begellhouse
since 2008, Prof. Dr. S. Beale
Member of the Editorial Board

Renewable Energy Research Association (FVEE)
since 2009, Dr. B. Emonts
Representative of Forschungszentrum Jülich GmbH for Fuel Cells

h2-netzwerk-ruhr
since 2009, Dr. B. Emonts
Member of the Advisory Board

since 2012, Dr. B. Emonts
Vice-Chair of the Advisory Board

since 2015, Dr. B. Emonts
Chair of the Advisory Board

ASME K-20 Heat Transfer Technical Committee (computational heat transfer)
since 2010, Prof. Dr. S. Beale
Member

ASME Research Committee on Energy-Water Nexus
since 2010, Prof. Dr. S. Beale
Member

ASME Research Committee on Sustainable Products and Processes
since 2010, Prof. Dr. S. Beale
Member

Thermopedia Journal, begellhouse
since 2010, Prof. Dr. S. Beale
Member of the Editorial Board

Max Planck Institute for Dynamics of Complex Technical Systems Magdeburg
since 2011, Prof. D. Stolten
Member of the Scientific Advisory Board

Society for Chemical Engineering and Biotechnology e.V. (DECHEMA)
since 2011, Prof. D. Stolten
Member

VDI Society Chemical and Process Engineering (VDI-GVC)
since 2011, Prof. D. Stolten
Member of the Executive Board and Advisory Council

VDI-Vieweg publishing house – VDI-Fachbuch, Berlin
since 2011, Prof. R. Peters
Member of the Advisory Board

Fuel Cells and Hydrogen Network NRW
since 2012, Dr. B. Emonts and Dr. T. Grube
Chairmen of the Hydrogen Platform and the Working Group for H_2 Systems

Wuppertal Institute for Climate, Environment and Energy
since 2012, Prof. D. Stolten
Member of the Supervisory Board

International Association of Hydrogen Energy (IAHE)
since 2012, Prof. D. Stolten
Vice President of the Board of Directors

since 2012, Dr. B. Emonts
Member

Applied Energy Journal, Elsevier
since 2012, Prof. D. Stolten
Member of the Editorial Board

since 2015–2016, Prof. D. Stolten
Specialist editor

Institute of Electrochemistry and Energy Systems of the Bulgarian Academy of Sciences
since 2012, Prof. Dr. W. Lehnert
Member of the Advisory Board

Clean Power Net
since 2012, Dr. M. Müller
Member

Hydrogen Power Storage & Solutions East Germany (HYPOS)
2013–2015, Prof. D. Stolten
Member of the Board

VDMA Fuel Cells Group PG HT-BZ (SOFC)
since 2013, Prof. L. Blum
Member

Journal of Hydrogen Energy, Elsevier
since 2014, Prof. D. Stolten
Member of the Editorial Board

Journal of Energy Storage, Elsevier
since 2014, Prof. D. Stolten
Member of the editorial board and the editorial committee

TRENDS2017 – Transition to Renewable Energy Devices, Aachen
2017, Prof. D. Stolten
Chairman of the Conference and the Organizing Committee

2017, Prof. R. Peters
Vice-Chairman of the Conference and the Organizing Committee

Project House TESA – Technology-Based Energy System Analysis
since 2015, Prof. D. Stolten
Spokesman of the Steering Committee

since 2015, Dr. B. Emonts
Office manager

Profile Area Energy, Chemical & Process Engineering (ECPE) of RWTH Aachen University
since 2015, Prof. D. Stolten
Member

JARA-Energy – Processes Pillar
since 2015, Prof. D. Stolten
Head of department (together with Prof. Leitner, RWTH Aachen University)

Guideline committee VDI 4657 on the planning and integration of energy storage systems
since 2015, Dr. P. Stenzel
Member

Scientific Advisory Committee for the 12th European SOFC & SOE Forum, Switzerland
2016, Prof. D. Stolten
Member

German National Academy of Science and Engineering (acatech)
since 2016, Dr. M. Robinius
Member of the working group on pathway dependendes and decision strategies

BMWI research network on entire systems analysis: working group on model coupling and overall system
since 2016, Dr. P. Markewitz
Group spokesman

Advances Journal of the Royal Society of Chemistry
since 2016 – Dr. J. Pasel
Co-editor

German Association for Electrical, Electronic and Information Technologies (VDE)
since 2016, Dr. M. Robinius
Member

Hydrogen Implementing Agreement der International Energy Agency – Task 38 Power to Hydrogen to X
since 2016, Dr. M. Robinius
Member

GEE Gesellschaft für Energiewissenschaft und Energiepolitik
since 2017, Dr. M. Robinius
Member

VDI Society for Vehicle and Traffic Systems Technology/steering committee on drives and energy management
since 2017, Prof. D. Stolten
Member

Kopernikus project "ENavi"
since 2017, Dr. T. Grube
Member of the mobility competence team

6th International Conference on Advances in Energy Research, India
2017, Prof. D. Stolten
Member of the International Advisory Committee

European Fuel Cell Conference & Exhibition – Piero Lunghi Conference EFC 2017, Italy
2017, Prof. D. Stolten
Member of the Organizing Committee

Expert panel for the evaluation of the hydrogen and fuel cell center ZBT GmbH in Duisburg
2018, Prof. D. Stolten
Member of the working group "Evaluation JRF (Johannes-Rau-Stiftung)"

Grand Renewable Energy 2018 International Conference, Japan
2018, Prof. D. Stolten
Member of the International Advisory Committee

6.6 Contributions to trade fairs and exhibitions

IEK-3 showcases its innovativeness and R&D results at trade fairs and exhibitions which provide an excellent environment for establishing contact with interested visitors and exchanging information with partners and experts with similar specializations. In 2017, IEK-3 took part in five trade fairs and exhibitions in Düsseldorf, Hannover, Munich, and Stuttgart. Details of these fairs and exhibitions are listed below:

2017

11 IRES 2017 14 –16.03.2017, Düsseldorf *Sustainable energy and raw material pathways*
Hannover Messe 2017 24 –28.04.2017, Hannover *Fuel cell and electrolysis research*
Intersolar 2017 31.05. –02.06.2017, Munich *MW electrolysis plant as a system contribution to the Energy Lab 2.0*
ECS30 9 –11.10.2017, Stuttgart *Systems research for electromobility*
SHELL Energie-Dialog H_2 11.12.2017, Düsseldorf *H_2 – Building block of sector coupling and electrofuel*

The annual highlight of IEK-3's trade fair activities is its joint stand on hydrogen, fuel cells, and batteries at the technology trade fair in Hannover (see Fig. 94). In 2017, IEK-3 presented the latest technological developments in the field of fuel cell and electrolysis research. Ready-for-series-production reactors for autothermal reforming, water–gas shift, and catalytic combustion were presented as the state of the art in developments for fuel gas production from diesel or kerosene. The newest HT-PEFC components were presented on a screen alongside the respective multiscale modeling and simulation. Furthermore, cell and stack components demonstrated the structure and function of a system using a ceramic cell, which can be operated as a fuel cell or an electrolyzer according to requirements. A novel model offered insights into the structure of the functional layers of a PEM electrolysis cell. On the back wall of the trade fair stand, integrated into the map of the energy supply of the future, IEK-3's process and systems analysis presented specific analysis results for the traffic, industry, and household sectors. Within the scope of the Technical Forum, Professor Blum held a talk entitled "rSOC plant: efficient design and operation behavior", during which he spoke about the latest dimensioning and operation results of a plant with a stack of reversibly operable solid oxide cells. Meanwhile at the Public Forum, Markus Reus answered the moderator's questions on the topic of "Linking the power and transport sectors – A sector coupling scenario for Germany".

Fig. 94: Hannover Messe 2017 – Jülich exhibition stand and team

An overview of the events in which IEK-3 participated in 2018 and the topics concerned is given below.

2018

Hannover Messe 2018
23 –27.04.2018, Hannover
Fuel cell and electrolysis research

Forschen:Gesellschaft:Zukunft
14.06.2018, Jülich
H2 – an important building block of sector coupling

22nd World Hydrogen Energy Conference 2016
17 –22.06.2018, Rio de Janeiro, Brazil
Research for the efficient production and use of hydrogen

13th European SOFC & SOE Forum
3 –6.07.2018, Lucerne/Switzerland
Research into energy converters using ceramic electrolytes

f-cell 2018
18 –19.09.2018, Stuttgart
Energy research for electromobility

Under the tag line “Technologies & Systems Design for the Energy Transition”, the IEK-3 team presented itself at Hannover Messe 2018 (see Fig. 95, left). The team’s exhibits ranged from cell components, cells, and stacks for PEM electrolysis, rSOC, and PEFC to a flow cell for PEM electrolysis on a square-meter scale and a jet loop reactor for the synthesis of liquid fuels. As part of the forums for visitors to the trade fair, Dr. Grube presented the results of a contract study entitled “Batteries and hydrogen – a comparative analysis of infrastructure

costs". At the Public Forum, Dr. Martin Müller spoke about PEM electrolyzers from Jülich, stack components, and entire systems on a kW scale.

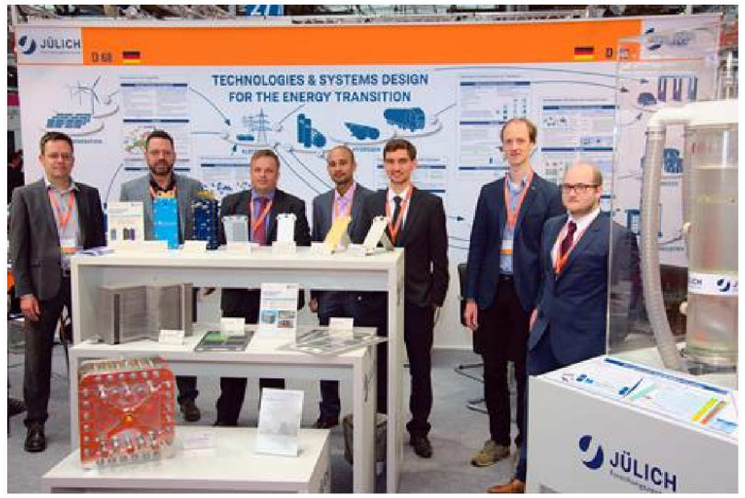

Fig. 95: Hannover Messe 2018 – Jülich exhibition stand and team

6.7 How to reach us

6.7.1 By car

Coming from Cologne on the A4 motorway (Cologne–Aachen) leave the motorway at the Düren exit, then turn right towards Jülich (B56). After about 10 km, turn off to the right onto the L253, and follow the signs for “Forschungszentrum”.

Coming from Aachen on the A44 motorway (Aachen–Düsseldorf) take the “Jülich-West” exit. At the first roundabout turn left towards Jülich, and at the second roundabout turn right towards Düren (B56). After about 5 km, turn left onto the L253 and follow the signs for “Forschungszentrum”.

Coming from Düsseldorf Airport, take the A52 motorway (towards Düsseldorf/Mönchengladbach) followed by the A57 (towards Cologne (Köln)) to Neuss-West. Then take the A46 (towards Jüchen/Grevenbroich), before turning onto the A44 (towards Aachen). Continue as described in “Coming from Düsseldorf”.

Coming from Düsseldorf on the A44 motorway (Düsseldorf–Aachen) you have two choices:

1. (Shorter route but more traffic) turn right at the Jülich-Ost exit onto the B55n, which you should follow for approx. 500 m before turning right towards Jülich. After 200 m, before the radio masts, turn left and continue until you reach the “Merscher Höhe” roundabout. Turn left here, drive past the Solar Campus belonging to Aachen University of Applied Sciences and continue straight along Brunnenstrasse. Cross the Römerstrasse junction, continue straight ahead onto Wiesenstrasse, and then after the roundabout and the caravan dealers, turn left towards “Forschungszentrum” (signposted).

2. (Longer but quicker route) drive until you reach the “Jülich-West” exit. At the first roundabout turn left towards Jülich, and at the second roundabout turn right towards Düren (B56). After about 5 km, turn left onto the L253 and follow the signs for “Forschungszentrum”.

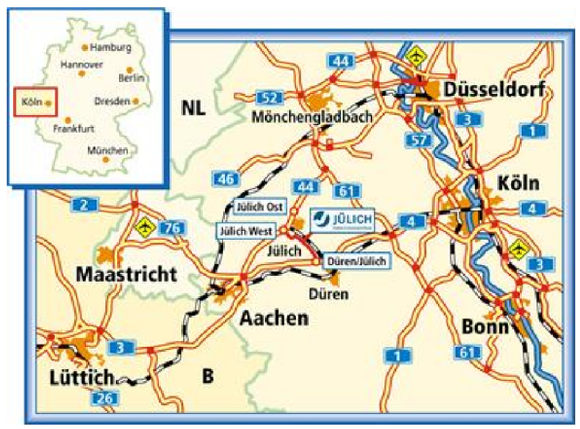

Fig. 96 Euregio Rheinland map

Navigation systems: In your navigation system, enter “Wilhelm-Johnen-Strasse” as the destination. From here, it is only a few hundred meters to the main entrance – simply follow

the signs. Forschungszentrum Jülich itself is not part of the network of public roads and is therefore not recognized by navigation systems.

6.7.2 By plane

Cologne Bonn Airport: From the railway station at the airport, either take the S13 to Cologne main train station (Köln Hauptbahnhof) and then continue with the regional express to Düren, or go to Köln-Ehrenfeld by regional express and then take the S12 to Düren. Continue from Düren as described under “By train”.

By train from **Düsseldorf Airport**: From the railway station at the airport, travel to Cologne main train station (Köln Hauptbahnhof) and then continue on to Düren. Some trains go directly to Düren whereas other connections involve a change at Cologne main train station. Continue from Düren as described under “By train”.

6.7.3 By train

Take the train from Aachen or Cologne to Düren’s main train station (Hauptbahnhof). Then take the local train to Jülich (“Rurtalbahn”) and get out at the “Forschungszentrum” stop. From here, you need to keep right and walk towards the main road before turning right towards Forschungszentrum Jülich. The main entrance to Forschungszentrum Jülich is about 20 minutes by foot.

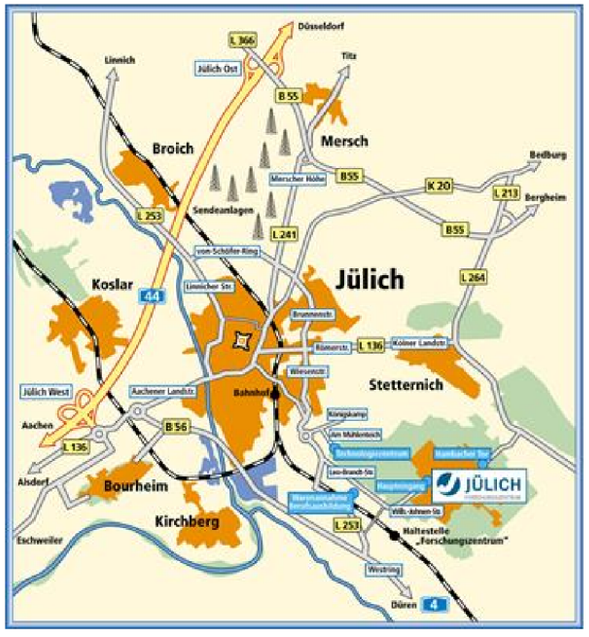

Fig. 97: **Forschungszentrum Jülich campus map**

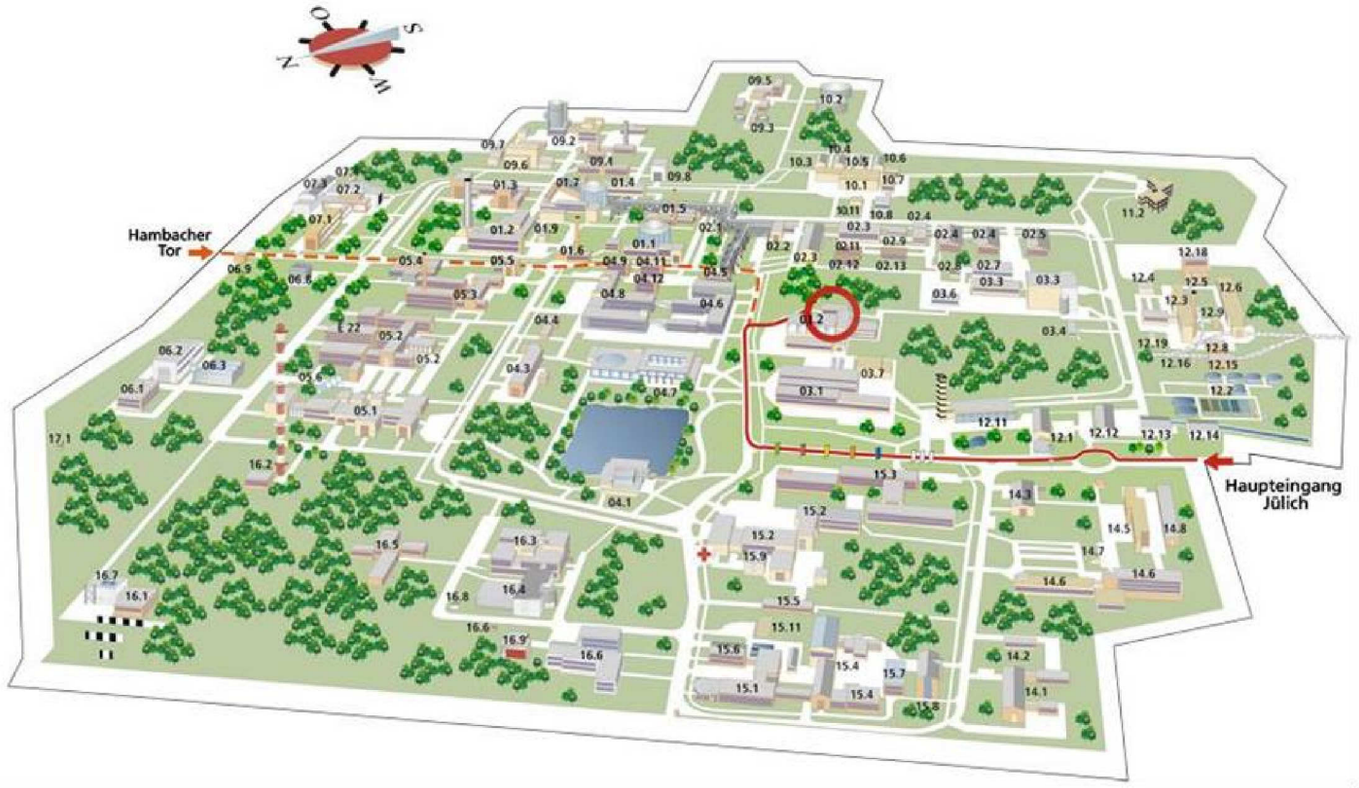

Fig. 98: **Location of Institute of Energy and Climate Research, IEK-3: Electrochemical Process Engineering, Helmholtz Ring H8, building 03.2**

6.8 List of Abbreviations

AAe	Alfa Aesar
acatech	German National Academy of Science and Engineering
AFM	atomic force microscopy
AGEF	Working Group of Electrochemical Research Facilities
APU	auxiliary power unit
AP-XPS	appearance potential X-ray photoemission spectroscopy
ASC	anode-supported cell
ASME	American Society of Mechanical Engineers
ASR	area-specific resistance
ATR	Autothermal reforming
BASF	Badische Anilin- & Soda-Fabrik: German chemical group based in Ludwigshafen
BET	analytical technique for the determination of surface area (Brunauer-Emmett-Teller)
BGS	Fuel Processing and Systems group
Bio CH	biologically produced methane
BMBF	German Federal Ministry of Education and Research
BMVI	German Federal Ministry of Transport and Digital Infrastructure
BMWi	German Federal Ministry for Economic Affairs and Energy
BPP	bipolar plate
BREZEL	fuel cells expert committee of the Association of German Engineers (VDI)
BTL	biomass-to-liquid
BZ	fuel cell
CAB	catalytic burner
CAN	Center for Applied Nanotechnology
CAPM	capital asset pricing model
CC-MEA	catalyst-coated membrane electrode assembly
CCM	catalyst-coated membrane
CFD	computational fluid dynamics
CFD	computational fluid dynamics
CGO	cerium-gadolinium oxide: Ce0.8Gd0.2O2-δ
CP	credit point
CPLEX	program system for modeling & solving optimization problems
CS	cassette-substrate concept
CT	X-ray tomography
CV	cyclic voltammetry
DBG	German Bunsen Society for Physical Chemistry
DC	direct current
DC/DC network	direct current/direct current network
DECHEMA	Society for Chemical Engineering and Biotechnology e.V.
DLR	German Aerospace Center
DME	Dimethyl ether
DMFC	direct methanol fuel cell
DOSY	diffusion ordered spectroscopy
DPG	German Physical Society

DRT	distribution of relaxation times
DSC	differential scanning calorimeter
DTU	Technical University of Denmark
DWV	German Hydrogen and Fuel Cell Association
EC	ethylene carbonate
ECPE	Energy, Chemical & Process Engineering
ECS	Electrochemical Society
EDX	energy-dispersive X-ray spectroscopy
EEL	electrochemistry electrolysis group
EFC	European Fuel Cell Conference & Exhibition
EIS	electrochemical impedance spectroscopy
ELKE	project for the development of high-performance and low-cost electrode structures for alkaline electrolysis
EU	European Union
FEM	finite element method
FH Aachen	Aachen University of Applied Sciences
FINE	framework for integrated energy system assessment
FOB	solid oxide fuel cells
FTIR	Fourier-transform infrared spectroscopy
R&D	research and development
FVEE	German Renewable Energy Research Association
FZJ	Forschungszentrum Jülich GmbH
GC	gas chromatograph
GC/MS	gas chromatograph coupled with a mass spectrometer
GDAL	geospatial data abstraction library
GDCh	German Chemical Society
GDL	gaseous diffusion plant
GEE	German affiliate of the International Association for Energy Economics (IAEE)
GFZ	German Research Centre for Geosciences
GLAES	Geospatial Land Availability for Energy Systems
GW	gigawatt
HAADF	high-angle annular dark field imaging analysis technique
HT-PEFC	high-temperature polymer electrolyte fuel cells
HT-SOC	high-temperature solid oxide cell
HC kerosene	Hydrocarbon kerosene
HGF	Helmholtz Association of German Research Centres
HIFIPEFC	collaborative project funded by BMWi for characterizing ionic liquids for use as electrolytes in fuel cells with polymer membranes
HiKAB	hierarchical composite nanoparticle systems for application in fuel cells
HPC	high-performance computer
H-SEM	high-resolution scanning electron microscope
HT-PEM	high-temperature polymer electrolyte membrane
HTS	high-temperature shift stage
HYPOS	Hydrogen Power Storage & Solutions East Germany, a BMBF project for building a hydrogen infrastructure
HZB	Helmholtz-Zentrum Berlin
IAHE	International Association for Hydrogen Energy

IAS-JSC	Institute for Advanced Simulation at the Jülich Supercomputing Centre
IEA	International Energy Agency
IEEE	Institute of Electrical and Electronics Engineers
IEK-1	Institute of Energy and Climate Research – Materials Synthesis and Processing
IEK-3	Institute of Energy and Climate Research – Electrochemical Process Engineering
IEK-9	Institute of Energy and Climate Research – Fundamental Electrochemistry
IL	ionic liquid
IMechE	Institution of Mechanical Engineers
IQ-BZ	Fuel Cell Qualification Initiative
ISE	International Society of Electrochemistry
JARA	Jülich Aachen Research Alliance
JSC	Jülich Supercomputing Centre
JuLab	Jülich schools laboratory
JURECA	Jülich Research on Exascale Cluster Architectures
KIT/IMVT	Karlsruhe Institute of Technology/Institute for Micro Process Engineering
KOH	potassium hydroxide
CHP	combined heat and power generation
LHV	lower heating value
LNMO	spinel-type cathode material $LiNi_{0.5}Mn_{1.5}O_4$
LOHC	liquid organic hydrogen carrier
LP	linear programming
LSCF	lanthanum strontium cobaltite ferrite
LT-PEFC	low-temperature polymer electrolyte fuel cell
LTS	low-temperature shift stage
MCFC	molten carbonate fuel cell
MEA	membrane electrode assembly
MEMS	micro-electro-mechanical system
METIS	models for energy transformation and integration systems
MODEX-NET	model comparison of power grid models in the European context
N.ERGHY	society of research institutions in the European hydrogen and fuel cells initiative
NDIR	non-dispersive infrared adsorption analyser
NESTOR	National Energy System model with integrated sector coupling
NOW	National Organization for Hydrogen and Fuel Cell Technology
NRW	North Rhine-Westphalia
LT-PEFC	low-temperature polymer electrolyte fuel cell
LTS	low-temperature shift stage
NUTS	Nomenclature of territorial units for statistics (from the French *Nomenclature des unités territoriales statistiques*)
OCV	open cell voltage
ODD	upper average pressure drop
OER	oxygen evolution reaction
OME	oxymethylene ether
OpenFOAM	Open Source Field Operation and Manipulation (free simulation software package for continuum-mechanics problems)
ORR	oxygen reduction reaction
P2X	Power-to-X

PAFC	phosphoric acid fuel cell
PBI	polybenzimidazole
PCEC	proton-conducting electrolysis cell
PCFC	proton-conducting fuel cell
PCL	physico-chemical laboratory
PEFC	polymer electrolyte fuel cell
PEM	polymer electrolyte membrane
PEM-EL	Polymer Electrolyte Membrane Electrolysis
PET	positron emission tomography
PIL	proton-conducting ionic liquids
PoF	programme-oriented funding from the Helmholtz Association
ProMINat	academy for students
PSI	Paul Scherrer Institute
PTF	power-to-fuel processes
PTFE	polytetrafluoroethylene
PtG	power-to-gas
PTX	Power-to-X
PV	Photovoltaics
PV-BESS	photovoltaic battery storage systems
Raman/IR	Raman/infrared spectroscopy
RDE	rotating disk electrode
SEM	scanning electron microscope
SEM/EDX	scanning electron microscope combined with energy-dispersive X-ray spectroscopy
rSOC	reversible solid oxide cell
RWTH	RWTH Aachen University
RWÜ	tube bundle heat exchanger
SCT	segmented cell technology
SDEWES	Conference of Sustainable Development of Energy, Water and Environment Systems
SEI	solid electrolyte interface
SFC	SFC Energy: listed manufacturer of fuel cells based in Brunnthal near Munich
SGL	SGL Carbon SE: international manufacturer of carbon products based in Wiesbaden
SOC	solid oxide cell
SOE	solid oxide electrolysis
SOFC	solid oxide fuel cell
sPEEK	sulfonated polyether ether ketone
SRMS	spatial resolution mass spectroscopy
SS	summer semester
SSI-21	International Conference of Solid State Ionics
STEM	scanning transmission electron microscope
SuPER	ProcessNet Section on sustainable production, energy, and resources
SVI	Storage and Cross-Linked Infrastructure
SWOT	method for evaluating strengths, weaknesses, opportunities, and threats
TAP	temporal analysis of products
TEM	transmission electron microscope

TESYS	Project House Technology-Based Energy System Analysis
TG	thermogravimetric analysis
TGA	thermogravimetric analyzer
TMFB	tailor-made fuels from biomass
TRENDS	conference for the transition to renewable energy devices and systems
TSA	techno-economic energy systems analysis
TU Berlin	Technische Universität Berlin
UDD	lower average pressure drop
UNIFAC	universal quasichemical functional group activity coefficients
US DOE	Department of Energy, USA.
UPS	uninterruptible power supply unit
VDE	German Association for Electrical, Electronic and Information Technologies
VDI	Association of German Engineers
VDI-GVC	Association of German Engineers – Society for Process Engineering and Chemical Engineering
VEL	Process Engineering Electrolysis group
VOF	volume of fluid (method in computational fluid dynamics)
VSA	process and systems analysis group
WACC	method of evaluating companies based on weighted average cost of capital
WGS	water-gas shift reaction
WILEY-VCH	WILEY Verlag Chemie publishing house
WPS	wet powder spraying
WS	Winter semester
WTW	well-to-wheel
XRD	X-ray diffraction
XRR	Reflectometry
ZEA-3	Central Institute of Engineering, Electronics and Analytics

Schriften des Forschungszentrums Jülich
Reihe Energie & Umwelt / Energy & Environment

Band / Volume 470
Entwicklung von Reparaturmethoden für Nickel-Superlegierungen mittels thermischer Spritzverfahren
T. Kalfhaus (2019), VI, 126, XXX pp
ISBN: 978-3-95806-418-8

Band / Volume 471
Entwicklung von korrosionsstabilen Schutzschichten für oxidische Faserverbundwerkstoffe
C. S. Gatzen (2019), II, 143 pp
ISBN: 978-3-95806-422-5

Band / Volume 472
Coatings for Metallic Bipolar Plates in High-Temperature Polymer Electrolyte Fuel Cells
R. Li (2019), II, 119 pp
ISBN: 978-3-95806-425-6

Band / Volume 473
Thermochemische Eigenschaften von kombinierten Katalysator- und Sauerstoffträgersystemen für die partielle Oxidation von Teeren aus der Biomassevergasung
M. Ma (2019), VII, 157 pp
ISBN: 978-3-95806-426-3

Band / Volume 474
Einfluss der klimatischen Fertigungsumgebung auf die Mechanik und Rissstrukturierung der elektrodenbeschichteten Membran einer PEM-Brennstoffzelle
B. Wienk-Borgert (2019), IV, 141 pp
ISBN: 978-3-95806-428-7

Band / Volume 475
Reversible wasserstoffbetriebene Festoxidzellensysteme
M. H. Frank (2019), 187 pp
ISBN: 978-3-95806-430-0

Band / Volume 476
Partitioning of carbon dioxide exchange in rapidly and slowly changing ecosystems
P. Ney (2019), xvi, 95 pp
ISBN: 978-3-95806-431-7

Band / Volume 477
Massentransportphänomene in Schichtsystemen eines Elektrolyseurs
U. Panchenko (2019), 107 pp
ISBN: 978-3-95806-433-1

Schriften des Forschungszentrums Jülich
Reihe Energie & Umwelt / Energy & Environment

Band / Volume 478
Mechanische Eigenschaften von Polymer-Elektrolyt-Membran-Brennstoffzellen
P. Irmscher (2019), vii, 177 pp
ISBN: 978-3-95806-435-5

Band / Volume 479
Morphology and Degradation of High Temperature Polymer Electrolyte Fuel Cell Electrodes
S. Liu (2019), III, 162 pp
ISBN: 978-3-95806-436-2

Band / Volume 480
Structural uptake and retention of safety relevant radionuclides by cementitious materials
S. Lange (2019), 133 pp
ISBN: 978-3-95806-437-9

Band / Volume 481
Quantifying the Impact of Inhomogeneity, Transport and Recombination in Emerging Thin-Film Solar Cells
P. Kaienburg (2019), vii, 258 pp
ISBN: 978-3-95806-440-9

Band / Volume 482
Studies of oxidation resistant tungsten alloys at temperatures of 1100K to 1475K
F. Klein (2019), 158 pp
ISBN: 978-3-95806-444-7

Band / Volume 483
Impact Assessment of Land-Use Change and Agricultural Treatments on Greenhouse Gas Emissions from Wetlands of Uganda and Tanzania
K. X. X. Wagner (2019), 144 pp
ISBN: 978-3-95806-447-8

Band / Volume 484
IEK-3 Report 2019
Tailor-Made Energy Conversion for Sustainable Fuels
D. Stolten, B. Emonts (Eds.) (2020), 162 pp
ISBN: 978-3-95806-451-5

There is an urgent need to reduce carbon dioxide emissions from the burning of fossil fuels in the transport sector. Through its focused efforts in technology research on water electrolysis and in the technoeconomic evaluation of future transport solutions in the period under review, IEK-3 succeeded in improving the technological maturity of advanced water electrolysis and gaining ground-breaking insights into process engineering for the production of synthetic fuels from H_2 and CO_2.

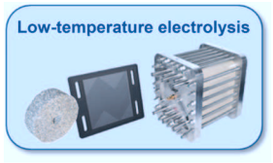

Water electrolysis at temperatures of roughly 70 °C permits highly dynamic operation with fast start-up and shut-down procedures. Electrolyzers with polymer electrolyte membranes or potassium hydroxide solution have reached a sufficient degree of maturity to facilitate the construction of large plants on the megawatt scale, with current and future R&D activities focusing on improving performance, increasing lifetimes, and reducing investment and operating costs. Rolling out large-scale plants for electrochemical H_2 production serves as a test for their integration in the energy system

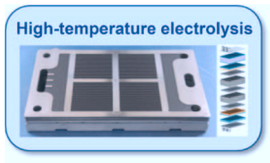

Steam electrolysis at temperatures of up to approximately 800 °C permits the use of surplus high-temperature heat produced in many industrial processes. The maturity of electrolyzers based on solid oxide cells depends on that of the relevant fuel cells and is now sufficiently high to enable plants to be constructed on the kilowatt scale. Current and future R&D activities focus on resolving issues related to material changes that reduce performance and lifetime; other priorities include designing a reversible system for electrolysis and fuel cell operation and achieving application-relevant cost targets.

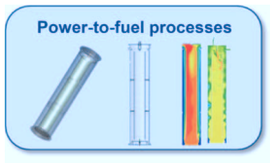

The targeted processing of hydrogen from renewable sources and carbon dioxide from climate-neutral sources produces a synthetic, liquid fuel that in its ideal form substitutes today's kerosene or diesel and at the same time burns without harmful residues. Dimensioning tools and methods are being used to design a synthesis reactor – comprising an autothermal reformer, WGS reactor, and catalytic burner – which will synthesize the two source gases, H_2 and CO_2, into a synfuel with high selectivity and low conversion losses.

Energie & Umwelt / Energy & Environment
Band / Volume 484
ISBN 978-3-95806-451-5

Mitglied der Helmholtz-Gemeinschaft

JÜLICH
Forschungszentrum